

Holographic CFTs on $AdS_d \times S^n$ and conformal defects

Ahmad Ghodsi^a, Elias Kiritsis^{b,c} and Francesco Nitti^b

^a *Department of Physics, Faculty of Science, Ferdowsi University of Mashhad, Mashhad, Iran.*

^b *Université Paris Cité, CNRS, Astroparticule et Cosmologie, F-75013 Paris, France.*

^c *Crete Center for Theoretical Physics, Institute for Theoretical and Computational Physics, Department of Physics University of Crete, Heraklion, Greece*

ABSTRACT: We consider $(d + n + 1)$ -dimensional solutions of Einstein gravity with constant negative curvature. Regular solutions of this type are expected to be dual to the ground states of $(d + n)$ -dimensional holographic CFTs on $AdS_d \times S^n$. Their only dimensionless parameter is the ratio of radii of curvatures of AdS_d and S^n . The same solutions may also be dual to $(d - 1)$ -dimensional conformal defects in holographic QFT _{$d+n$} . We solve the gravity equations with an associated conifold ansatz, and we classify all solutions both singular and regular by a combination of analytical and numerical techniques. There are no solutions, regular or singular, with two boundaries along the holographic direction. Out of the infinite class of regular solutions, only one is diffeomorphic to AdS_{d+n+1} and another to $AdS_d \times AdS_{n+1}$. For the regular solutions, we compute the on-shell action as a function of the relevant parameters.

KEYWORDS: Holography, CFT, AdS, conformal defects.

Contents

| | |
|---|-----------|
| 1. Introduction, results and outlook | 2 |
| 1.1 Results | 5 |
| 1.2 Conformal Defects | 8 |
| 1.3 Outlook | 10 |
| 2. Constant negative curvature solutions with $AdS_d \times S^n$ slices | 10 |
| 2.1 The general conifold ansatz | 10 |
| 2.2 The $AdS_d \times S^n$ slice | 12 |
| 3. Regular and singular asymptotic of the solutions | 13 |
| 3.1 Near-boundary expansions | 14 |
| 3.2 Regular and singular end-points | 15 |
| 3.2.1 Singular end-points | 17 |
| 3.2.2 Regular end-points | 17 |
| 3.3 Solutions with A-bounces and monotonic solutions | 19 |
| 3.3.1 AdS_d bounce | 20 |
| 3.3.2 S^n bounce | 22 |
| 4. Exact solutions | 23 |
| 5. Numerical solutions | 24 |
| 5.1 Solutions with one regular end-point | 25 |
| 5.2 Solutions with A-bounces | 28 |
| 5.3 A_1 -bounce space of solutions | 31 |
| 5.4 A_2 -bounce space of solutions | 33 |
| 5.5 Monotonic solutions | 35 |
| 6. The space of all solutions | 35 |
| 7. The boundary CFT data | 37 |
| 7.1 Boundary data of (R, B)-type | 38 |
| 8. The on-shell action and the free energy | 39 |
| 8.1 Regularization | 42 |
| 8.2 Fixing the scheme | 44 |

| | |
|--|-----------|
| 9. Solutions with $AdS_d \times S^1$ slices | 45 |
| 9.1 Asymptotics | 46 |
| 9.2 Exact solutions | 48 |
| 9.3 The global AdS_{d+2} solution | 52 |
| 9.4 Relations between parameters in two coordinates | 52 |
| 10. On general Einstein manifold solutions with constant negative curvature. | 55 |
| Acknowledgements | 56 |
| Appendices | 57 |
| A. Product space ansatz for the slice | 57 |
| A.1 The curvature invariants | 59 |
| B. Various global coordinates on AdS_{d+n+1} and its Euclidean version | 60 |
| B.1 Standard global coordinates on AdS_{d+n+1} | 60 |
| B.2 Coordinates fibered over $AdS_d \times S^n$ | 61 |
| B.3 The special case $n = 0$ | 63 |
| C. Analytic solutions for other signatures | 63 |
| C.1 The uniform solution | 63 |
| C.2 The constant A_2 solution | 65 |
| D. The stress-energy tensor | 65 |
| E. Perturbations around the product space solution | 67 |
| F. Topological Black holes with a negative cosmological constant | 69 |

1. Introduction, results and outlook

Quantum field theories are usually considered in flat background space-time. They can be studied, however, in background space-times that have non-zero curvature. Space-time curvature is irrelevant in the UV, as at short distances any regular manifold is flat. However, the curvature is relevant in the IR and can affect the low-energy structure of the QFT.

There are several reasons to consider QFT in curved backgrounds.

- Partition functions of QFTs on compact manifolds (spheres), are important elements in the study of the monotonicity of the RG Flow and the definition of generalized C-functions, especially in odd dimensions, [1, 2, 3].
- Many observables in CFTs and other massless QFTs (supersymmetric indices are examples) are well-defined when a mass gap is introduced. This can be generated by putting the theory on a positive curvature manifold, like a sphere. Sphere compactifications have been used in calculating supersymmetric indices in CFTs, [4]. They have also been used as regulators of IR divergences of perturbation theory in QFT, [5, 6, 7] and string theory, [8].
- Curvature in QFT, although UV-irrelevant is IR-relevant and importantly affects the IR physics. It can drive (quantum) phase transitions in the QFT, [9, 10].
- The ground-states of holographic QFTs on curved manifolds lead to constant (negative) curvature metrics sliced by curved slices. The Fefferman-Graham theorem indicates that such regular metrics exist near the asymptotically *AdS* boundary, [11]. However, it is not known whether such solutions can be extended to globally regular solutions in the Euclidean case. If yes, then there may exist associated Minkowski signature solutions with horizons¹. The few (mathematical) facts that are known can be found in [13, 14].

Holography suggests that because we can put any holographic CFT on any manifold we choose, there should be dual regular saddle point solutions. This argument has, however, a loophole: it may be that for a regular solution to exist, more bulk fields need to be turned-on (spontaneously), via asymptotically vev solutions².

- Cosmology has always given a motivation to study QFT in curved space-time, [16, 17]. In particular, QFT in de Sitter or almost de Sitter space is expected to describe early universe inflation as well as the current acceleration of the universe.
- The issue of quantum effects in approximate de Sitter backgrounds is a controversial issue even today, [18]–[23].
- Partition functions of holographic QFTs on curved manifolds are important building blocks in the no-boundary proposal of the wave-function of the universe, [24, 25]. They serve to determine probabilities for various universe geometries.

¹Such metrics have been discussed in section 5 of [12].

²A milder version of this phenomenon associated with spontaneous symmetry breaking of a parity-like Z_2 symmetry has been observed in [15].

Many examples of holographic QFTs living on non-trivial geometries have been already discussed in the past.

The simplest case of $(S^1)^n$ has already been systematically studied in the case where all circles have the same radius as well as when there are two different radii, [26, 27, 28].

The case of $S^1 \times S^{d-1}$ has been studied extensively but not systematically. It contains AdS_{d+1} in global coordinates, as well as (Euclidean) Schwarzschild- AdS , and some RG flows have been analyzed in this case.

A systematic analysis of curved space-time holographic RG flows in Einstein-dilaton theories has been initiated in [10], when the boundary field theory is defined on an Einstein space with positive or negative curvature. For positive curvature, the RG flow pattern is not very different from that of flat space field theories. The main difference is that curvature dominates in the IR and provides a gap to the theory before the deep IR regime is reached. On the other hand, many quantum phase transitions appear, driven by the positive curvature.

The general problem where the boundary is a product of constant (positive) curvature manifolds and the QFT is a CFT has been addressed in [29]. Phase transitions were found, generalizing the Hawking-Page transition (which is relevant in the $S^1 \times S^{d-1}$ case), [30]. Efimov resonances were also found that were explored in [31] to generate a class of associated black hole solutions. The general case of QFTs on $S^2 \times S^2$ was addressed in [15]. Among other things, it was found that a Z_2 parity-like symmetry that exists when the two spheres have the same size is always spontaneously broken by quantum effects. Therefore the vacuum is always doubly degenerate.

In the case where the boundary has negative curvature, however, the holographic QFT interpretation of the solutions is *very* different from that of a standard RG flow. The reason is that, when the bulk is foliated by constant negative curvature d -dimensional slices, the solution has *two* asymptotically AdS_{d+1} boundaries. This corresponds to two UV CFTs that are interacting through the bulk.

Solutions in string theory, with asymptotic boundary metrics being AdS , have been studied for some time, [32]–[44]. They have two (apparently) distinct conformal boundaries at the two end-points of the holographic coordinate. However, as the slices involve a non-compact manifold, which has also a conformal boundary, the two boundaries are connected. This results in a single conformal boundary.

If the bulk is $d + 1$ dimensional, and the slices are AdS_d , the total boundary is conformal to two pieces of S^d separated by an overlap on the equator³ S^{d-1} . The two endpoints of the flow can have different sources, the two holographically-dual theories can have different couplings and they are separated by an interface, justifying the name “Janus solutions”. A similar class of solutions contains a single boundary and

³In the context of holography, this description is most appropriate when the bulk AdS_{d+1} is written in global coordinates, see [44].

is delimited in the bulk by a brane that ends on “the boundary of the boundary”. They are also *AdS*-sliced and a prototypical example was discussed in [45]. They have been proposed as holographic duals of boundary CFTs, [46, 47]. Related holographic RG flows have been considered in [48, 49].

There is another incarnation of such solutions. In Euclidean cases, where the slice manifold is a constant negative curvature manifold with finite volume and no boundary, such a solution is an example of a Euclidean wormhole. This is an object that still holds mysteries for the holographic correspondence, [50, 51, 52, 53]. The holographic interpretation of such solutions is still debated and for this reason, their occurrence is also an interesting datum.

AdS-sliced solutions were studied systematically in [44] with three purposes

- The holographic construction of QFTs on *AdS* manifolds.
- The exploration of the space of holographic interfaces.
- The study of “proximity of QFTs” defined by which ones can be connected by wormholes.

A specific potential landscape was fully analyzed by a combination of analytical and numerical methods. It was found that the solution space contained many exotic RG flow solutions that realized unusual asymptotics, as boundaries of different regions in the space of solutions. Phenomena like “walking” flows and the generation of extra boundaries via “flow fragmentation” were found.

The purpose of the present paper is to pursue the research program started in [26] and [10], and to study a further example along similar lines: holographic CFTs on product manifolds of the type⁴ $AdS_d \times S^n$. Such manifolds are interesting as they combine a piece that has constant negative curvature and one that has constant positive curvature.

Moreover, these geometries are also interesting since upon (generalized) dimensional reduction on S^n they give rise to the infrared region of confining field theories defined on AdS_d [54, 55]. This connection, and the space of solutions of the reduced theory, will be thoroughly analyzed in a forthcoming work.

1.1 Results

We consider an Einstein theory with a negative cosmological constant in $d + n + 1$ dimensions. The ansatz used is a conifold ansatz that contains a holographic (radial) coordinate and a product of a d -dimensional constant negative curvature manifold and an n -dimensional constant positive curvature manifold.

$$ds^2 = du^2 + e^{2A_1(u)} ds_{AdS_d}^2 + e^{2A_2(u)} ds_{S^n}^2 . \quad (1.1)$$

⁴All our results are valid if we replace AdS_d with any d -dimensional negative constant curvature manifold, with or without finite volume. A similar statement holds for S^n .

The solutions should have a $d + n$ -dimensional conformal boundary, where a holographic CFT lives. In this context, we obtain and solve the equations of motion and compute the scalar curvature invariants, which are necessary ingredients to check the regularity/singularity of the solutions.

- **Classification of the solutions:** We classify the solutions according to their “end-points,” which we define as limiting values of the radial coordinate of the conifold. A detailed analysis shows that we have four classes of end-points:
 1. An *AdS*-like boundary where the scale factors of *AdS* and the sphere diverge. We shall denote this end-point as **B**.
 2. A regular end-point where the scale factor of the sphere shrinks to zero sizes while the *AdS* factor asymptotes to a constant value. We shall denote this end-point as **R**.
 3. A singular end-point in which the size of *AdS* vanishes while the size of the sphere diverges. We shall denote this end-point as **A**.
 4. A singular end-point in which the size of the sphere vanishes while the size of *AdS* diverges. We shall denote this end-point as **S**.

Only the first two of the four end-points correspond to a regular geometry. A solution is characterized by its two end-points along the radial (holographic) direction. We denote the class of a solution by its two end points, ie. (\mathbf{B}, \mathbf{R}) or (\mathbf{B}, \mathbf{S}) , etc.

In addition to end-points, a generic solution may or may not have an *A-bounce*: this is a stationary point of one or both of the scale factors which then displays a local minimum or maximum away from the end-points.

By analyzing the behavior of the scale factors near the A-bounces we recognize that the AdS_d or S^n can have at most one A-bounce. This restricts the classes of solutions with the above-mentioned end-points.

Our analytical and numerical analysis leads to the following results:

1. There is only one class of solutions that are everywhere regular: these are solutions that have one regular end-point and one *AdS*-like boundary, i.e. (\mathbf{B}, \mathbf{R}) .
2. If a solution has an A-bounce, then it also has at least one singular end-point. Therefore, we do not find any regular wormhole-like solution.
3. There do not exist solutions in which at both end-points the scale factor of the sphere shrinks to zero sizes, ie. solutions of the type (\mathbf{R}, \mathbf{R}) , (\mathbf{R}, \mathbf{S}) and (\mathbf{S}, \mathbf{S}) do not exist.

4. We find two exact solutions of the Einstein equations: one of them is the global AdS_{d+n+1} space-time; the other is the product solution $AdS_d \times AdS_{n+1}$.

- **Space of solutions:** The space of solutions is three-dimensional as three initial conditions are needed to solve the equations. From the holographic point of view, these correspond to the two curvature scales of AdS_d and S^n and one vev parameter of the dual stress-energy tensor. However, one of these parameters can be scaled out and the physics of such solutions depends on two dimensionless parameters. They can be taken as the ratio of curvatures of AdS_d and S^n and the associated ratio for the vev.

We analyze the transition between the above-mentioned solutions in the parameter space. In this space, we can follow how different regular/singular solutions change to each other as we move inside this space. There is a codimension-one subspace (a two dimensional surface) for regular solutions which ends on one side to the product space solution.

- **QFT data on the boundary:** The Fefferman-Graham expansion near the AdS -like boundary (UV boundary) contains three parameters: two of them are the AdS and sphere curvatures (R_{AdS}^{UV}, R_S^{UV}). Since the dual CFT is conformally invariant, the physics only depends on the ratio of these curvatures. The last parameter (C), is related to the vacuum expectation value and corresponds to parts of the vev of the components of the stress tensor. We can construct another dimensionless parameter from C and one of the AdS or sphere curvatures. Overall, we have two dimensionless ratios that describe the holographic QFT on the conformal boundary of a bulk solution. The value of C depends on the data of the IR end-point. Here the IR is the location of the regular end-point and the only relevant parameter remaining is the curvature of the AdS slice at this point. The value of C for the product space solution, $AdS_d \times AdS_{n+1}$, diverges and for the global AdS space solution, it is zero as expected. For other regular solutions, it can be a positive or a negative number.
- **Free energy:** The computation of the free energy for regular solutions shows that among these solutions, the global AdS solution has the maximum value. This implies that if one constructs the no-boundary wave-function along the lines of [24] the global AdS solution is the least probable state.

All the previous conclusions hold when $n > 1$, as in this case, the sphere has non-zero positive curvature. The case $n = 1$ needs a separate analysis that is performed in section 9. The S^1 can be interpreted as a Euclidean time, and the structure of the solutions is that of a black hole with a hyperbolic horizon. Such black holes are

known as topological back holes, [61, 62]. In this case, we only have the following classes of solutions:

1. The regular solutions of (\mathbf{R}, \mathbf{B}) type. This describes the solution outside the horizon of the black hole i.e. stretched from the horizon to the asymptotic boundary.
2. The singular solutions of (\mathbf{R}, \mathbf{A}) type. This describes the solution behind the horizon of the black hole i.e. stretched from horizon to singularity.
3. The singular solutions of (\mathbf{A}, \mathbf{B}) type. This describes a solution that is stretched from singularity to boundary (solutions with a naked singularity).

The regular solutions appear in two classes:

- Black holes with two horizons (one event and one Cauchy horizon). In the limit where the two horizons coincide, we have an extremal black hole solution.
- Solutions with a single horizon. At the boundary of these solutions is the global AdS_{d+2} solution.

Known facts about topological black holes are collected in appendix F.

We finally remark, that the techniques of the conifold ansatz with constant curvature slices can be used to find solutions at higher dimensions while solving only ODEs. It is not clear whether this algorithm captures all negative constant curvature metrics.

1.2 Conformal Defects

There is another context where conifold geometries with $AdS \times S$ slices are relevant, namely in the study of conformal defects, [56]-[60].

Consider a D -dimensional QFT $_D$, with a d -dimensional defect in it. If the QFT $_D$ is defined on flat space then its generic symmetry is $ISO(D)$. If it is a CFT $_D$, the symmetry is enhanced to conformal symmetry, i.e. $O(D+1, 1)$. Consider now a d -dimensional flat space defect, in QFT $_D$, localized on a d -dimensional hyperplane in R^D . The symmetries that remain unbroken by the defect that is assumed to be a flat d -dimensional hyperplane, are $ISO(d) \times SO(D-d)$. If the defect is conformally invariant on the d -dimensional world-volume⁵ then $ISO(d)$ is enhanced to $O(d+1, 1)$ and the total symmetry becomes $O(d+1, 1) \times SO(D-d)$.

In a holographic theory such a symmetry will be geometrically realized by a $AdS_{d+1} \times S^{D-d-1}$ manifold⁶.

A special case is a conformal interface that has $d = D - 1$. In that case, the symmetry becomes $O(D, 1)$ and is geometrically realized by AdS_D . Moreover, $SO(1)$ is realized by S^0 which are two distinct points (and this explains why in this case we

⁵The generic case is that the bulk theory is a QFT $_D$ without conformal invariance, but that the defect theory is tuned to be conformally invariant. Examples of such theories can be found in [60]. The most common case, however, studied in the literature is that where the theory in the bulk is a CFT $_D$.

⁶Interestingly, the flat D -dimensional metric is conformal to the metric of $AdS_{d+1} \times S^{D-d-1}$ with the d -dimensional defect being identified with the d -dimensional boundary of AdS_{d+1} .

have two boundaries). The holographic dual of this is given by holographic solutions with the $(D + 1)$ -dimensional metric to be a conifold with AdS_D slices realizing the aforementioned symmetry.

Similarly, in the case of general d , we expect that the holographic ansatz will be a $(D + 1)$ -dimensional conifold with $AdS_{d+1} \times S^{D-d-1}$ slices. Therefore, the holographic ansatz we study in this paper is expected to also describe conformal d -dimensional defects in a holographic QFT $_D$. In particular, the structure of the generic solutions is such that their boundary has two components. One is the boundary of the total space, and this is conformal to $AdS_{d+1} \times S^{D-d-1}$, which is also conformal to flat space⁷. There is another boundary, namely the union of the boundaries of the AdS_{d+1} slices. Insertions on that boundary correspond to defect operators.

The bulk operators are in one-to-one correspondence with the gravitational fields, and their correlators are calculated by putting Dirichlet boundary conditions at the $AdS_{d+1} \times S^{D-d-1}$ boundary⁸. The defect operators are in one-to-one correspondence again with the bulk gravitational fields but their correlators are now determined by putting boundary conditions at the boundary of AdS_{d+1} . Clearly, this picture describes defects that do not carry additional degrees of freedom.

The special analytic solutions found in this paper are interesting from this point of view. We consider the case $n > 1$ that corresponds to defects with codimension $D - d \geq 3$. The global AdS_{D+1} solution seems to imply that the defect does not back-react in the induced CFT geometry as the total space is the same as the holographic dual of a CFT without the defect. Therefore this seems to correspond to trivial conformal defects associated with the identity operator of the CFT.

The $AdS_{d+1} \times AdS_{D-d}$ solution, on the other hand, seems to imply a complete decoupling between the defect and its transverse space. The boundary structure of this solution is different and it has two independent boundaries that in Poincaré coordinates are R^d and S^{D-d-1} . Insertions on these boundaries provide correlators for the defect and its transverse theory. Obviously, these correlators are completely independent. In particular, all one-point functions vanish. The study of small graviton fluctuations around this geometry indicates that there is no flow of energy between defect and bulk.

In the case of $n = 1$ or $D - d = 2$, again the global AdS_{D+1} solution should correspond to trivial defects. On the other hand, the product solution is now $AdS_{d+1} \times \mathcal{M}_2$ where \mathcal{M}_2 are the three spaces $EAdS_2^{\pm,0}$ described in section 9.2. They have one or two AdS_2 boundaries. In analogy with extremal black holes whose horizon contains AdS_2 factors, we would expect also here similar phenomena: a one-dimensional scale invariance as well as a quantum mode that does not decouple at low temperatures.

Further analysis is needed in order to substantiate such claims.

⁷There is a conical singularity around the defect if the curvatures of AdS_{d+1} and S^{D-d-1} are not the same.

⁸When there are non-trivial dynamical degrees of freedom on the defect this ceases to be true.

1.3 Outlook

There is one more case of constant negative curvature manifolds that can be written as conifolds that remains to be systematically studied: that where the slices are products of negative curvature manifolds.

The regular solutions found here descend via dimensional reduction on S^n to solutions of Einstein dilaton gravity with a dilaton potential that has confining asymptotics, [54]. They imply the correct way of desingularizing the asymptotic singular solutions of the Einstein-dilaton theory. This is an interesting domain as it will teach us about confining theories on AdS .

Finally, the implications of our solutions for conformal defects need to be examined. There are several questions in this direction that involve quantitative questions like correlation functions both in the bulk and the defect as well as the dynamics of symmetries broken by the defect. In particular, an interesting question involves the construction of non-trivial defect flows in the holographic context. This is in principle straightforward in the holographic context, as such flows will involve solutions that will depend on two radial coordinates, u and the radial coordinate of the AdS slice. The relevant boundary conditions are that the solutions are vev only at the u -boundary while they have sources on the slice AdS boundary. Special solutions of this type have been considered in [41]. We plan to study this further in the near future.

The structure of this paper is as follows:

In section 2 we derive the equations of motion for a metric with a domain wall holographic coordinate and slices which in general are the product of Einstein manifolds. In section 3 we compute the asymptotic expansions near the boundary, singular and regular end-points for $AdS_d \times S^n$ slices. We also explore the possibility of having A-bounces in the scale factors of AdS_d or S^n . In section 4, we present two exact solutions of the theory, the global AdS_{d+n+1} and product space solution $AdS_d \times AdS_{n+1}$. In sections 5 and 6, we show all the numerical solutions that we found and how they are related to each other through a three-dimensional space of solutions. In section 7, we extract the boundary CFT data of the regular solutions and identify the dimensionless parameters that characterize the CFT. Using this data, we calculate the on-shell action and the renormalized free energy in section 8. In section 9, we focus on the special case of $AdS_d \times S^1$ and use a suitable coordinate transformation to obtain exact solutions of the equations of motion. Then we discuss their properties. In section 10, we comment on how to generalize our solutions to conifolds of conifolds.

2. Constant negative curvature solutions with $AdS_d \times S^n$ slices

2.1 The general conifold ansatz

We consider an Einstein theory in a $d + 1$ dimensional bulk space-time parametrized

by coordinates $x^a \equiv (u, x^\mu)$ where u is the holographic coordinate. The most general two-derivative action is

$$S = M_P^{d-1} \int d^{d+1}x \sqrt{-g} (R - \Lambda) + S_{GHY}, \quad (2.1)$$

where M_P is the $d+1$ dimensional Plank mass. In this action g_{ab} is the bulk metric, R is its associated Ricci scalar and Λ is a cosmological constant. The surface term S_{GHY} is the Gibbons-Hawking-York term at the space-time boundary (e.g. the UV boundary if the bulk is asymptotically AdS). The bulk field equations of motion are given by

$$R_{ab} - \frac{1}{2}g_{ab}(R - \Lambda) = 0. \quad (2.2)$$

We shall consider a (holographic) boundary QFT defined on a space that is a product of Einstein manifolds. The natural bulk metric ansatz that preserves all the original symmetries of the boundary metric, is given in terms of a domain wall holographic coordinate u and a conifold ansatz (for both Euclidean and Lorentzian signatures)

$$ds^2 = g_{ab}dx^a dx^b = du^2 + \sum_{i=1}^n e^{2A_i(u)} \zeta_{\alpha_i, \beta_i}^i dx^{\alpha_i} dx^{\beta_i}. \quad (2.3)$$

Here the geometry of the constant u slices are products of n Einstein manifolds, each with metric $\zeta_{\alpha_i, \beta_i}^i$, dimension d_i and coordinates x^{α_i} , $\alpha_i = 1, 2, \dots, d_i$. Each Einstein manifold is associated with a different scale factor $A_i(u)$, which depends on the coordinate u only. Therefore, every d -dimensional slice at constant u is given by the product of n Einstein manifolds of dimension d_1, \dots, d_n . This is the conifold ansatz.

Since $\zeta_{\mu\nu}^i$ are Einstein manifolds, the following relations hold

$$R_{\mu\nu}^{(\zeta^i)} = \kappa_i \zeta_{\mu\nu}^i, \quad R^{(\zeta^i)} = d_i \kappa_i, \quad (2.4)$$

where κ_i is the (constant) scalar curvature scale of the i th manifold and no sum on i is implied. We have the identity

$$\sum_{i=1}^n d_i = d. \quad (2.5)$$

In the case of maximal symmetry, the scalar curvatures are

$$\kappa_i = \begin{cases} \frac{(d_i - 1)}{\alpha_i^2} & dS_{d_i} \text{ or } S^{d_i} \\ 0 & \mathcal{M}_{d_i} \\ -\frac{(d_i - 1)}{\alpha_i^2} & AdS_{d_i} \end{cases}, \quad (2.6)$$

where α_i are associate radii and \mathcal{M}_{d_i} denotes d_i -dimensional Minkowski space.

The non-trivial components of Einstein's equation from (2.2) are

$$\left(\sum_{k=1}^n d_k \dot{A}_k\right)^2 - \sum_{k=1}^n d_k \dot{A}_k^2 - \sum_{k=1}^n e^{-2A_k} R^{\zeta^k} + \Lambda = 0 \quad , \quad uu \quad (2.7)$$

$$2\left(1 - \frac{1}{d}\right) \sum_{k=1}^n d_k \ddot{A}_k + \frac{1}{d} \sum_{i,j=1}^n d_i d_j (\dot{A}_i - \dot{A}_j)^2 + \frac{2}{d} \sum_{k=1}^n e^{-2A_k} R^{\zeta^k} = 0 \quad , \quad ii \quad (2.8)$$

$$\ddot{A}_i + \dot{A}_i \sum_{k=1}^n d_k \dot{A}_k - \frac{1}{d_i} e^{-2A_i} R^{\zeta^i} = \ddot{A}_j + \dot{A}_j \sum_{k=1}^n d_k \dot{A}_k - \frac{1}{d_j} e^{-2A_j} R^{\zeta^j} \quad , \quad i \neq j \quad (2.9)$$

where the derivatives with respect to u are denoted by a dot. The details of computations are found in appendix A. The above equations are the same for both Lorentzian and Euclidean signatures of the slices, so all our results hold for both cases.

Holographic saddle points are in one-to-one correspondence with the regular solutions to the equations (2.7)–(2.9). Hence, in the following, we shall be interested in the structure and properties of solutions to these equations, specifically for a negative cosmological constant Λ .

To check the regularity of the solutions, we analyze scalar invariants of curvatures. For example (see appendix A.1 for more details) the Ricci scalar is given by:

$$R = -2 \sum_{i=1}^n d_i \ddot{A}_i - \left(\sum_{i=1}^n d_i \dot{A}_i\right)^2 - \sum_{i=1}^n d_i \dot{A}_i^2 + \sum_{i=1}^n e^{-2A_i} R^{\zeta^i} \quad , \quad (2.10)$$

while the Ricci squared scalar reads

$$R_{ab} R^{ab} = \left(\sum_{i=1}^n d_i (\ddot{A}_i + \dot{A}_i^2)\right)^2 + \sum_{i=1}^n d_i \left(e^{-2A_i} \kappa - (\ddot{A}_i + \dot{A}_i \sum_{j=1}^n d_j \dot{A}_j)\right)^2 \quad . \quad (2.11)$$

Moreover, the Kretschmann scalar, $\mathcal{K} = R_{abcd} R^{abcd}$ is given by

$$\begin{aligned} \mathcal{K} = & \sum_{i=1}^n \left(e^{-4A_i} \mathcal{K}^{\zeta^i} - 4e^{-2A_i} \dot{A}_i^2 R^{\zeta^i} - 2d_i \dot{A}_i^4 \right. \\ & \left. + 4d_i (\ddot{A}_i + \dot{A}_i^2)^2 \right) + \sum_{i,j=1}^n 2d_i d_j (\dot{A}_i \dot{A}_j)^2 \quad , \quad (2.12) \end{aligned}$$

where \mathcal{K}^{ζ^i} is the Kretschmann scalar of the ζ^i metric.

2.2 The $AdS_d \times S^n$ slice

We now specialize the general conifold ansatz to the main subject of investigation of this paper, namely the bulk holographic description of QFTs living on $AdS_d \times S^n$ space-time. The metric (2.3) in this case is

$$ds^2 = du^2 + e^{2A_1(u)} \zeta_{\alpha\beta}^1 dx^\alpha dx^\beta + e^{2A_2(u)} \zeta_{\mu\nu}^2 dx^\mu dx^\nu \quad , \quad (2.13)$$

where ζ^1 and ζ^2 are the AdS_d and S^n metrics respectively.

We have set the dimensions of the Einstein manifolds to $d_1 = d$ and $d_2 = n$. The non-trivial components of Einstein's equation are

$$(d\dot{A}_1 + n\dot{A}_2)^2 - d\dot{A}_1^2 - n\dot{A}_2^2 - e^{-2A_1}R_1 - e^{-2A_2}R_2 + \Lambda = 0, \quad (2.14)$$

$$(d+n-1)(d\ddot{A}_1 + n\ddot{A}_2) + dn(\dot{A}_1 - \dot{A}_2)^2 + e^{-2A_1}R_1 + e^{-2A_2}R_2 = 0, \quad (2.15)$$

$$\ddot{A}_1 + \dot{A}_1(d\dot{A}_1 + n\dot{A}_2) - \frac{1}{d}e^{-2A_1}R_1 = \ddot{A}_2 + \dot{A}_2(d\dot{A}_1 + n\dot{A}_2) - \frac{1}{n}e^{-2A_2}R_2, \quad (2.16)$$

where we have defined

$$R_1 \equiv R^{\zeta^1}, \quad R_2 \equiv R^{\zeta^2}.$$

To check the regularity of the solutions we need to know the Kretschmann scalar from (2.12). In the geometry (2.13), it is given by

$$\begin{aligned} \mathcal{K} = & e^{-4A_1}\mathcal{K}_1 + e^{-4A_2}\mathcal{K}_2 - 4e^{-2A_1}R_1\dot{A}_1^2 - 4e^{-2A_2}R_2\dot{A}_2^2 + 2d(d-1)\dot{A}_1^4 \\ & + 2n(n-1)\dot{A}_2^4 + 4nd\dot{A}_1^2\dot{A}_2^2 + 4d(\ddot{A}_1 + \dot{A}_1^2)^2 + 4n(\ddot{A}_2 + \dot{A}_2^2)^2, \end{aligned} \quad (2.17)$$

where \mathcal{K}_1 and \mathcal{K}_2 are the Kretschmann scalars for AdS_d and S^n respectively

$$\mathcal{K}_1 = \frac{2}{d(d-1)}R_1^2, \quad \mathcal{K}_2 = \frac{2}{n(n-1)}R_2^2. \quad (2.18)$$

3. Regular and singular asymptotic of the solutions

In the rest of this paper we parametrize the value of the cosmological constant as

$$\Lambda = -\frac{1}{\ell^2}(d+n)(d+n-1). \quad (3.1)$$

The gravitational equations demand a constant negative curvature Einstein manifold and read

$$(d\dot{A}_1 + n\dot{A}_2)^2 - d\dot{A}_1^2 - n\dot{A}_2^2 - e^{-2A_1}R_1 - e^{-2A_2}R_2 = \frac{1}{\ell^2}(d+n)(d+n-1), \quad (3.2)$$

$$(d+n-1)(d\ddot{A}_1 + n\ddot{A}_2) + dn(\dot{A}_1 - \dot{A}_2)^2 + e^{-2A_1}R_1 + e^{-2A_2}R_2 = 0, \quad (3.3)$$

$$\ddot{A}_1 + \dot{A}_1(d\dot{A}_1 + n\dot{A}_2) - \frac{1}{d}e^{-2A_1}R_1 = \ddot{A}_2 + \dot{A}_2(d\dot{A}_1 + n\dot{A}_2) - \frac{1}{n}e^{-2A_2}R_2. \quad (3.4)$$

In this section, we find the expansions of the AdS_d and S^n scale factors (A_1 and A_2) near the AdS (UV) boundary, the end-points, and the A-bounces⁹. Using these expansions we can search and classify various regular and singular bulk solutions and extract the values of sources and vevs of the dual boundary CFTs.

⁹A-bounces are points where any scale factor A changes direction, i.e. $\dot{A} = 0$.

3.1 Near-boundary expansions

The Fefferman-Graham expansion of the (2.13) metric near a UV boundary, which can be reached either as $u \rightarrow +\infty$ or at $u \rightarrow -\infty$, is

$$\begin{aligned} ds^2 &= du^2 + e^{\pm \frac{2u}{\ell}} (ds_{QFT}^2 + \dots) \\ &= du^2 + e^{\pm \frac{2u}{\ell}} \left[e^{2\bar{A}_1} \zeta_{\alpha\beta}^1 dx^\alpha dx^\beta + e^{2\bar{A}_2} \zeta_{\mu\nu}^2 dx^\mu dx^\nu \right] + \text{sub-leading}, \end{aligned} \quad (3.5)$$

where \bar{A}_1, \bar{A}_2 are arbitrary constants. Therefore, the holographic CFT will be living on a boundary with geometry $AdS_d \times S^n$, with metric given by the square bracket in equation (3.5) and with the corresponding curvatures given by

$$R_1^{UV} = e^{-2\bar{A}_1} R_1, \quad R_2^{UV} = e^{-2\bar{A}_2} R_2. \quad (3.6)$$

In the expression above, R_1 and R_2 are the scalar curvatures of the metrics ζ_1 and ζ_2 of AdS_d and S^n , respectively. We parametrize them by introducing the corresponding curvature radii

$$R_1 = -\frac{d(d-1)}{\alpha_1^2}, \quad R_2 = \frac{n(n-1)}{\alpha_2^2}, \quad (3.7)$$

where α_1 and α_2 are the associated radii of the AdS and S spaces.

As equations (3.2)–(3.4) show, we have two second-order equations plus one first-order constraint for the two scale factors $A_1(u)$ and $A_2(u)$. This system has three integration constants. Two of them are shifts of \bar{A}_1 and \bar{A}_2 which can be fixed by demanding that R_1 and R_2 coincide with the actual curvatures of the manifold on which the UV boundary theory is defined according to the holographic dictionary, i.e. the relations in (3.6).

The last integration constant enters at sub-leading order in the asymptotic (UV) expansion in (3.5), and therefore it corresponds to a vacuum expectation value. Since in our model, the only non-trivial bulk field is the metric, it must correspond to parts of the vev of the components of the stress tensor. As we have shown in appendix D for the specific cases of $d = n = 2$, this constant, called C , appears in the expectation values of the stress-energy tensor of both AdS_2 and S^2 , as seen in equations (D.9a) and (D.9b).

The value of the third constant will be fixed once we impose the regularity in the interior. Since the dual CFT is conformally invariant, the physics depends only on the ratio of the curvature scales of AdS_d and S^n which is the only dimensionless source parameter of our problem.

Solving the equations of motion (3.2)–(3.4), near the putative boundary either at $u \rightarrow +\infty$ or $u \rightarrow -\infty$ gives expansions for scale factors of AdS_d and S^n spaces. For $d = n = 4$ we find the following expansions,¹⁰

¹⁰The formulae can be generalized to arbitrary d, n .

$$\begin{aligned}
A_1(u) = & \bar{A}_1 \pm \frac{u}{\ell} - \frac{1}{2^4 3^1 7^1} (5\mathcal{R}_1 - 2\mathcal{R}_2) e^{\mp \frac{2u}{\ell}} - \frac{1}{2^9 3^2 7^2} (46\mathcal{R}_1^2 - 20\mathcal{R}_1\mathcal{R}_2 - 17\mathcal{R}_2^2) e^{\mp \frac{4u}{\ell}} \\
& - \left(\frac{1}{2^{12} 3^4 7^3} (356\mathcal{R}_1^3 - 66\mathcal{R}_1^2\mathcal{R}_2 - 171\mathcal{R}_1\mathcal{R}_2^2 - 92\mathcal{R}_2^3) \right) e^{\mp \frac{6u}{\ell}} \\
& - \left(\frac{1}{2^{19} 3^4 7^4} (2111\mathcal{R}_1^4 - 1160\mathcal{R}_1^3\mathcal{R}_2 - 1740\mathcal{R}_1^2\mathcal{R}_2^2 - 1160\mathcal{R}_1\mathcal{R}_2^3 + 2111\mathcal{R}_2^4) + C \right) e^{\mp \frac{8u}{\ell}} \\
& \pm \frac{1}{2^{16} 3^3 7^3} (23\mathcal{R}_1^4 - 52\mathcal{R}_1^3\mathcal{R}_2 + 52\mathcal{R}_1\mathcal{R}_2^3 - 23\mathcal{R}_2^4) \frac{u}{\ell} e^{\mp \frac{8u}{\ell}} + \mathcal{O}(e^{\mp \frac{10u}{\ell}}), \tag{3.8a}
\end{aligned}$$

$$\begin{aligned}
A_2(u) = & \bar{A}_2 \pm \frac{u}{\ell} + \frac{1}{2^4 3^1 7^1} (2\mathcal{R}_1 - 5\mathcal{R}_2) e^{\mp \frac{2u}{\ell}} + \frac{1}{2^9 3^2 7^2} (17\mathcal{R}_1^2 + 20\mathcal{R}_1\mathcal{R}_2 - 46\mathcal{R}_2^2) e^{\mp \frac{4u}{\ell}} \\
& + \left(\frac{1}{2^{12} 3^4 7^3} (92\mathcal{R}_1^3 + 171\mathcal{R}_1^2\mathcal{R}_2 + 66\mathcal{R}_1\mathcal{R}_2^2 - 365\mathcal{R}_2^3) \right) e^{\mp \frac{6u}{\ell}} \\
& - \left(\frac{1}{2^{19} 3^4 7^4} (2111\mathcal{R}_1^4 - 1160\mathcal{R}_1^3\mathcal{R}_2 - 1740\mathcal{R}_1^2\mathcal{R}_2^2 - 1160\mathcal{R}_1\mathcal{R}_2^3 + 2111\mathcal{R}_2^4) - C \right) e^{\mp \frac{8u}{\ell}} \\
& \mp \frac{1}{2^{16} 3^3 7^3} (23\mathcal{R}_1^4 - 52\mathcal{R}_1^3\mathcal{R}_2 + 52\mathcal{R}_1\mathcal{R}_2^3 - 23\mathcal{R}_2^4) \frac{u}{\ell} e^{\mp \frac{8u}{\ell}} + \mathcal{O}(e^{\mp \frac{10u}{\ell}}). \tag{3.8b}
\end{aligned}$$

Here \mathcal{R}_1 and \mathcal{R}_2 are dimensionless curvature parameters, defined as

$$\mathcal{R}_1 \equiv \ell^2 R_1 e^{-2\bar{A}_1} = \ell^2 R_1^{UV} \quad , \quad \mathcal{R}_2 \equiv \ell^2 R_2 e^{-2\bar{A}_2} = \ell^2 R_2^{UV} . \tag{3.9}$$

The constant C that appeared in the above equations is proportional to the vev of the stress-energy tensor of the boundary CFT that we already discussed above, see also appendix D for more details. A similar argument can be found in [15] for holographic CFTs on $S^2 \times S^2$.

We also note that the coefficients of $\frac{u}{\ell} e^{\mp \frac{8u}{\ell}}$ in (3.8a) and (3.8b) reflect the conformal anomaly in $d+n=8$ dimensions. To see more details in $d+n=4$ see appendix D or [63, 64].

3.2 Regular and singular end-points

We now study the geometry close to an (IR) end-point, i.e. a point $u = u_0$ where one or both scale factors of the AdS and S shrink to zero. At this point, the u direction terminates¹¹. Such an end-point may be regular, or it may be a curvature singularity. In the latter case, from the point of view of holography, the associated solution has to be rejected.

Given such an endpoint, we now work out an expansion of the solution near it and compute the Kretschmann scalar. This will determine if this end-point is regular or singular.

¹¹If it is the AdS_d scale factor that shrinks to zero, and the AdS has Minkowski signature, this point is a horizon, [12]. However, as we shall see, this kind of end-point is always singular.

To solve equations of motion near $u = u_0$ ($u \rightarrow u_0^+$), we consider the following expansions for scale factors¹²

$$A_1(u) = \lambda_1 \log \frac{u - u_0}{\ell} + \frac{1}{2} \log a_0 + a_1 \frac{u - u_0}{\ell} + a_2 \frac{(u - u_0)^2}{\ell^2} + \mathcal{O}(u - u_0)^3, \quad (3.10a)$$

$$A_2(u) = \lambda_2 \log \frac{u - u_0}{\ell} + \frac{1}{2} \log s_0 + s_1 \frac{u - u_0}{\ell} + s_2 \frac{(u - u_0)^2}{\ell^2} + \mathcal{O}(u - u_0)^3. \quad (3.10b)$$

The constants appearing in the above expansions determine the behavior (regularity or singularity) of the end-point at $u = u_0$.

Inserting the first two leading terms in the above expansions into the equations of motion (3.2)–(3.4) we obtain

$$\frac{(d+n-1)(d+n)}{\ell^2} + \frac{\frac{r_1}{\ell^2}}{(u-u_0)^{2\lambda_1}} + \frac{\frac{r_2}{\ell^2}}{(u-u_0)^{2\lambda_2}} - \frac{(d\lambda_1 + n\lambda_2)^2 - d\lambda_1^2 - n\lambda_2^2}{(u-u_0)^2} + \dots = 0, \quad (3.11)$$

$$dn(\lambda_1 - \lambda_2)^2 - (d+n-1)(d\lambda_1 + \lambda_2 n) + \frac{\frac{r_1}{\ell^2}}{(u-u_0)^{2\lambda_1-2}} + \frac{\frac{r_2}{\ell^2}}{(u-u_0)^{2\lambda_2-2}} + \dots = 0, \quad (3.12)$$

$$\frac{n\frac{r_1}{\ell^2}}{(u-u_0)^{2\lambda_1-2}} - \frac{d\frac{r_2}{\ell^2}}{(u-u_0)^{2\lambda_2-2}} + dn(\lambda_2 - \lambda_1)(d\lambda_1 + n\lambda_2 - 1) + \dots = 0, \quad (3.13)$$

where we have defined

$$r_1 \equiv \frac{\ell^2 R_1}{a_0}, \quad r_2 \equiv \frac{\ell^2 R_2}{s_0}. \quad (3.14)$$

By an exhaustive analysis of the above equations for various regions of λ_1 and λ_2 , we find the following possibilities for λ_1 and λ_2 :

- Singular end-point: ($1 > \lambda_1 > 0$ and $0 > \lambda_2 > -1$) or ($0 > \lambda_1 > -1$ and $1 > \lambda_2 > 0$).
- Regular end-point (sphere shrinking): $\lambda_1 = 0, \lambda_2 = 1$. For other values of λ_1 and λ_2 , for example, $\lambda_1 > 1$ or $\lambda_2 > 1$ or both, or for example when $\lambda_1 = 1, \lambda_2 = 0$ where the *AdS* is shrinking to zero sizes, we find no solution for equations (3.11)–(3.13).

When solving equations (3.11)–(3.13), the values of λ_1 and λ_2 are fixed. Moreover, we find a_0 and s_0 (and u_0) as free parameters and

$$a_1 = s_1 = 0, \quad (3.15a)$$

$$a_2 = \frac{(d+n)(d(2\lambda_1 - 2\lambda_2 - 1) - n + 1)}{4d(\lambda_1 - \lambda_2)(2d\lambda_1 + 2n\lambda_2 + 1)}, \quad (3.15b)$$

$$s_2 = \frac{(d+n)(n(2\lambda_1 - 2\lambda_2 + 1) + d - 1)}{4n(\lambda_1 - \lambda_2)(2d\lambda_1 + 2n\lambda_2 + 1)}, \quad (3.15c)$$

and all higher coefficients of the expansion can be similarly determined.

¹²A power-law leading behavior, $A_1 = \kappa_1(u - u_0)^a + \dots$ and $A_2 = \kappa_2(u - u_0)^b + \dots$ in which $a, b < 0$ cannot solve Einstein's equations near $u = u_0$, as one can show along the lines of [15]. Other non-power-law behaviors do not produce solutions.

3.2.1 Singular end-points

We may have solutions that one of the scale factors shrinks but the other one blows up when $u \rightarrow u_0^+$. Here we find only two possible cases:

- $1 > \lambda_1 > 0$, $0 > \lambda_2 > -1$:

In this case, the AdS_d scale factor vanishes and the S^n scale factor diverges. We have named this asymptotic A_0S_∞ . We obtain

$$\lambda_1 = \frac{\sqrt{dn(d+n-1)} + d}{d(d+n)} > 0 \quad , \quad \lambda_2 = \frac{n - \sqrt{dn(d+n-1)}}{n(d+n)} < 0. \quad (3.16)$$

- $1 > \lambda_2 > 0$, $0 > \lambda_1 > -1$:

In this class of solutions, the AdS_d size is growing and the S^n size is shrinking. We have named this asymptotic $A_\infty S_0$. We have the following solution

$$\lambda_1 = \frac{d - \sqrt{dn(d+n-1)}}{d(d+n)} \quad , \quad \lambda_2 = \frac{n + \sqrt{dn(d+n-1)}}{n(d+n)}. \quad (3.17)$$

For both cases above, the Kretschmann scalar is singular as $u \rightarrow u_0$

$$\begin{aligned} \mathcal{K} = & -\frac{4\lambda_1^2 r_1}{\ell^4} \left(\frac{u - u_0}{\ell} \right)^{-2\lambda_1 - 2} - \frac{4\lambda_2^2 r_2}{\ell^4} \left(\frac{u - u_0}{\ell} \right)^{-2\lambda_2 - 2} \\ & + \mathcal{O}\left(\frac{u - u_0}{\ell} \right)^{-4\lambda_1} + \mathcal{O}\left(\frac{u - u_0}{\ell} \right)^{-4\lambda_2}. \end{aligned} \quad (3.18)$$

3.2.2 Regular end-points

Consider the case when the scale factor of S^n shrinks to zero sizes as $u \rightarrow u_0^+$, but the AdS_d has a finite size at this point, corresponding to $(\lambda_1 = 0, \lambda_2 = 1)$. The position u_0 is arbitrary, as it can be changed by a shift in u (which however may change the value of the near-boundary parameters).

Solving the equations of motion using the expansion (3.10a) and (3.10b), we find the following expansions for the scale factors ($\lambda_1 = 0, \lambda_2 = 1$)

$$\begin{aligned} e^{2A_1(u)} = & a_0 + \frac{a_0 d(d+n) + \ell^2 R_1}{d\ell^2(1+n)} (u - u_0)^2 \\ & - \frac{(a_0 d(d+n) + \ell^2 R_1)(a_0 d(d-n-4)(d+n) + (d-3)\ell^2 R_1)}{3a_0 d^2 \ell^4 (1+n)^2 (3+n)} (u - u_0)^4 \\ & + \mathcal{O}(u - u_0)^6, \end{aligned} \quad (3.19a)$$

$$\begin{aligned} e^{2A_2(u)} = & \frac{R_2}{n(n-1)} (u - u_0)^2 + \frac{(a_0(d-d^2+n+n^2) - \ell^2 R_1)R_2}{3a_0 \ell^2 n^2 (n^2 - 1)} (u - u_0)^4 \\ & + \mathcal{O}(u - u_0)^6, \end{aligned} \quad (3.19b)$$

which is valid for all values of $d, n > 1$. The quantity a_0 is a non-zero positive (but otherwise arbitrary) constant.

Computing the Kretschmann scalar (2.17) at $u = u_0$ we shows that

$$\mathcal{K} = \frac{2(d+n)^2}{\ell^4 n(n+1)} \left[(d-2)d + (n+1)^2 + \frac{(d+n-1)(2\bar{a}_0(d-1)d+1)}{\bar{a}_0^2(d-1)d(d+n)} \right] + \mathcal{O}(u - u_0), \quad (3.20)$$

where

$$\bar{a}_0 \equiv \frac{a_0}{\ell^2 R_1}. \quad (3.21)$$

Equation (3.20) implies that at this end-point the geometry is regular. For comparison, the Kretschmann scalar of an AdS_{d+n+1} space with length scale ℓ is constant everywhere and is given by

$$\mathcal{K}_{AdS} = \frac{2(d+n)(d+n+1)}{\ell^4}. \quad (3.22)$$

We obtain

$$\mathcal{K} - \mathcal{K}_{AdS} = \frac{2(d+n)(d+n-1)}{\ell^4 \bar{a}_0^2 d(d-1)n(n+1)} (d(d-1)\bar{a}_0 + 1)^2 + \mathcal{O}(u - u_0), \quad (3.23)$$

which suggests that at $\bar{a}_0 = -\frac{1}{d(d-1)}$ we obtain AdS_{n+d+1} . We shall verify this in section 4.

This class of solutions has only two arbitrary parameters, a_0, u_0 , and is, therefore, a ‘‘tuned’’ solution as we implemented regularity.

We should note that at this regular end-point, we always have

$$\dot{A}_1 \sim (u - u_0) \quad , \quad \dot{A}_2 \sim \frac{1}{u - u_0}, \quad (3.24)$$

and

$$\begin{cases} \ddot{A}_1 \geq 0, & a_0 \geq -\frac{\ell^2 R_1}{d(d+n)}, \\ \ddot{A}_1 < 0, & \text{otherwise.} \end{cases} \quad (3.25)$$

When $\ddot{A}_1 < 0$ it might be expected that the AdS space shrinks to zero at some point $u > u_0$. We shall find such solutions in the next sections.

On the other hand, we may also consider that AdS_d shrinks to zero sizes while the size of S^n is finite. This corresponds to $\lambda_1 = 1, \lambda_2 = 0$ in the expansions (3.10a) and (3.10b), and from them, the expansions of the scale factors can be written as

$$e^{2A_1(u)} = a_2 \frac{(u - u_0)^2}{\ell^2} + \mathcal{O}(u - u_0)^3 \quad , \quad e^{2A_2(u)} = s_0 + 2s_0 s_1 \frac{u - u_0}{\ell} + \mathcal{O}(u - u_0)^2, \quad (3.26)$$

which by inserting into the equations of motion we find that

$$a_2 = \frac{R_1}{d(d-1)} < 0. \quad (3.27)$$

With our initial signature, $e^{A_1} > 0$, and therefore this case is not possible. *We can not have a solution that the AdS scale factor vanishes while the sphere scale is finite.*

3.3 Solutions with A-bounces and monotonic solutions

Except for the shrinking of AdS_d and S^n factors, we can also have places where $\dot{A}_{1,2} = 0$ and then the evolution of scale factors is not monotonic. We call points where $\dot{A}_{1,2} = 0$ ‘‘A-bounces’’. We shall investigate such a regime in this section.

Consider the case in which the arbitrary point $u = u_0$ is an A-bounce. In general, the expansions of the scale factors around such a point (that is a regular point of the equations) can be written as ¹³

$$A_1(u) = \frac{1}{2} \log \hat{a}_0 + \hat{a}_1 \frac{u - u_0}{\ell} + \hat{a}_2 \frac{(u - u_0)^2}{\ell^2} + \mathcal{O}(u - u_0)^3, \quad (3.28a)$$

$$A_2(u) = \frac{1}{2} \log \hat{s}_0 + \hat{s}_1 \frac{u - u_0}{\ell} + \hat{s}_2 \frac{(u - u_0)^2}{\ell^2} + \mathcal{O}(u - u_0)^3. \quad (3.28b)$$

From equations of motion (3.2)–(3.4) we know that all unknown coefficients above can be written as functions of three arbitrary constants. We choose these constants to be \hat{a}_0, \hat{s}_0 and \hat{s}_1 . From the equations, we obtain

$$\hat{a}_1 = \frac{-nd\hat{a}_0\hat{s}_0\hat{s}_1 \pm \chi}{d(d-1)\hat{a}_0\hat{s}_0}, \quad (3.29a)$$

$$\begin{aligned} \hat{a}_2 = & \frac{-(d(n(d+n)\hat{s}_0 + \ell^2 R_2)\hat{a}_0 + \ell^2 R_1\hat{s}_0)}{2(d-1)d\hat{a}_0\hat{s}_0} \\ & + \frac{dn(1-d-2n)\hat{a}_0\hat{s}_0\hat{s}_1^2 \pm (d+1)n\hat{s}_1\chi}{2\hat{a}_0(d-1)^2 d\hat{s}_0}, \end{aligned} \quad (3.29b)$$

$$\hat{s}_2 = \frac{(d-1)\hat{a}_0(n(d+n)\hat{s}_0 + \ell^2 R_2) + n^2\hat{a}_0\hat{s}_0\hat{s}_1^2 \mp n\hat{s}_1\chi}{2(d-1)n\hat{a}_0\hat{s}_0}, \quad (3.29c)$$

where

$$\begin{aligned} \chi \equiv & \left(d\hat{a}_0\hat{s}_0[(d-1)((d+n-1)(d+n)\hat{a}_0\hat{s}_0 + \ell^2(\hat{a}_0 R_2 + \hat{s}_0 R_1)) \right. \\ & \left. + n(d+n-1)\hat{a}_0\hat{s}_0\hat{s}_1^2] \right)^{\frac{1}{2}}. \end{aligned} \quad (3.30)$$

The reality of (3.30) restricts the parameters to

$$|\hat{s}_1| \geq \sqrt{-\frac{(d-1)((d+n)(d+n-1)\hat{a}_0\hat{s}_0 + \ell^2 R_2\hat{a}_0 + \ell^2 R_1\hat{s}_0)}{n(d+n-1)\hat{a}_0\hat{s}_0}}, \quad (3.31a)$$

$$R_1 + \frac{\hat{a}_0(\ell^2 R_2 + (d+n)^2 \hat{s}_0)}{\ell^2 \hat{s}_0} < \frac{\hat{a}_0(d+n)}{\ell^2}. \quad (3.31b)$$

According to the above expansions, we can divide the solutions of Einstein’s equations into two sets of solutions:

¹³These expansions are the expansion in (3.10a) and (3.10b) for $\lambda_1 = \lambda_2 = 0$. The constant parameters are denoted by a hat to distinguish them from the end-point parameters.

- Solutions with A-bounce: There is at least one point where either \hat{a}_1 or \hat{s}_1 or both are zero
- Monotonic solutions: There is no point where \hat{a}_1 or \hat{s}_1 are zero.

As we already mentioned, we may have solutions that one or both of the scale factors have an A -bounce. At this point, the scale factor reaches a non-zero minimum or a finite maximum. Similar bounces were found in flat RG flows in [26], in which what changed direction (bounced) was the scalar field. Scale factor bounces, or A -bounces in short, were instead found to be ubiquitous in curved RG-flows with AdS slices, [32, 10, 44].

In the subsequent sections, we shall study the properties of the solutions with A -bounces. A subset of monotonic solutions was studied in section 3.2.2. Other monotonic solutions will be studied numerically in section 5.5.

3.3.1 AdS_d bounce

Consider the case when the scale factor of AdS_d displays a bounce at some radial position $u = u_0$. We call this an A_1 -bounce ($\dot{A}_1 = 0, \dot{A}_2 \neq 0$). This corresponds to consider $\hat{a}_1 = 0$ in (3.28a), i.e.

$$A_1(u) = \frac{1}{2} \log(\hat{a}_0) + \hat{a}_2 \frac{(u - u_0)^2}{\ell^2} + \mathcal{O}((u - u_0)^3), \quad (3.32a)$$

$$A_2(u) = \frac{1}{2} \log(\hat{s}_0) + \hat{s}_1 \frac{(u - u_0)}{\ell} + \hat{s}_2 \frac{(u - u_0)^2}{\ell^2} + \mathcal{O}((u - u_0)^3), \quad (3.32b)$$

where \hat{a}_0 and \hat{s}_0 are the sizes of AdS and the sphere at the bounce. Moreover, one finds

$$\hat{s}_1 = \pm \frac{\sqrt{(d+n)(d+n-1) + (\hat{r}_1 + \hat{r}_2)}}{\sqrt{(n-1)n}}, \quad (3.33a)$$

$$\hat{s}_2 = -\frac{d^2n + dn^2 + (n\hat{r}_1 + \hat{r}_2)}{2(n-1)n}, \quad (3.33b)$$

$$\hat{a}_2 = \frac{d^2 + dn + \hat{r}_1}{2d}, \quad (3.33c)$$

and

$$\hat{r}_1 \equiv \frac{\ell^2 R_1}{\hat{a}_0} < 0 \quad , \quad \hat{r}_2 \equiv \frac{\ell^2 R_2}{\hat{s}_0} > 0. \quad (3.34)$$

The expansions (3.32a) and (3.32b) show the following properties for solutions of equations of motion with an A_1 -bounce:

- Since $R_1 < 0$, then

$$\begin{cases} \hat{a}_2 \geq 0, & \text{for } \hat{a}_0 \geq -\frac{\ell^2 R_1}{d(d+n)}, \\ \hat{a}_2 < 0, & \text{for } -\frac{\ell^2 R_1}{d(d+n)} > \hat{a}_0 > \hat{a}_0^{min}, \end{cases} \quad (3.35)$$

where the reality of the value of \hat{s}_1 in (3.33a) puts a lower bound on \hat{a}_0 for any positive value of \hat{s}_0

$$\hat{a}_0^{\min} = -\frac{\ell^2 R_1 \hat{s}_0}{\hat{s}_0(d+n)(d+n-1) + \ell^2 R_2}. \quad (3.36)$$

- $\hat{s}_1 \in \mathbb{R}$ also indicates that at A_1 -bounce always $\hat{s}_2 < 0$.
- At a specific value

$$\hat{a}_0 = a_0^c \equiv -\frac{\ell^2 R_1}{d(d+n)}, \quad (3.37)$$

the bounce disappears and we can find an exact solution

$$e^{2A_1(u)} = -\frac{\ell^2 R_1}{d(d+n)}, \quad (3.38a)$$

$$\begin{aligned} e^{2A_2(u)} &= \hat{s}_0 \left(\lambda_0 \sinh \left[k \frac{u-u_0}{\ell} \right] + \cosh \left[k \frac{u-u_0}{\ell} \right] \right)^2, \\ &= \hat{s}_0 (\lambda_0^2 - 1) \sinh^2 \left[k \frac{u-u_0}{\ell} - \frac{1}{2} \log \left(\frac{\lambda_0 - 1}{\lambda_0 + 1} \right) \right], \end{aligned} \quad (3.38b)$$

where

$$\lambda_0 = \sqrt{\frac{\ell^2 R_2}{(n-1)(d+n)\hat{s}_0} + 1}, \quad k = \sqrt{\frac{d}{n} + 1}. \quad (3.39)$$

This solution will be discussed in more detail in section 4.

- If we have two A-bounces, both for AdS_d and S^n at the same point $u = u_0$ (equivalently, when $\hat{s}_1 = 0$) then

$$\hat{a}_0 = a_0^b \equiv \frac{-\ell^2 R_1}{(d+n)(d+n-1)} > 0, \quad (3.40)$$

and

$$\hat{a}_2 = -\frac{1}{2} \left(\frac{\ell^2 R_2}{\hat{s}_0} + (d+n)(d+n-2) \right) < 0, \quad (3.41)$$

which implies that the AdS scale factor has a finite *maximum* at this point. As we shall see, the solutions with this property have two end-points where the AdS space shrinks to zero sizes.

To summarize, the space of solutions with an A_1 -bounce is parametrized by three free parameters \hat{a}_0 and \hat{s}_0 and u_0 which represent the size of AdS and sphere at the bounce as well as the position of the bounce. The analysis above shows that:

1) From equation (3.35) we deduce that the AdS scale factor has at most one A-bounce. To see this, consider two neighboring bounces that one of them is a local maximum ($\hat{a}_2 < 0$) and the other is a local minimum ($\hat{a}_2 > 0$). According to (3.35) the value of the AdS scale factor (\hat{a}_0) for the local minimum should be greater than

its local maximum neighbor, which is impossible, therefore we can not have more than one A_1 -bounce in a solution.

2) There is a lower bound (3.36) on \hat{a}_0 for an A_1 -bounce to exist. \hat{a}_0 controls the minimum size of AdS at the A_1 -bounce.

3) We have a special solution with a constant scale factor of AdS . This is an exact solution that will be discussed later in section 4.

4) If both AdS and the sphere have A-bounces at the same point, at this point, AdS has a finite maximum size but the sphere reaches a nonzero minimum.

3.3.2 S^n bounce

An alternative possibility occurs when S^n has a bounce (A_2 -bounce). This is the case with $\hat{s}_1 = 0$ in (3.28b). Then we obtain

$$A_1(u) = \frac{1}{2} \log(\hat{a}_0) + \hat{a}_1 \frac{(u - u_0)}{\ell} + \hat{a}_2 \frac{(u - u_0)^2}{\ell^2} + \mathcal{O}(u - u_0)^3, \quad (3.42a)$$

$$A_2(u) = \frac{1}{2} \log(\hat{s}_0) + \hat{s}_2 \frac{(u - u_0)^2}{\ell^2} + \mathcal{O}(u - u_0)^3, \quad (3.42b)$$

with the following values for the above coefficients

$$\hat{a}_1 = \pm \frac{\sqrt{(d+n)(d+n-1) + (\hat{r}_1 + \hat{r}_2)}}{\sqrt{(d-1)d}}, \quad (3.43a)$$

$$\hat{a}_2 = -\frac{d^2n + dn^2 + (d\hat{r}_2 + \hat{r}_1)}{2(d-1)d}, \quad (3.43b)$$

$$\hat{s}_2 = \frac{n^2 + dn + \hat{r}_2}{2n}. \quad (3.43c)$$

Here unlike the A_1 -bounce case, we always have $\hat{s}_2 > 0$, therefore, we do not expect to have a solution with two shrinking end-points for S^n . However, there is a constraint for the reality of \hat{a}_1 in equation (3.43a)

$$\begin{cases} \hat{a}_0 \leq a_0^b & \Rightarrow 0 < \hat{s}_0 \leq \frac{-\hat{a}_0 \ell^2 R_2}{\ell^2 R_1 + \hat{a}_0 (d+n)(d+n-1)}, \\ \hat{a}_0 > a_0^b & \Rightarrow 0 < \hat{s}_0, \end{cases} \quad (3.44)$$

where a_0^b is given in equation (3.40). Moreover, the reality of \hat{a}_1 in (3.43a) shows that $\hat{a}_2 < 0$ at the A_2 -bounce.

To summarize:

1) Since at an A_2 -bounce we always have a minimum size for the sphere scale factor ($\hat{s}_2 > 0$) we can not have a solution with more than one A_2 -bounce.

2) If there is an A_2 -bounce, we do not expect to find a solution that has two end-points with a shrinking sphere.

3) According to (3.44) in the space of solutions described by the two parameters (\hat{a}_0, \hat{s}_0) , there is an upper bound on the size of the sphere at the bounce, as far as $\hat{a}_0 \leq a_0^b$.

4. Exact solutions

In this section, we shall find some exact solutions for the equations of motion (3.2)–(3.4). There are several special cases in which we can solve equations of motion exactly. The expansions in (3.19a) and (3.19b) also can help us to find these solutions.

- **$AdS_d \times AdS_{n+1}$ (product space) solution**

As we can observe from equation (3.19a), in the special case where

$$a_0 = a_0^c = -\frac{\ell^2 R_1}{d(d+n)}, \quad (4.1)$$

the scale factor of AdS_d is fixed and is independent of the u coordinate. In this situation, the equations of motion are exactly solvable and we find for $n > 1$

$$e^{2A_1(u)} = -\frac{\ell^2 R_1}{d(d+n)}, \quad e^{2A_2(u)} = \left(ce^{\sqrt{\frac{d+n}{n}} \frac{u}{\ell}} - \frac{\ell^2 R_2}{4c(n-1)(d+n)} e^{-\sqrt{\frac{d+n}{n}} \frac{u}{\ell}} \right)^2, \quad (4.2)$$

where c is the constant of integration. This solution in general has an end-point for the sphere at

$$u_0 = -\frac{1}{2}\ell \sqrt{\frac{n}{d+n}} \log \left(\frac{4c^2(n-1)(d+n)}{\ell^2 R_2} \right). \quad (4.3)$$

Therefore, we can rewrite the scale factors as

$$e^{2A_1(u)} = -\frac{\ell^2 R_1}{d(d+n)}, \quad e^{2A_2(u)} = \frac{\ell^2 R_2}{(n-1)(d+n)} \sinh^2 \left(\sqrt{\frac{d+n}{n}} \frac{u - u_0}{\ell} \right), \quad (4.4)$$

which means that the metric describes a product space $AdS_d \times AdS_{n+1}$.

The Kretschmann scalar for this solution is a constant

$$\mathcal{K} = \frac{2(d+n)^2(2dn + d - n - 1)}{n(d-1)\ell^4}, \quad (4.5)$$

and differs from the AdS_{d+n+1} value which is

$$\mathcal{K} = \frac{2(d+n)(d+n+1)}{\ell^4}. \quad (4.6)$$

We should remind the reader that we already encountered this solution when we studied the A_1 -bounces, where at the critical value of a_0^c , the AdS bounce disappeared and we found a similar exact solution in (3.38b). In appendix E we have considered the fluctuations around this solution to show that the asymptotic behavior changes completely near the boundary of this solution. In particular, the boundary of this solution (in Euclidean signature) has two components: $AdS_d \times S^n \cup S^{d-1} \times AdS_{n+1}$.

- **Global AdS_{d+n+1} solution**

Another exact solution for equations of motion is the global AdS solution

$$ds^2 = du^2 + e^{2\bar{A}_1} \cosh^2 \frac{u - u_0}{\ell} ds_{AdS_d}^2 + e^{2\bar{A}_2} \sinh^2 \frac{u - u_0}{\ell} d\Omega_n^2, \quad (4.7)$$

where equations of motion fix the coefficients to

$$e^{2\bar{A}_1} = -\frac{\ell^2 R_1}{d(d-1)}, \quad e^{2\bar{A}_2} = \frac{\ell^2 R_2}{n(n-1)}. \quad (4.8)$$

We obtain

$$\bar{a}_0 = -\frac{1}{d(d-1)}, \quad (4.9)$$

for this solution, verifying the claim below (3.23). We also obtain

$$R_1^{UV} = 4e^{-2\bar{A}_1} R_1 = -\frac{4d(d-1)}{\ell^2}, \quad R_2^{UV} = 4e^{-2\bar{A}_2} R_2 = \frac{4n(n-1)}{\ell^2}, \quad (4.10)$$

or the ratio of dimensionless curvatures are fixed by dimensions of AdS_d and S^n spaces

$$\frac{\mathcal{R}_1}{\mathcal{R}_2} = -\frac{d(d-1)}{n(n-1)}. \quad (4.11)$$

This can be confirmed also in the specific case of $d = n = 4$ which we have the UV expansions in (3.8a) and (3.8b). Here we realize that the global solution is equivalent to considering the vev $C = 0$ and $\mathcal{R}_1 = -\mathcal{R}_2 = -48$. For a discussion on AdS space in various coordinates including the ones discussed here, see appendix B.

5. Numerical solutions

We employ numerical techniques to uncover every potential solution to equations of motion and verify our analytical results obtained from the asymptotics. The independent equations we solve are (2.14) and (2.15) and they require three constants of integration.

We assume that at a generic point $u = u_0$, the following expansions of the scale factors satisfy the equations of motion

$$A_1(u) = \frac{1}{2} \log \hat{a}_0 + \hat{a}_1 \frac{u - u_0}{\ell} + \hat{a}_2 \frac{(u - u_0)^2}{\ell^2} + \mathcal{O}(u - u_0)^3, \quad (5.1a)$$

$$A_2(u) = \frac{1}{2} \log \hat{s}_0 + \hat{s}_1 \frac{u - u_0}{\ell} + \hat{s}_2 \frac{(u - u_0)^2}{\ell^2} + \mathcal{O}(u - u_0)^3. \quad (5.1b)$$

Among the constant coefficients in these expansions, we select \hat{a}_0 , \hat{s}_0 and \hat{s}_1 as our free parameters. Using the aforementioned expansions we can read the initial conditions required for solving the equations of motion on both sides of $u = u_0$. This approach will lead us to four classes of end-points for solutions:

- **B**: An *AdS*-like boundary¹⁴ where both sphere and *AdS* sizes diverge. The behavior of the scale factors close to this boundary is given in section 3.1.
- **R**: A regular end-point where the sphere shrinks to a zero size and the *AdS* scale factor asymptotes to a constant value. Properties of this end-point are discussed in section 3.2.2.
- **A**: This is a singular end-point where the sphere size diverges while the *AdS* size vanishes, as discussed in section 3.2.1.
- **S**: This is another singular end-point where the sphere size vanishes while the *AdS* size diverges, as discussed in section 3.2.1.

According to the above possible end-points, we find the following types of solutions. Each solution is characterized by its end-points:

- **(B, R)**-type: This is a regular class of solutions.
- **(R, A)**-type, **(S, B)**-type, **(A, B)**-type, **(A, A)**-type and **(S, A)**-type: These are all singular solutions.

In the subsequent sections, we show examples of the above solutions.

When S^n or AdS_d shrinks to zero size, this signals in Euclidean signature an endpoint of the flow. From our findings, a sphere can shrink to zero sizes, and the solution is regular there. But AdS_d cannot shrink to zero sizes and the solution to be regular at that point¹⁵.

5.1 Solutions with one regular end-point

Among the solutions that we have, two classes of solutions have a regular end-point **(R)**. The product space solution $AdS_d \times AdS_{n+1}$ also has a regular end-point. As we already showed in section 3.2.2, the regular end-point at an arbitrary value $u = u_0$ has the following expansions for scale factors

$$e^{2A_1(u)} = a_0 + \frac{a_0 d(d+n) + \ell^2 R_1}{d\ell^2(1+n)} \left((u-u_0)^2 - \frac{a_0 d(d-n-4)(d+n) + (d-3)\ell^2 R_1}{3a_0 d\ell^2(1+n)(3+n)} (u-u_0)^4 + \mathcal{O}(u-u_0)^6 \right), \quad (5.2a)$$

$$e^{2A_2(u)} = \frac{R_2}{n(n-1)} (u-u_0)^2 + \frac{(a_0(d-d^2+n+n^2) - \ell^2 R_1) R_2}{3a_0 \ell^2 n^2 (n^2-1)} (u-u_0)^4 + \mathcal{O}(u-u_0)^6. \quad (5.2b)$$

¹⁴In our solutions we have only one boundary which we consider to be located at $u = +\infty$.

¹⁵Unless the holographic direction is timelike.

Here we have a free parameter $a_0 = e^{2A_1(u_0)}$. Varying u_0 does not give more solutions as such a variation can be undone by a translation in u .

For a point at $u = u_0 + \epsilon$ with $\epsilon > 0$ the initial conditions required to numerically solve the equations of motion are

$$A_1(\epsilon) = \frac{1}{2} \log a_0 + \mathcal{O}(\epsilon^2) \quad , \quad \dot{A}_1(\epsilon) = \frac{a_0 d(d+n) + \ell^2 R_1}{a_0 d \ell^2 (1+n)} \epsilon + \mathcal{O}(\epsilon^3) \quad , \quad (5.3a)$$

$$A_2(\epsilon) = \frac{1}{2} \log \left(\frac{R_2}{n(n-1)} \epsilon^2 \right) + \mathcal{O}(\epsilon^2) \quad , \quad \dot{A}_2(\epsilon) = \frac{1}{\epsilon} + \mathcal{O}(\epsilon) \quad , \quad (5.3b)$$

where the higher order terms depend on a_0 . According to the value of the only parameter a_0 in this class, we find three different types of answers.¹⁶

- **(R, B)–type:** This is a solution that starts from a regular end-point at $u = u_0$ and asymptotes to an AdS boundary at $u \rightarrow +\infty$. At the end-point, the scale factor of the sphere is zero but the AdS space has a finite size. This solution exists as far as $a_0 > a_0^c$ where

$$a_0^c \equiv -\frac{\ell^2 R_1}{d(d+n)} \quad . \quad (5.4)$$

An example of this type is sketched in figure 1.

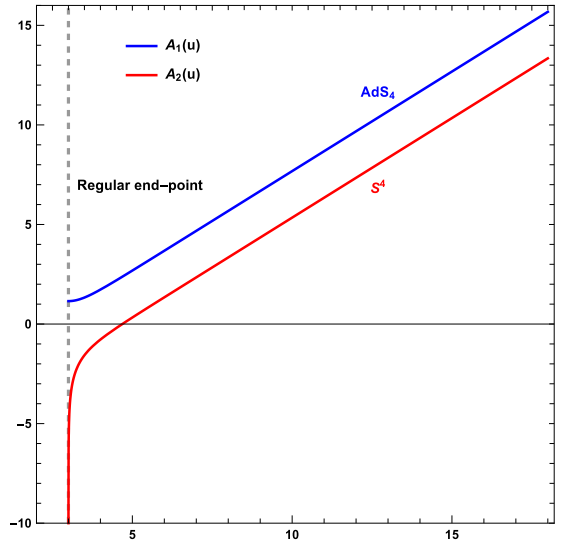


Figure 1: (R, B)–type: The scale factor for AdS (blue curve), and the scale factor of S (red curve), start at a regular end-point (dashed line). At this point, the sphere scale factor shrinks to a zero size but AdS has a finite non-zero size. Both scale factors reach the AdS boundary ($u \rightarrow +\infty$).

¹⁶In the rest of this paper, for the numerical solutions we fix $d = n = 4$, $R_1 = -1$, $R_2 = 2$, and $\ell = 1$.

- The product space solution: This is an $AdS_d \times AdS_{n+1}$ solution that we discussed in section 4. While the scale factor of AdS_d is fixed, the scale factor of $S^n \subset AdS_{n+1}$ starts from a zero value at the end-point and reaches the UV boundary at $u \rightarrow +\infty$. This is a single solution corresponding to choosing $a_0 = a_0^c$ from (5.4). Figure 2 shows this solution.

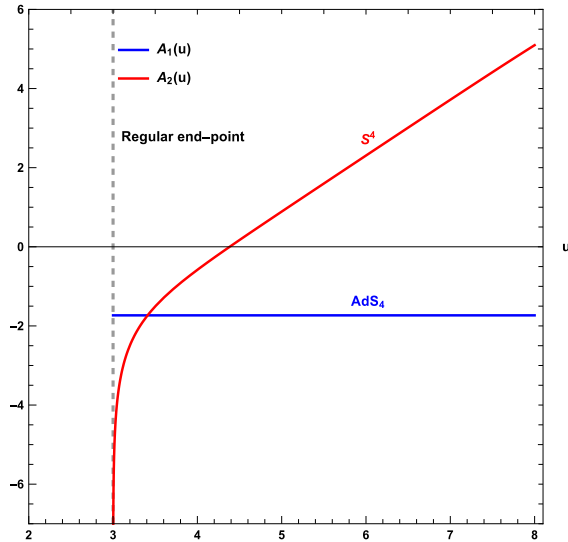


Figure 2: $AdS_d \times AdS_{n+1}$ solution.

- **(R, A)–type:** If we choose the value of a_0 such that according to (3.25) $\ddot{A}_1(u_0) < 0$, or equivalently if $a_0 < a_0^c$, then although we start from a regular end-point at $u = u_0$, the AdS scale factor decreases until it reaches zero at a finite $u > u_0$. At this point, we can check that the scale factors behave as

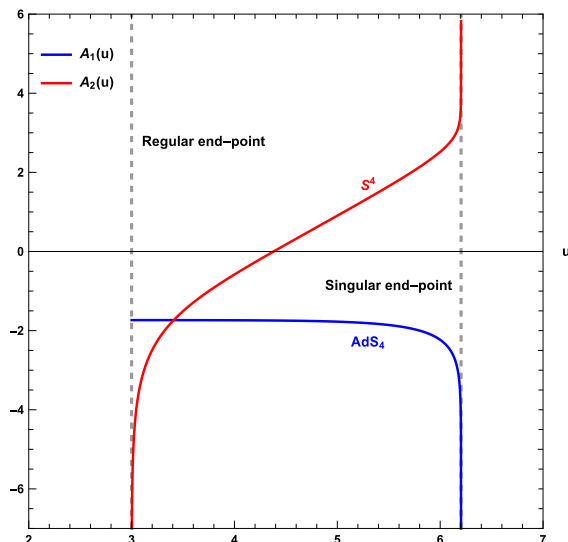


Figure 3: (R, A)–type: A singular solution that starts at a regular end-point (left dashed line) and reaches a singular end-point (right dashed line).

(3.10a) and (3.10b) with λ_1 and λ_2 coefficients in (3.16), so we have a singular end-point here. An example of this singular solution is given in figure 3.

At an arbitrary regular end-point u_0 , as we decrease the scale factor of AdS_d i.e. $a_0 = e^{2A_1(u_0)}$, we observe the transition between the above solutions. This is sketched in figure 4a. Figure 4b shows how the Kretschmann scalar changes for three different types of solutions. For (R, A)-type at the singular end-point, this scalar is diverging.

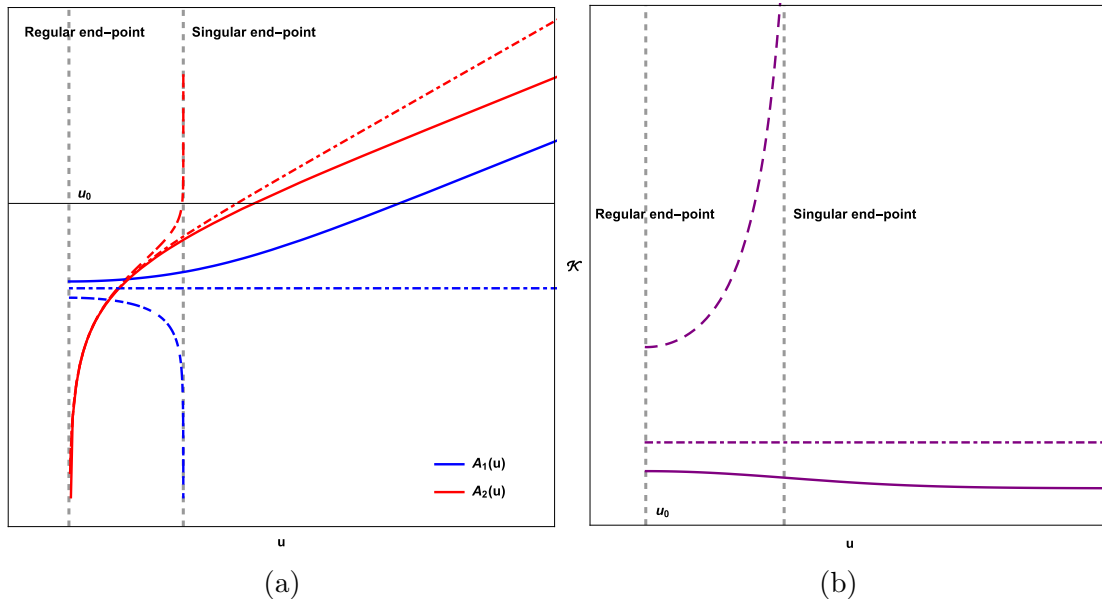


Figure 4: (a): Transition between solutions as we change the initial value of the AdS_d scalar factor, a_0 . The solid curves show an example of (R, B)-type. By decreasing a_0 and at a specific point $a_0 = a_0^c$ we have the $AdS_d \times AdS_{n+1}$ solution (dot-dashed curves). Below that point, all solutions are the (R, A)-type. (b): The Kretschmann scalar \mathcal{K} vs u . For all solutions in figure (a) we have sketched the Kretschmann scalar.

5.2 Solutions with A-bounces

If we assume that there is either an A_1 -bounce or A_2 -bounce at an arbitrary point $u = u_0$, we find three different types of singular solutions. We observe that the existence of an A-bounce is always accompanied by one or two singular end-points.

If we consider that at $u = u_0$ there is an A_1 -bounce then according to expansions of (3.32a) and (3.32b) the initial conditions to solve the equations of motion are

$$A_1(u_0) = \frac{1}{2} \log(\hat{a}_0) \quad , \quad \dot{A}_1(u_0) = 0 \quad , \quad A_2(u_0) = \frac{1}{2} \log(\hat{s}_0) \quad , \quad (5.5a)$$

$$\dot{A}_2(u_0) = \pm \frac{\sqrt{(d+n)(d+n-1) + \left(\frac{\ell^2 R_1}{\hat{a}_0} + \frac{\ell^2 R_2}{\hat{s}_0}\right)}}{\ell \sqrt{(n-1)n}} \quad . \quad (5.5b)$$

Here we find two types of solutions. A solution with just one A_1 -bounce and another solution with one A_1 -bounce and one A_2 -bounce:

(S, B)–type: Figure 5 shows a solution with an A_1 -bounce. On the left-hand side of the bounce, the solution has a singular end-point i.e. the sphere shrinks but the scale factor of AdS diverges. On the right-hand side, there is an AdS boundary at $u \rightarrow +\infty$. This solution corresponds to the plus sign in (5.5b). With the minus sign, we find the mirror image where the AdS boundary is at $u \rightarrow -\infty$.

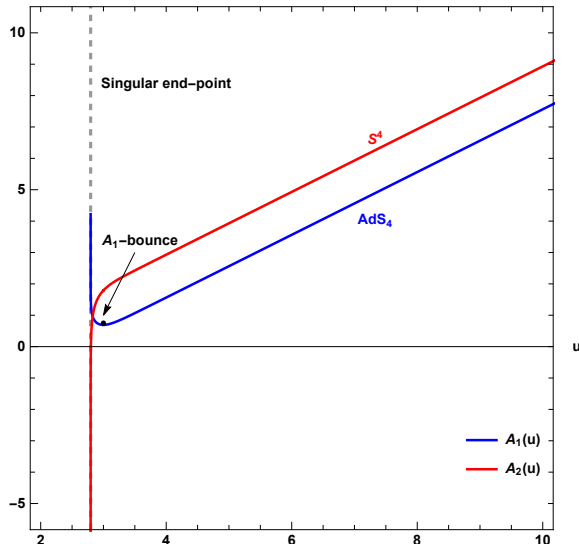


Figure 5: (S, B)–type: Left to the A_1 -bounce there is a singular IR end-point. Both scale factors reach the UV boundary at $u \rightarrow +\infty$.

(A, A)–type: There is another type of solution with one A_1 -bounces and one A_2 -bounce. Here the bounces are not necessarily at the same point in the u coordinate. Figure 6 shows a solution of this type. On both sides of these bounces the scale factor of the sphere is diverging but for AdS space it shrinks to zero and so on both sides, we have singular end-points.

We can consider that at $u = u_0$ there is an A_2 -bounce. Looking at the expansions (3.42a) and (3.42b) we can read the initial conditions required to solve the equations of motion

$$A_1(u_0) = \frac{1}{2} \log(\hat{a}_0) \quad , \quad A_2(u_0) = \frac{1}{2} \log(\hat{s}_0) \quad , \quad \dot{A}_2(u_0) = 0, \quad (5.6a)$$

$$\dot{A}_1(u_0) = \pm \frac{\sqrt{(d+n)(d+n-1) + \left(\frac{\ell^2 R_1}{\hat{a}_0} + \frac{\ell^2 R_2}{\hat{s}_0}\right)}}{\ell \sqrt{(d-1)d}}. \quad (5.6b)$$

Once again we may have solutions with just one A_2 -bounce or solutions with one A_2 -bounce and one A_1 -bounce which we already showed in figure 6.

(A, B)–type: Figure 7 shows an example of solutions with just one A_2 -bounce. On the left-hand side of the sphere bounce, the solution has a singular end-point

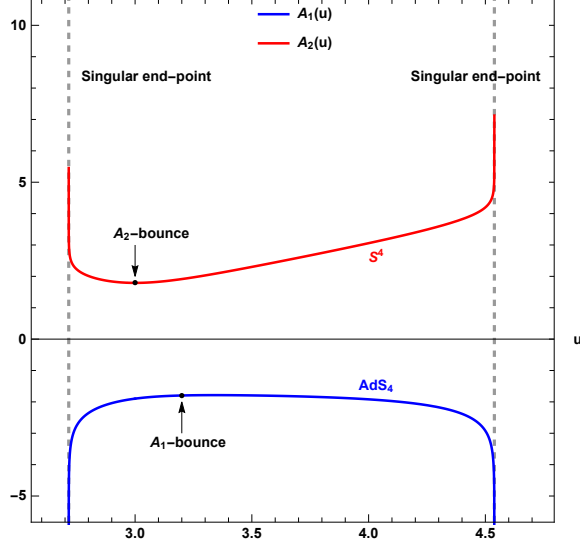


Figure 6: (A, A)–type: An example of solutions with two singular end-points. Both AdS and the sphere has a bounce.

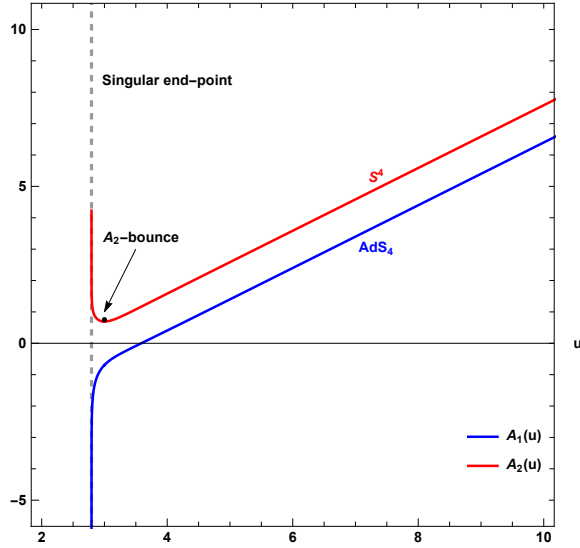


Figure 7: (A, B)–type: Left to the A_2 -bounce there is a singular end-point where the AdS scale factor is zero but sphere scale factor diverges. Both scale factors reach the AdS boundary at $u \rightarrow +\infty$.

where the scale factor of the sphere diverges but the AdS scale shrinks to zero. On the right-hand side, there is an AdS boundary as $u \rightarrow +\infty$. This solution corresponds to the plus sign in (5.6b) and its mirror image is given by the minus sign.

The behavior of the sphere scale factor that we observe in (A, B)–type and (A, A)–type is consistent with what we already found in section 3.3.2 where we show that at the A_2 -bounce always $\ddot{A}_2 > 0$ because $\hat{s}_2 > 0$ in (3.43c).

5.3 A_1 -bounce space of solutions

To see how the different solutions with A_1 -bounce change under the variation of the initial values at the bounce, we can draw the space of these solutions.

The initial conditions for solutions with an A_1 -bounce in (5.5a) and (5.5b) depend on two free parameters \hat{a}_0 and \hat{s}_0 . These two parameters describe the coordinates of the space of the solutions with an A_1 -bounce, see figure 8.

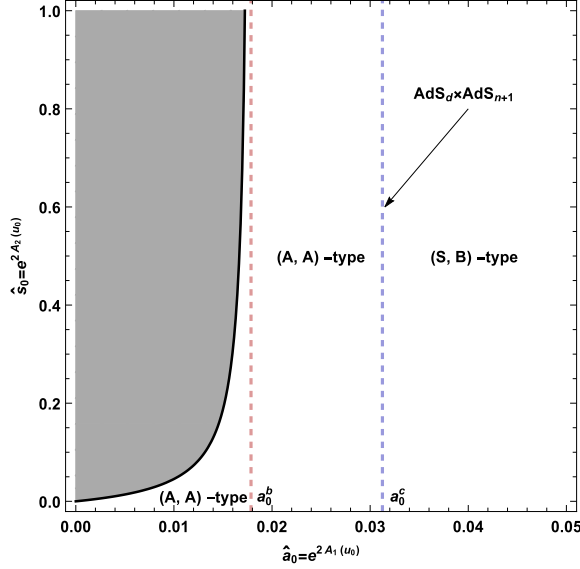


Figure 8: The A_1 -bounce space of solutions: The (S, B)-type solutions are living on $\hat{a}_0 > a_0^c$, the right-hand side of the blue dashed line. The (A, A)-type solutions are limited from right to the $a_0 = a_0^c$ and are bounded from left to the gray region. There is no solution in the gray region. Exactly on the blue dashed line we have the product space solutions. On the red dashed line, AdS_d and S^n have a bounce at the same point. Here again, the solutions are the (A, A)-type.

This space has the following properties:

1. For values $\hat{a}_0 > a_0^c$ where a_0^c is defined in (3.37), and for all the values of $\hat{s}_0 > 0$, only solutions of the (S, B)-type can exist.
2. In the place indicated by the blue dashed line at $\hat{a}_0 = a_0^c$ in figure 8, we have the product space solution.
3. Left to the blue dashed line and right to the gray region only the solutions of (A, A)-type can exist.
4. The boundary of the gray region is given by equation (3.36). Inside the gray region, there is no real solution for equations of motion.
5. The red dashed line at $\hat{a}_0 = a_0^b$, given in equation (3.40), shows the solutions that have two bounces for AdS_d and S^n at the same point $u = u_0$.

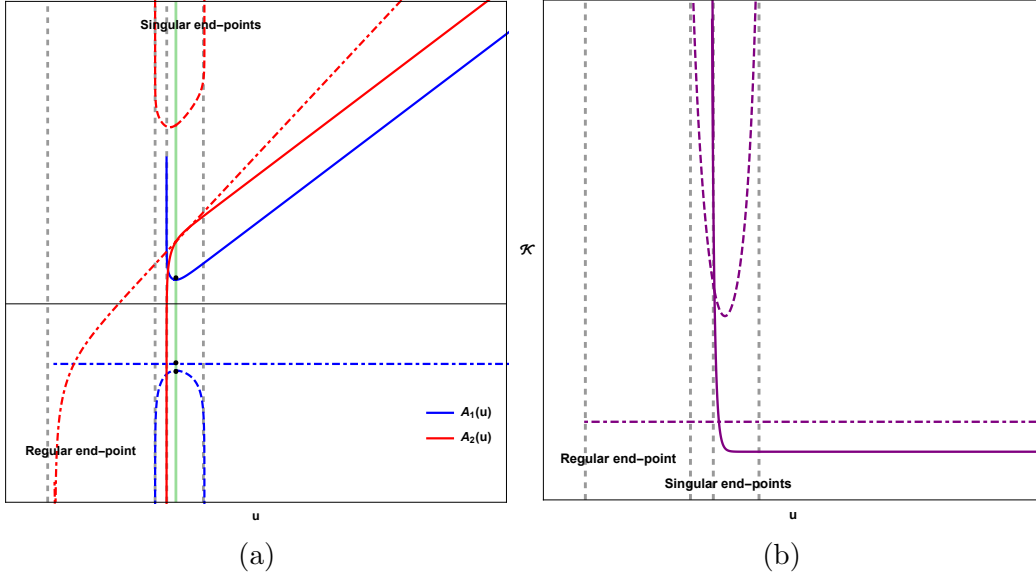


Figure 9: (a): At a fixed value of $\hat{s}_0 = e^{A_2(u_0)}$ (u_0 is the location of the green vertical line), and by decreasing the initial value of \hat{a}_0 (moving down on the green line) we first observe the solid curves which show an (S, B)-type solution. At a specific value $\hat{a}_0 = a_0^c$ a new solution (dot-dashed curves) will appear, This is a product space solution. Below a_0^c , the solutions (dashed curves) are the (A, A)-type ones. There is a lower bound for \hat{a}_0 given by (3.36). (b): The Kretschmann scalar for solutions in figure (a).

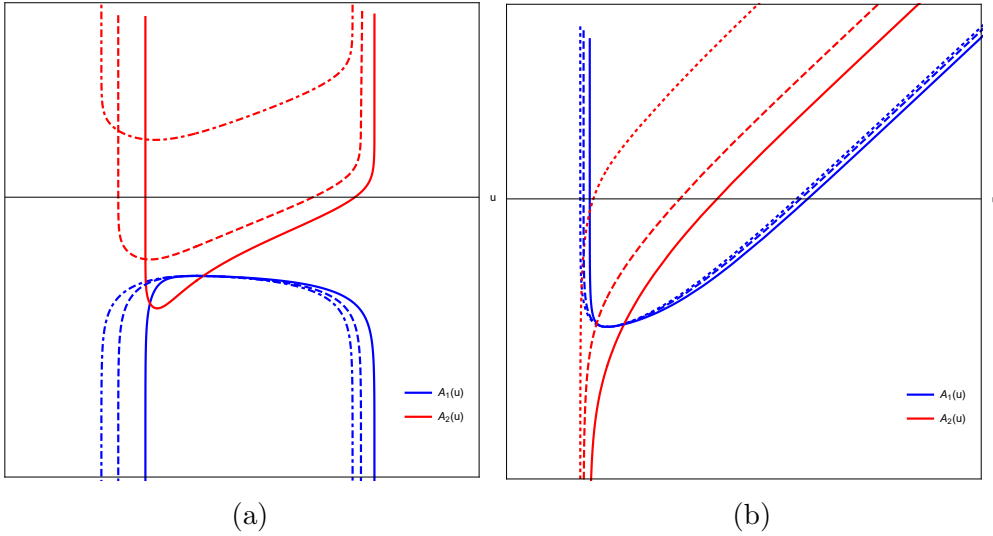


Figure 10: Consider solutions with A_1 -bounce at a fixed $u = u_0$ (the common point through which all the blue curves pass). (a) Shows the transformation of the solutions as we change the value of \hat{s}_0 for a fixed $\hat{a}_0 < a_0^c$. (b) Shows this transformation for a fixed $\hat{a}_0 > a_0^c$.

Consider an arbitrary point in $u = u_0$ where the A_1 -bounce is happening and then change the value of \hat{a}_0 while the value of \hat{s}_0 is kept fixed (move horizontally in figure

8). Figure 9a shows the transition between solutions as we change the parameter \hat{a}_0 of the A_1 -bounce. Figure 9b shows how the Kretschmann scalar diverges at the singular end-points of the solutions in figure 9a.

We can also move vertically on the space of solution in figure 8, i.e. keep \hat{a}_0 fixed and change \hat{s}_0 . Depending on which region we are in figure 8 we either have figure 10a or 10b.

5.4 A_2 -bounce space of solutions

The initial conditions for solutions with an A_2 -bounce in (5.6a) and (5.6b) depend on two free parameters \hat{a}_0 and \hat{s}_0 . These two parameters describe the coordinates of the space of the solutions with an A_2 -bounce, see figure 11.

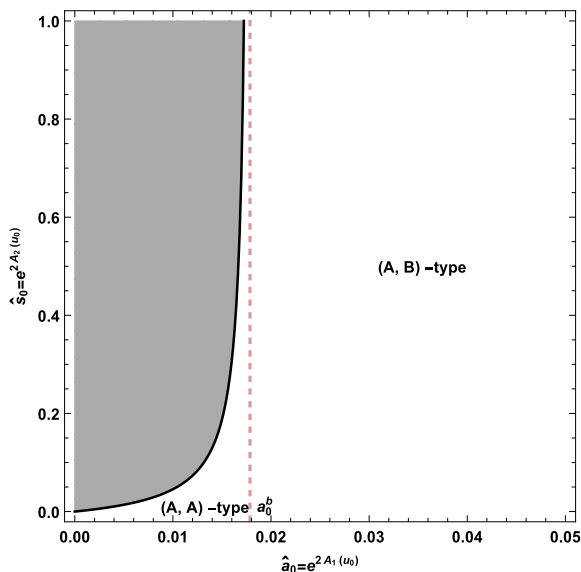


Figure 11: A_2 -bounce space of solutions: (A, B)-type solutions are living on the right-hand side of the red dashed line which is drawn at $\hat{a}_0 = a_0^b$, see equation (3.40). (A, A)-type solutions are limited from the right to the dashed line and are bounded from the left. In the gray region, we do not have any solution. Exactly on the dashed line, both AdS_d and S^n scale factors bounce at the same point $u = u_0$. Here we have the (A, A)-type solutions.

This space has the following properties:

1. For every value of $\hat{a}_0 > a_0^b$ (right to the red dashed line in figure 11) and for all values of $\hat{s}_0 > 0$, only solutions of (A, B)-type can exist.
2. Exactly on the dashed line where $\hat{a}_0 = a_0^b$ (defined in (3.40)) both the AdS and sphere have a bounce at the same point $u = u_0$. At this point as we already discussed we have (A, A)-type solutions.
3. Left to the dashed line and right to the gray region only the (A, A)-type solutions can exist.

4. The reality of solutions forbids the parameters inside the gray region, see equation (3.43a).

Figures 12a, 12b and 13 show the transformations and transitions between solutions with A_2 -bounce as we move inside the space of solutions in figure 11.

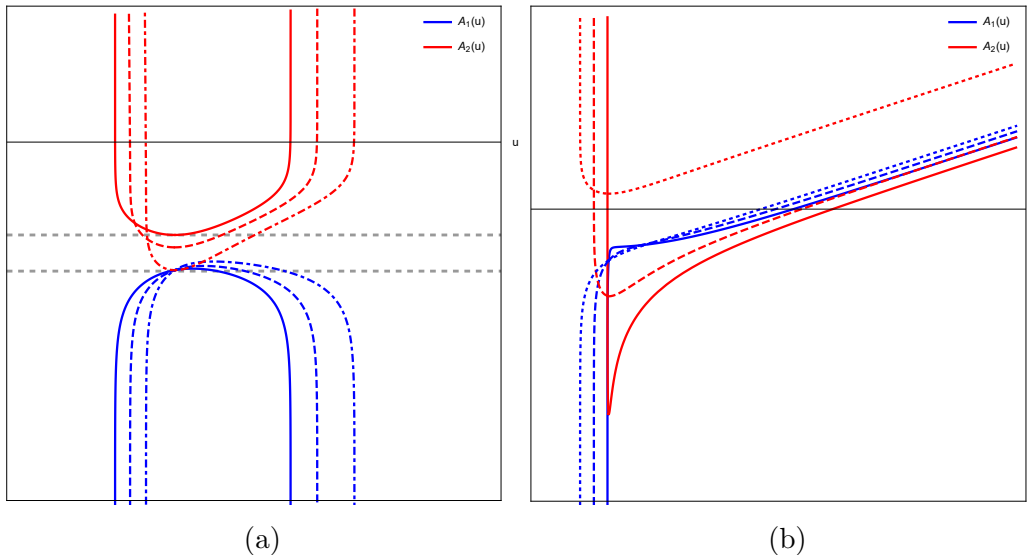


Figure 12: (a): For certain values of $\hat{a}_0 < a_0^b$ (for example at the lower horizontal dashed line which is the intersection of all the blue curves), the parameter \hat{s}_0 (the location of A_2 -bounces) is bounded by equation (3.44) (the upper dashed horizontal line). All the solutions in this region are the (A, A)-type. (b): For a fixed $\hat{a}_0 > a_0^b$ the value of \hat{s}_0 is unbounded. In this case, all the solutions are the (A, B)-type.

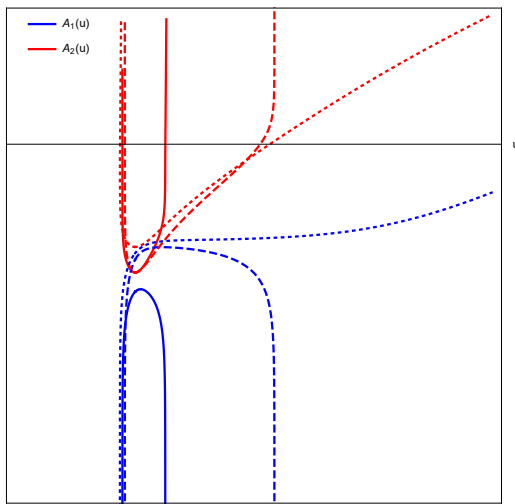


Figure 13: For a fixed value of \hat{s}_0 by decreasing the value of \hat{a}_0 (moving horizontally to the left in figure 11) we see a transition from the (A, B)-type to (A, A)-type solutions.

5.5 Monotonic solutions

As we already discussed in section 3.3, we may have solutions that do not have any A-bounce. These are solutions with monotonic scale factors. There are two types of solutions with this monotonic behavior:

- Solutions with one regular end-point which we already found in section 5.1. The other end-point of these solutions was either at the UV boundary or was a singular end-point.
- **(S, A)–type:** These are solutions with two singular end-points. If we read the initial conditions for a point at $u = u_0$ from the upper signs in (3.29a)–(3.29c), we find a solution which at the left end-point $u_L < u_0$, the AdS_d scale factor diverges but S^n shrinks.

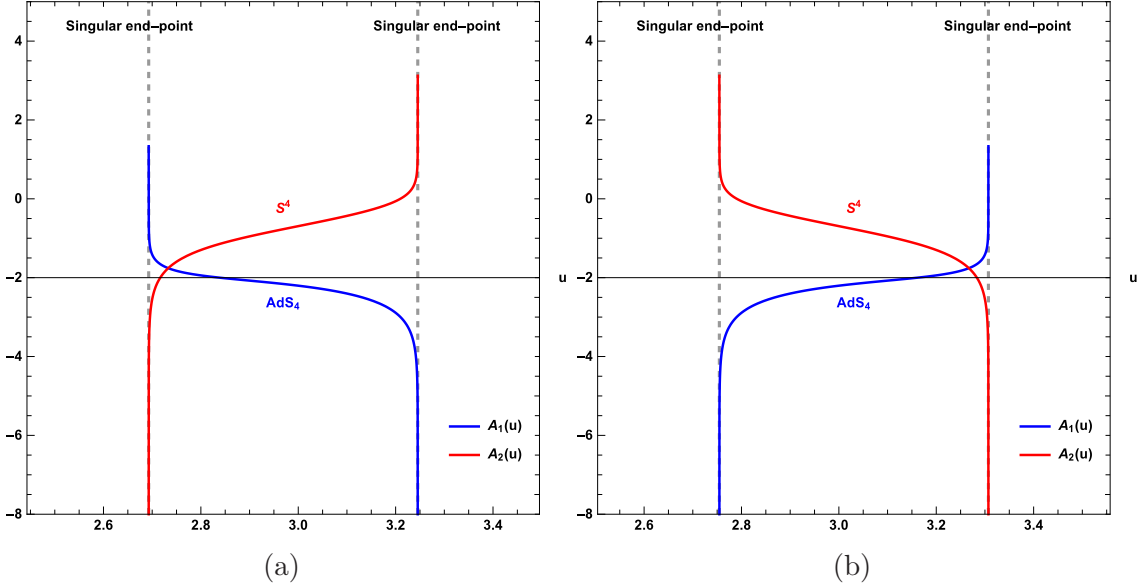


Figure 14: (a): An example of (S, A)–type, a monotonic solution with two singular end-points. Here the free parameters are fixed to $\hat{a}_0 = \frac{1}{82}$, $\hat{s}_0 = \frac{1}{4}$ and $\hat{s}_1 = \frac{5}{2}$. (b): (A, S)–type: A mirror image of the figure (a) with parameters $\hat{a}_0 = \frac{1}{82}$, $\hat{s}_0 = \frac{1}{4}$ and $\hat{s}_1 = -\frac{5}{2}$.

On the right end-point $u_R > u_0$ however, the AdS_d shrinks and S^n diverges, see figure 14a. There is a mirror image of this solution, (A, S)–type, in which at the left end-point the AdS_d shrinks but S^n diverges and at the right end-point the AdS_d diverges and S^n shrinks, see figure 14b. This solution is obtained by choosing the lower signs in (3.29a)–(3.29c) and keeping the values of \hat{a}_0 and \hat{s}_0 fixed but $\hat{s}_1 \rightarrow -\hat{s}_1$.

6. The space of all solutions

We can observe various types of transitions between different solutions if we carefully

describe the space of solutions. To do this, we choose a generic point u_0 with the following scale factor expansions

$$A_1(u) = \frac{1}{2} \log \hat{a}_0 + \hat{a}_1 \frac{u - u_0}{\ell} + \hat{a}_2 \frac{(u - u_0)^2}{\ell^2} + \mathcal{O}(u - u_0)^3, \quad (6.1a)$$

$$A_2(u) = \frac{1}{2} \log \hat{s}_0 + \hat{s}_1 \frac{u - u_0}{\ell} + \hat{s}_2 \frac{(u - u_0)^2}{\ell^2} + \mathcal{O}(u - u_0)^3. \quad (6.1b)$$

Assuming these expansions satisfy the equations of motion, we have three free parameters, here for example we select $(\hat{a}_0, \hat{s}_0, \hat{s}_1)$. These parameters construct the three dimensional space of solutions with $(\hat{a}_0, \hat{s}_0, \hat{s}_1)$ coordinates. Figure 15 shows this space for some fixed slices of \hat{s}_0 . According to figure 15, we observe the following properties:

- As mentioned, in some regions of this space we have no solution. For example in the slice with $\hat{a}_0 = 0.01$ there is a void space inside the blue region. This is coming from the reality of χ in equation (3.30) which implies that both conditions (3.31a) and (3.31b) should be satisfied.
- For fixed values of \hat{a}_0 which $\hat{a}_0 < a_0^c = \frac{1}{32} \approx 0.031$, by increasing \hat{s}_1 we observe the transition: $(\mathbf{A}, \mathbf{B}) \rightarrow (\mathbf{A}, \mathbf{A}) \rightarrow (\mathbf{R}, \mathbf{A}) \rightarrow (\mathbf{S}, \mathbf{A})$. We should emphasize that the (\mathbf{R}, \mathbf{A}) -type solutions are at the boundary of the blue and green regions in figure 15.
- At the critical value of $\hat{a}_0 = a_0^c = \frac{1}{32}$, equation (4.1), we should have the product space solution. Fixing \hat{a}_0 to this value gives a relation between \hat{s}_1 and \hat{s}_0 which draws the black curved in figure 15. This curve is the place where the blue region $((\mathbf{A}, \mathbf{A})$ -type) and the yellow region $((\mathbf{S}, \mathbf{B})$ -type) are terminated. We saw the same behavior in figure 8 when we studied the A_1 -bounce space of solutions. Moreover, this curve is the boundary between the green $((\mathbf{S}, \mathbf{A})$ -type) and red $((\mathbf{A}, \mathbf{B})$ -type) regions.
- For fixed values of \hat{a}_0 which $\hat{a}_0 > a_0^c$, by increasing \hat{s}_1 we observe the transition: $(\mathbf{A}, \mathbf{B}) \rightarrow (\mathbf{R}, \mathbf{B}) \rightarrow (\mathbf{S}, \mathbf{B}) \rightarrow (\mathbf{S}, \mathbf{A})$.
- There is an orange surface in figure 15 which belongs to the regular solutions, the (\mathbf{R}, \mathbf{B}) -type. This surface is the boundary between the yellow, (\mathbf{S}, \mathbf{B}) -type, and the red region (\mathbf{A}, \mathbf{B}) -type. It terminates at the black curve, the product space solution.

The above analysis is performed when we read the initial conditions from (3.29a)–(3.29c) by choosing the upper signs. We can start with the lower signs. The results are similar but we shall find the mirror solutions, i.e. at fixed (\hat{a}_0, \hat{s}_0) we should send $\hat{s}_1 \rightarrow -\hat{s}_1$.

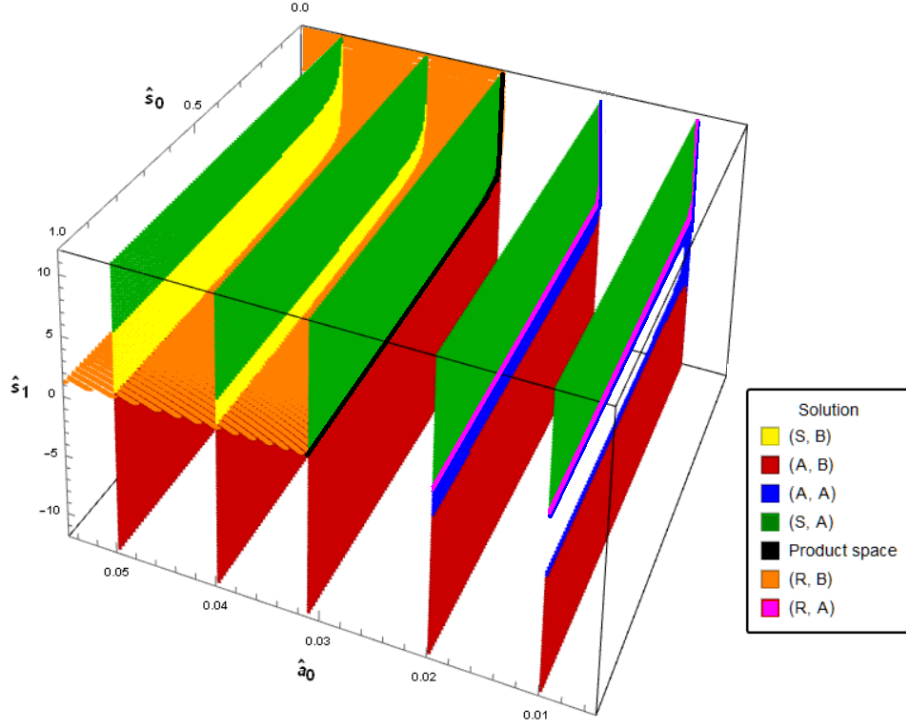


Figure 15: The space of solutions. To see all possible transitions between different solutions we have sketched five slices of this space. The void space inside the blue region on the slice $\hat{a}_0 = 0.01$ is a forbidden region where solutions are not real. Here we have fixed $u_0 = 3$. The orange surface belongs to the regular solutions, the (R, B)-type, which terminates at the black curve (product space solution). This surface is the boundary between the yellow and red regions. See table 1 for the related links to solutions.

| Color | Solution | Figure |
|---------|--------------------------|--------|
| Yellow | (S, B)-type | 5 |
| Red | (A, B)-type | 7 |
| Blue | (A, A)-type | 6 |
| Green | (S, A)-type | 14a |
| Black | $AdS_d \times AdS_{n+1}$ | 2 |
| Orange | (R, B)-type | 1 |
| Magenta | (R, A)-type | 3 |

Table 1: Different solutions in figure 15 and their related figures.

7. The boundary CFT data

As we observed so far, there are regular and singular solutions that reach the AdS boundary. In this section, we are returning to the holographic correspondence. In this, we need solutions that are everywhere regular, and therefore the only class to

consider is **(R, B)**.

For the regular solutions, we shall compute the near-boundary data that according to the holographic dictionary corresponds to data in the dual CFT. For example, we shall compute the dimensionless curvatures of AdS_d and S^n spaces at the UV boundary where the CFT is living. We are also interested in finding the parameter C which is proportional to the vev of stress-energy tensor of the boundary CFT.

7.1 Boundary data of **(R, B)**-type

There are two free parameters for regular IR end-points, the end-point location u_0 , and

$$T_{AdS}^{IR} \equiv R_1 e^{-2A_1(u_0)} = \frac{R_1}{a_0}, \quad (7.1)$$

with a_0 that has appeared in the expansions in equations (3.19a) and (3.19b). On the other hand, we have three free parameters on the UV boundary $R_{AdS}^{UV} = R_1^{UV}$, $R_S^{UV} = R_2^{UV}$ (3.6), and C , which represents the vev of stress-energy tensor of the boundary QFT, see appendix D and equations, (D.9a) and (D.9b). According to the asymptotic expansions of the scale factors, i.e. equations (3.8a) and (3.8b), under a shift $u \rightarrow u + u_\infty$ near the boundary we obtain

$$R_{AdS,S}^{UV} \sim e^{-\frac{2u_\infty}{\ell}}, \quad C \sim e^{-\frac{8u_\infty}{\ell}}, \quad (7.2)$$

so the following dimensionless ratios are independent of u_∞

$$\frac{R_{AdS}^{UV}}{R_S^{UV}}, \quad \frac{C}{(R_S^{UV})^4 \ell^8}. \quad (7.3)$$

Now we find the behavior of these UV parameters in terms of the T_{AdS}^{IR} on the IR side numerically. In the following figures we have fixed

$$R_1 = -1, \quad R_2 = 2, \quad \ell = 1, \quad d = n = 4. \quad (7.4)$$

With the above choices, the critical value of a_0 is $a_0^c = \frac{1}{32}$. We observe the following behaviors for the physical curvatures R_{AdS}^{UV} , R_S^{UV} and C as functions of the IR parameter T_{AdS}^{IR} :

- As $a_0 \rightarrow \infty$ or $T_{AdS}^{IR} \rightarrow 0$ the UV curvature $R_{AdS}^{UV} \rightarrow 0$ but R_S^{UV} has a finite value. At this point, C also has a positive finite value.
- As far as $R_S^{UV} > |R_{AdS}^{UV}|$ we have $C > 0$ and visa-versa and at the point where $R_S^{UV} = |R_{AdS}^{UV}|$ the value of C vanishes and we have the global solution (4.7).
- At the lowest value for regular solutions i.e. at $a_0 = a_0^c$ which is given in (4.1), we have the product space solution (4.4). As a_0 tends to this point $R_{AdS}^{UV} \rightarrow -\infty$ and $R_S^{UV} \rightarrow 0$ and $C \rightarrow -\infty$.

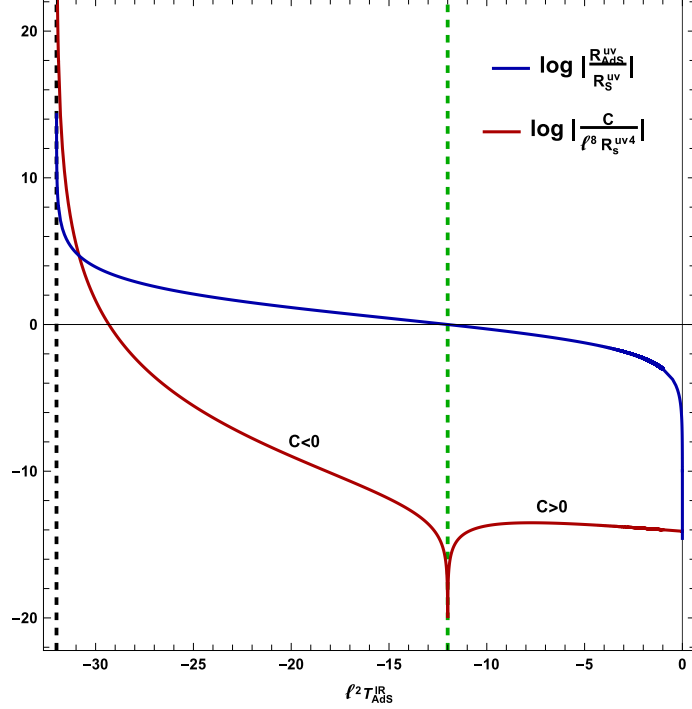


Figure 16: The logarithm of the dimensionless ratios of the UV parameters vs. $\ell^2 T_{AdS}^{IR}$. The black dashed line on the left corresponds to the lower bound $a_0 = a_0^c$ of regular IR end-point solutions where $|\ell^2 R_{AdS}^{UV}| \rightarrow +\infty$ and $\ell^2 R_S^{UV} \rightarrow 0$ (product space solution). The green dashed line shows the location where $|R_{AdS}^{UV}| = R_S^{UV}$ or $C = 0$. This point corresponds to the global solution.

- Below a_0^c we find solutions that have a singular end-point and do not reach the UV boundary at $u \rightarrow +\infty$.

The dimensionless ratios of the UV parameters i.e. R_{AdS}^{UV}/R_S^{UV} and $C/(\ell^2 R_S^{UV})^4$ in terms of $\ell^2 T_{AdS}^{IR}$ have been shown in figure 16.

8. The on-shell action and the free energy

In this section, we find the on-shell action and free energy for regular solutions of the theory. We begin again with the following action

$$S = M_P^{d+n-1} \int du d^{d+n} x \sqrt{|g|} \left(R^{(g)} - \frac{1}{2} \partial_a \varphi \partial^a \varphi - V(\varphi) \right) + S_{GHY}. \quad (8.1)$$

In this action we have

$$R^{(g)} = \frac{1}{2} (\partial \varphi)^2 - \frac{1+n+d}{1-n-d} V(\varphi) \quad , \quad \partial_a \varphi \partial^a \varphi = \dot{\varphi}^2 \quad , \quad \sqrt{|g|} = e^{dA_1 + nA_2} \sqrt{|\zeta^1| |\zeta^2|}. \quad (8.2)$$

Substituting into (8.1) we obtain the on-shell action ¹⁷

$$S_{on-shell} = \frac{2M_P^{d+n-1}}{d+n-1} V_{S^n} V_{AdS_d} \int_{u_0}^{+\infty} du e^{dA_1+nA_2} V(\varphi) + S_{GHY}, \quad (8.3)$$

where V_{S^n} and V_{AdS_d} are the volume of the sphere and AdS space respectively. However, we can write the potential in terms of the scale factors from the equation of motion (2.14) as follows

$$V(\varphi) = \frac{(d+n-1)e^{-2(A_1+A_2)}}{d+n} \left(R_1 e^{2A_2} + R_2 e^{2A_1} - e^{2(A_1+A_2)} (d\ddot{A}_1 + n\ddot{A}_2 + (d\dot{A}_1 + n\dot{A}_2)^2) \right). \quad (8.4)$$

Therefore, the on-shell action can be written in terms of the scale factors and their derivatives

$$S_{on-shell} = \frac{2M_P^{d+n-1}}{d+n} V_{S^n} V_{AdS_d} \left(\int_{u_0}^{+\infty} du e^{dA_1+nA_2} (R_1 e^{-2A_1} + R_2 e^{-2A_2}) - \left[e^{dA_1+nA_2} (d\dot{A}_1 + n\dot{A}_2) \right]_{u_0}^{+\infty} \right) + S_{GHY}. \quad (8.5)$$

The Gibbons Hawking York (GHY) term at the boundary $u = +\infty$, is given as

$$S_{GHY} = -2M_P^{d+n-1} \left[\int d^{d+n}x \sqrt{|\gamma|} K \right]^{u=+\infty}, \quad (8.6)$$

where γ_{ij} is the induced metric on the $AdS_d \times S^n$ slices and the extrinsic curvature is $K_{ij} = -\frac{1}{2} \partial_u \gamma_{ij}$. Therefore we find

$$K = -d\dot{A}_1 - n\dot{A}_2, \quad \sqrt{|\gamma|} = e^{dA_1+nA_2} \sqrt{|\zeta^1| |\zeta^2|}. \quad (8.7)$$

This gives

$$S_{GHY} = 2M_P^{d+n-1} V_{S^n} V_{AdS_d} \left[e^{dA_1+nA_2} (d\dot{A}_1 + n\dot{A}_2) \right]^{u=+\infty}. \quad (8.8)$$

Moreover, the contribution of the last term in (8.5) from the u_0 endpoint vanishes. This can be seen by calculating the derivative of $e^{2A_1(u)}$ and $e^{2A_2(u)}$ in (3.19a) and (3.19b) with respect to the u coordinate.

Using the previous observation and substituting (8.8) in equation (8.5) we obtain

$$S_{on-shell} = \frac{2M_P^{d+n-1}}{d+n} V_{S^n} V_{AdS_d} \left(\int_{u_0}^{+\infty} du e^{dA_1+nA_2} (R_1 e^{-2A_1} + R_2 e^{-2A_2}) + (d+n-1) \left[e^{dA_1+nA_2} (d\dot{A}_1 + n\dot{A}_2) \right]_{u_0}^{+\infty} \right). \quad (8.9)$$

¹⁷Here we consider solutions in which the boundary (UV) is at $u = +\infty$ while the S^n -shrinking end-point (IR) is at $u = u_0$ in (8.5).

We introduce two potentials $U_1(u)$ and $U_2(u)$ which satisfy the following differential equations

$$((n-2)\dot{A}_2 + d\dot{A}_1)U_1 + \dot{U}_1 = -1, \quad (8.10a)$$

$$((d-2)\dot{A}_1 + n\dot{A}_2)U_2 + \dot{U}_2 = -1. \quad (8.10b)$$

Then we can use these potentials to write the free energy ($\mathcal{F} = -S_{on-shell}$) as

$$\begin{aligned} \mathcal{F} = & -\frac{2M_P^{d+n-1}}{d+n} V_{S^n} V_{AdS_d} \left(-e^{dA_1+nA_2} \left(\frac{U_2 R_1}{e^{2A_1}} + \frac{U_1 R_2}{e^{2A_2}} \right) \Big|_{u_0}^{+\infty} \right. \\ & \left. + (d+n-1)e^{dA_1+nA_2} (d\dot{A}_1 + n\dot{A}_2) \Big|^{u=+\infty} \right). \end{aligned} \quad (8.11)$$

The volume of the n -sphere in slices is finite and is given in terms of its curvature by

$$V_{S^n} \equiv \frac{V_S}{R_2^{\frac{n}{2}}} = \frac{2\pi^{\frac{n+1}{2}}}{\Gamma(\frac{n+1}{2})} \left[\frac{(n(n-1))}{R_2} \right]^{\frac{n}{2}}. \quad (8.12)$$

The volume of AdS_d space, on the other hand, is infinite and we should regularize it. Starting from the Poincaré coordinates with length scale $\hat{\ell}$

$$ds_{AdS_d}^2 = \frac{\hat{\ell}^2}{z^2} (dz^2 + dx_i dx^i), \quad (8.13)$$

the volume can be regularized as

$$V_{AdS_d} = \int_0^L d^{d-1}x \int_{\hat{\epsilon}}^{\infty} dz \frac{\hat{\ell}^d}{z^d} = \frac{\hat{\ell}^d}{d-1} \frac{L^{d-1}}{\hat{\epsilon}^{d-1}}. \quad (8.14)$$

Using the value of AdS_d curvature $R_1 = -\frac{d(d-1)}{\hat{\ell}^2}$ we can rewrite the volume as

$$V_{AdS_d} \equiv \frac{V_A}{|R_1|^{\frac{d}{2}}} = \frac{1}{d-1} \left(\frac{L}{\hat{\epsilon}} \right)^{d-1} \left[\frac{d(d-1)}{|R_1|} \right]^{\frac{d}{2}}. \quad (8.15)$$

By the above values for the volumes, we can write the free energy as

$$\begin{aligned} \mathcal{F} = & \frac{2M_P^{d+n-1}}{d+n} \frac{V_S V_A}{|R_1|^{\frac{d}{2}} R_2^{\frac{n}{2}}} \left(e^{dA_1+nA_2} \left(\frac{U_2 R_1}{e^{2A_1}} + \frac{U_1 R_2}{e^{2A_2}} \right) \Big|_{u_0}^{+\infty} \right. \\ & \left. - (d+n-1)e^{dA_1+nA_2} (d\dot{A}_1 + n\dot{A}_2) \Big|^{u=+\infty} \right). \end{aligned} \quad (8.16)$$

To find the free energy, we need to compute U_1 and U_2 from (8.10a) and (8.10b) at the AdS boundary and the IR end-point $u = u_0$. For $d = n = 4$, we already computed the scale factors near the AdS boundary in equations (3.8a) and (3.8b). Moreover, the expansion of these functions near the regular IR end-point is given

in (3.19a) and (3.19b). Therefore, we find the following expansions near the AdS boundary for U_1 and U_2 as $u \rightarrow +\infty$

$$U_1 = -\frac{\ell}{6} + \frac{\ell(8\mathcal{R}_1 + \mathcal{R}_2)}{2016} e^{-\frac{2u}{\ell}} + \frac{\ell(11\mathcal{R}_1^2 - 76\mathcal{R}_1\mathcal{R}_2 + 11\mathcal{R}_2^2)}{338688} e^{-\frac{4u}{\ell}} + \mathcal{B}_1 e^{-\frac{6u}{\ell}} + \frac{-26\mathcal{R}_1^3 + 216\mathcal{R}_1^2\mathcal{R}_2 - 78\mathcal{R}_1\mathcal{R}_2^2 + 23\mathcal{R}_2^3}{9483264} u e^{-\frac{6u}{\ell}} + \dots, \quad (8.17a)$$

$$U_2 = -\frac{\ell}{6} + \frac{\ell(8\mathcal{R}_2 + \mathcal{R}_1)}{2016} e^{-\frac{2u}{\ell}} + \frac{\ell(11\mathcal{R}_1^2 - 76\mathcal{R}_1\mathcal{R}_2 + 11\mathcal{R}_2^2)}{338688} e^{-\frac{4u}{\ell}} + \mathcal{B}_2 e^{-\frac{6u}{\ell}} + \frac{-26\mathcal{R}_2^3 + 216\mathcal{R}_2^2\mathcal{R}_1 - 78\mathcal{R}_2\mathcal{R}_1^2 + 23\mathcal{R}_1^3}{9483264} u e^{-\frac{6u}{\ell}} + \dots, \quad (8.17b)$$

and at the end-point, we obtain ($u \rightarrow u_0^+$)

$$U_1 = -\frac{12a_0\ell^2\mathbf{b}_1}{40a_0 + \ell^2 R_1} \frac{1}{(u - u_0)^2} + \mathbf{b}_1 - \frac{1}{3}(u - u_0) - \frac{\mathbf{b}_1(20768a_0^2 + 1168a_0\ell^2 R_1 + 17\ell^4 R_1^2)}{250a_0\ell^2(40a_0 + \ell^2 R_1)} (u - u_0)^2 + \dots, \quad (8.18a)$$

$$U_2 = \frac{126000a_0^2\ell^4\mathbf{b}_2}{264512a_0^2 + 6112a_0\ell^2 R_1 + 53\ell^4 R_1^2} \frac{1}{(u - u_0)^4} - \frac{2100a_0\ell^2\mathbf{b}_2(112a_0 + \ell^2 R_1)}{264512a_0^2 + 6112a_0\ell^2 R_1 + 53\ell^4 R_1^2} \frac{1}{(u - u_0)^2} - \frac{1}{5}(u - u_0) + \dots, \quad (8.18b)$$

where $\mathcal{B}_1, \mathcal{B}_2, \mathbf{b}_1$ and \mathbf{b}_2 are constants of integration¹⁸.

8.1 Regularization

The on-shell action as defined is infinite due to the infinite volume of the total space. We now introduce a regulated boundary at $u = -\ell \log \epsilon$ and define a dimensionless cut-off

$$\Lambda \equiv \frac{e^{\frac{A_1 + A_2}{2}}}{\ell |\mathcal{R}_1 \mathcal{R}_2|^{\frac{1}{4}}} \Big|_{u = -\ell \log \epsilon} = \frac{1}{\epsilon |\mathcal{R}_1 \mathcal{R}_2|^{\frac{1}{4}}}. \quad (8.19)$$

The free energy can be computed as

$$\mathcal{F} = \mathcal{F}^\Lambda - \mathcal{F}^{u_0}, \quad (8.20)$$

¹⁸Since the free energy is dimensionless, $[L]^0$, then from (8.16) U_1 and U_2 should be $[L]^3$ and also \mathcal{B}_1 and \mathcal{B}_2 . Therefore we expect $\mathcal{B}_{1,2} = \ell^3 \mathcal{B}_{1,2}(\mathcal{R}_1^3, \mathcal{R}_2^3, \mathcal{R}_1^2 \mathcal{R}_2, \mathcal{R}_1 \mathcal{R}_2^2)$.

where we have

$$\begin{aligned}
\mathcal{F}^\Lambda = & -\frac{M_P^7 \ell^7}{4} V_S V_A \left(56\Lambda^8 + \frac{4}{3}\Lambda^6 \left(\left| \frac{\mathcal{R}_1}{\mathcal{R}_2} \right|^{\frac{1}{2}} - \left| \frac{\mathcal{R}_2}{\mathcal{R}_1} \right|^{\frac{1}{2}} \right) - \frac{\Lambda^4}{504} \left(\frac{\mathcal{R}_1}{\mathcal{R}_2} + 16 + \frac{\mathcal{R}_2}{\mathcal{R}_1} \right) \right. \\
& - \frac{\Lambda^2}{84672} \left(-2 \left| \frac{\mathcal{R}_1}{\mathcal{R}_2} \right|^{\frac{3}{2}} - 29 \left| \frac{\mathcal{R}_1}{\mathcal{R}_2} \right|^{\frac{1}{2}} + 29 \left| \frac{\mathcal{R}_2}{\mathcal{R}_1} \right|^{\frac{1}{2}} + 2 \left| \frac{\mathcal{R}_2}{\mathcal{R}_1} \right|^{\frac{3}{2}} \right) \\
& - \frac{\log(|\mathcal{R}_1 \mathcal{R}_2| \Lambda^4)}{37933056} \left(23 \left(\frac{\mathcal{R}_1}{\mathcal{R}_2} \right)^2 - 104 \frac{\mathcal{R}_1}{\mathcal{R}_2} + 432 - 104 \frac{\mathcal{R}_2}{\mathcal{R}_1} + 23 \left(\frac{\mathcal{R}_2}{\mathcal{R}_1} \right)^2 \right) \\
& - \frac{19}{113799168} \left(\left(\frac{\mathcal{R}_1}{\mathcal{R}_2} \right)^2 - 10 \frac{\mathcal{R}_1}{\mathcal{R}_2} + \frac{4041}{19} - 10 \frac{\mathcal{R}_2}{\mathcal{R}_1} + \left(\frac{\mathcal{R}_2}{\mathcal{R}_1} \right)^2 \right) - \frac{\mathcal{R}_2 \mathcal{B}_1 + \mathcal{R}_1 \mathcal{B}_2}{\ell \mathcal{R}_1^2 \mathcal{R}_2^2} \Big) \\
& + \mathcal{O}(\Lambda^{-2}), \tag{8.21}
\end{aligned}$$

where

$$\mathcal{R}_1 = \ell^2 R_1^{UV}, \quad \mathcal{R}_2 = \ell^2 R_2^{UV}, \tag{8.22}$$

and

$$\mathcal{F}^{u_0} = \frac{M_P^7}{4} V_S V_A \left(\frac{875 a_0^3 \ell^4 \mathbf{b}_2}{264512 a_0^2 R_1 + 6112 a_0 \ell^2 R_1^2 + 53 \ell^4 R_1^3} - \frac{a_0^3 \ell^2 \mathbf{b}_1}{R_1^2 (40 a_0 + \ell^2 R_1)} \right), \tag{8.23}$$

with

$$a_0 = e^{2A_1(u_0)}. \tag{8.24}$$

It should be noted that the free energy is independent of the constants of integration for U_1 and U_2 because it depends on the difference of the UV and IR parts i.e. equation (8.20). Therefore, we can choose $\mathbf{b}_1 = \mathbf{b}_2 = 0$ and use these conditions to find the values of \mathcal{B}_1 and \mathcal{B}_2 in the UV.

The free energy that we have found so far depends on the UV cut-off Λ . To find a renormalized free energy we can add counter-terms on the AdS boundary. The induced metric on this boundary is given by

$$ds^2 = \gamma_{\mu\nu} dx^\mu dx^\nu = e^{2A_1(u)} ds_{AdS_d}^2 + e^{2A_2(u)} ds_{S^n}^2 \Big|_{u=-\ell \log \epsilon}. \tag{8.25}$$

We can read some scalar tensors on the AdS boundary at $u = -\ell \log \epsilon$ as follows

$$\sqrt{\gamma} = e^{dA_1(u) + nA_2(u)} \sqrt{|\zeta^1| |\zeta^2|}, \tag{8.26a}$$

$$R^{(\gamma)} = e^{-2A_1(u)} R_1 + e^{-2A_2(u)} R_2, \tag{8.26b}$$

$$R_{\mu\nu}^{(\gamma)} R^{(\gamma)\mu\nu} = e^{-4A_1(u)} \frac{R_1^2}{d} + e^{-4A_2(u)} \frac{R_2^2}{n}. \tag{8.26c}$$

The counter-terms required to cancel the Λ -dependent terms in (8.21) are given by

$$\begin{aligned}
S^{ct} = & -\frac{M_P^7}{\ell} \int d^8 x \sqrt{\gamma} \left(14 + \frac{\ell^2}{6} R^{(\gamma)} + \frac{\ell^4}{144} (R_{\mu\nu}^{(\gamma)} R^{(\gamma)\mu\nu} - \frac{2}{7} R^{(\gamma)2}) \right. \\
& + \frac{\ell^6}{677376} (31 R^{(\gamma)3} - 140 R^{(\gamma)} R_{\mu\nu}^{(\gamma)} R^{(\gamma)\mu\nu}) - \frac{\ell^8}{303464448} (193 R^{(\gamma)4} \\
& \left. - 1960 R^{(\gamma)2} R_{\mu\nu}^{(\gamma)} R^{(\gamma)\mu\nu} + 5488 (R_{\mu\nu}^{(\gamma)} R^{(\gamma)\mu\nu})^2 \right) \log(\omega |\mathcal{R}_1 \mathcal{R}_2| \Lambda^4), \tag{8.27}
\end{aligned}$$

where ω is a constant and defines our scheme of free energy. Defining $\mathcal{F}^{ct} = -S^{ct}$ we find the regularized free energy as follow

$$\begin{aligned}
\mathcal{F}^{ren} &= \mathcal{F} + \mathcal{F}^{ct} \\
&= -M_P^7 \ell^7 V_S V_A \left(\frac{267\mathcal{R}_1^4 - 1004\mathcal{R}_1^3\mathcal{R}_2 - 2738\mathcal{R}_1^2\mathcal{R}_2^2 - 1004\mathcal{R}_1\mathcal{R}_2^3 + 267\mathcal{R}_2^4}{910393344\mathcal{R}_1^2\mathcal{R}_2^2} \right. \\
&\quad + \frac{(23\mathcal{R}_1^4 - 104\mathcal{R}_1^3\mathcal{R}_2 + 432\mathcal{R}_1^2\mathcal{R}_2^2 - 104\mathcal{R}_1\mathcal{R}_2^3 + 23\mathcal{R}_2^4)}{151732224\mathcal{R}_1^2\mathcal{R}_2^2} \log \omega \\
&\quad \left. - \frac{\mathcal{R}_2\mathcal{B}_1 + \mathcal{R}_1\mathcal{B}_2}{4\ell\mathcal{R}_1^2\mathcal{R}_2^2} \right). \tag{8.28}
\end{aligned}$$

8.2 Fixing the scheme

As it was already shown, an exact solution of equations of motion is the globally AdS_{d+n+1} solution (4.7). This solution among the regular solutions is a special case, for which $\mathcal{R}_1 = -\mathcal{R}_2$. For this solution, we can either compute the free energy directly from (8.9) or compute the potentials U_1 and U_2 . For example, we find

$$\begin{aligned}
U_1 &= \frac{1}{192\sinh^2(u-u_0)\cosh^4(u-u_0)} \left(3(c_1 + \sinh(2(u-u_0))) \right. \\
&\quad \left. - \sinh(4(u-u_0)) + 4u - \sinh(6(u-u_0)) \right), \tag{8.29a}
\end{aligned}$$

$$\begin{aligned}
U_2 &= \frac{1}{192\sinh^2(u-u_0)\cosh^4(u-u_0)} \left(3(c_2 + \sinh(2(u-u_0))) \right. \\
&\quad \left. + \sinh(4(u-u_0)) - 4u - \sinh(6(u-u_0)) \right), \tag{8.29b}
\end{aligned}$$

where c_1 and c_2 are constants of integration. The free energy before renormalization can be read as

$$\mathcal{F} = -M_P^7 \ell^7 V_S V_A \left(14\Lambda^8 - \frac{\Lambda^4}{144} - \frac{1}{55296} \log(4\sqrt{3}\Lambda) \right), \tag{8.30}$$

which is obviously independent of c_1 and c_2 . This result can be confirmed by using the results in equations (8.21) and (8.23) with IR boundary conditions $\mathfrak{b}_1 = \mathfrak{b}_2 = 0$ when we choose $\mathcal{R}_1 = -\mathcal{R}_2 = -48$ for the global solution.

To renormalize (8.30) we can use the counter-terms in (8.27) with an appropriate scheme

$$\omega = e^{-\frac{89}{42}}, \tag{8.31}$$

which finally gives the free energy of the global AdS

$$\mathcal{F}^{Global} = 0. \tag{8.32}$$

Now in this scheme, we can compute the free energy of all the regular solutions in

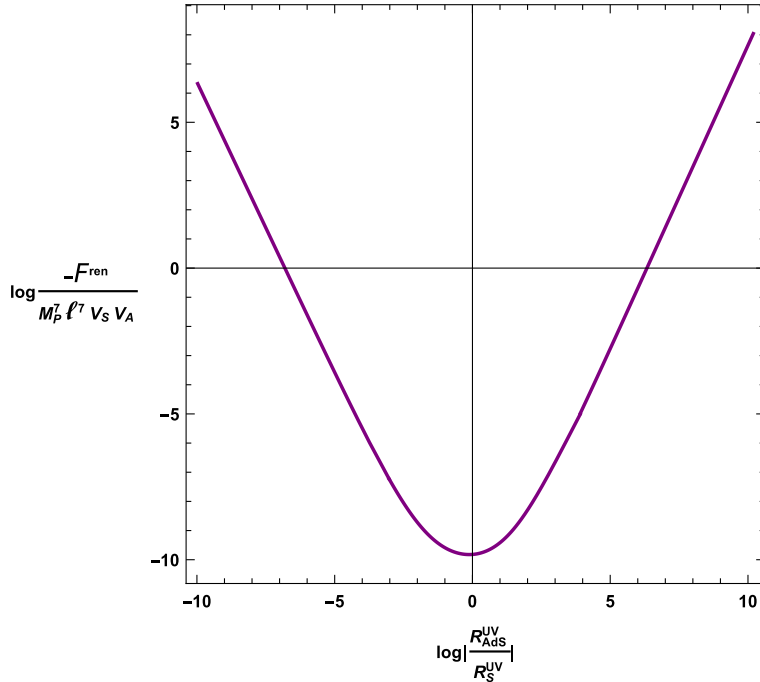


Figure 17: The logarithm of the renormalized free energy vs. the logarithm of the dimensionless ratio of UV curvatures. The free energy is maximum ($\mathcal{F}^{ren} \leq 0$) for global AdS_{d+n+1} solution ($|R_{AdS}^{UV}/R_S^{UV}| = 1$).

the theory. This is given by

$$\mathcal{F}^{ren} = M_P^7 \ell^7 V_S V_A \left(\frac{89\mathcal{R}_1^4 - 1114\mathcal{R}_1^3\mathcal{R}_2 + 28807\mathcal{R}_1^2\mathcal{R}_2^2 - 1114\mathcal{R}_1\mathcal{R}_2^3 + 89\mathcal{R}_2^4}{3186376704\mathcal{R}_1^2\mathcal{R}_2^2} + \frac{\mathcal{R}_2\mathcal{B}_1 + \mathcal{R}_1\mathcal{B}_2}{4\ell\mathcal{R}_1^2\mathcal{R}_2^2} \right). \quad (8.33)$$

The logarithm of the renormalized free energy in terms of the dimensionless ratio of UV curvatures is sketched in figure 17.

We should state that all different regular bulk solutions correspond to different UV sources and therefore to distinct CFTs. The distinct dual theories involve the same CFT but on $AdS \times S$ with a different ratio of radii of curvatures. There is therefore no competition between these saddle points. We observe, however, that the free energy (on shell action) is maximal for the globally AdS solution¹⁹.

9. Solutions with $AdS_d \times S^1$ slices

There is a special case of S^n , namely $n = 1$, that is not covered by our previous analysis, as S^1 has no curvature ($R_2 = 0$). In this section, we study this case. As

¹⁹The logarithm of the action in figure 17 should be $-\infty$ at the AdS solution. It is not because of a lack of perfect numerical accuracy.

in the previous cases studied, whatever we say is valid if replace AdS_d with any d -dimensional constant negative curvature manifold.

The equations of motion (3.2)–(3.4) simplify to

$$(d\dot{A}_1 + \dot{A}_2)^2 - d\dot{A}_1^2 - \dot{A}_2^2 - e^{-2A_1} R_1 = \frac{1}{\ell^2} d(d+1), \quad (9.1)$$

$$d(d\ddot{A}_1 + \ddot{A}_2) + d(\dot{A}_1 - \dot{A}_2)^2 + e^{-2A_1} R_1 = 0, \quad (9.2)$$

$$\ddot{A}_1 + \dot{A}_1(d\dot{A}_1 + \dot{A}_2) - \frac{1}{d} e^{-2A_1} R_1 = \ddot{A}_2 + \dot{A}_2(d\dot{A}_1 + \dot{A}_2). \quad (9.3)$$

By solving \dot{A}_2 and \ddot{A}_2 from equation (9.1) and (9.2) and then inserting in (9.3) we find the following equation for $A_1(u)$

$$de^{2A_1} \left(2\ell^2 \ddot{A}_1 + (d+1)(\ell^2 \dot{A}_1^2 - 1) \right) - \ell^2 R_1 = 0. \quad (9.4)$$

This equation can be integrated to obtain

$$e^{(d+1)A_1} \dot{A}_1^2 - \frac{e^{(d-1)A_1}}{d(d-1)\ell^2} (d(d-1)e^{2A_1} + \ell^2 R_1) + \alpha_1 = 0, \quad (9.5)$$

where α_1 is a constant of integration. Given A_1 , A_2 can be obtained from

$$d(d-1)\dot{A}_1^2 + 2d\dot{A}_1\dot{A}_2 = \frac{1}{\ell^2} d(d-1) + R_1 e^{-2A_1}. \quad (9.6)$$

9.1 Asymptotics

Performing the same analysis as in previous sections we find the following properties for solutions with $AdS_d \times S^1$ slices:

- **Near boundary expansions:** Solving the equations of motion (9.1)–(9.3), near the putative boundary either at $u \rightarrow +\infty$ or $u \rightarrow -\infty$ gives expansions for scale factors of AdS_d and S^1 spaces. For example, for $d = 3$ we find the following expansions:

$$A_1(u) = \bar{A}_1 \pm \frac{u}{\ell} - \frac{\mathcal{R}_1}{24} e^{\mp \frac{2u}{\ell}} - \left(\frac{\mathcal{R}_1^2}{1152} + \frac{C}{2} \right) e^{\mp \frac{4u}{\ell}} + \mathcal{O}(e^{\mp \frac{6u}{\ell}}), \quad (9.7a)$$

$$A_2(u) = \bar{A}_2 \pm \frac{u}{\ell} + \frac{\mathcal{R}_1}{24} e^{\mp \frac{2u}{\ell}} - \left(\frac{\mathcal{R}_1^2}{1152} - \frac{3C}{2} \right) e^{\mp \frac{4u}{\ell}} + \mathcal{O}(e^{\mp \frac{6u}{\ell}}), \quad (9.7b)$$

where $\mathcal{R}_1 = \ell^2 R_1 e^{-2\bar{A}_1}$ is the dimensionless curvature parameter.

- **Singular end-points:** Considering the expansions in (3.10a) and (3.10b), the only singular end-point possibility is when the AdS_d scale factor vanishes while the scale factor of the circle diverges i.e.

$$A_1(u) = \frac{2}{d+1} \log \frac{u - u_0}{\ell} + \frac{1}{2} \log a_0 + \mathcal{O}(u - u_0), \quad (9.8a)$$

$$A_2(u) = \frac{1-d}{1+d} \log \frac{u - u_0}{\ell} + \frac{1}{2} \log s_0 + \mathcal{O}(u - u_0). \quad (9.8b)$$

To see this, it is easy to put $n = 1$ in equation (3.16) which gives $\lambda_1 = \frac{2}{d+1}$ and $\lambda_2 = \frac{1-d}{d+1}$ while equation (3.17) gives $\lambda_1 = 0$ and $\lambda_2 = 1$ which describes a regular end-point.

- **Regular end-points:** Solving equations of motion (9.1)–(9.3) by inserting the expansions (3.10a) and (3.10b) for $\lambda_1 = 0$ and $\lambda_2 = 1$ we find the following scale factors near the regular end-point (S^1 shrinks but AdS_d has a finite size)

$$e^{2A_1(u)} = a_0 + \frac{a_0 d(d+1) + \ell^2 R_1}{2d\ell^2} (u - u_0)^2 - \frac{(a_0 d(d+1) + \ell^2 R_1)(a_0 d(d-5)(d+1) + (d-3)\ell^2 R_1)}{48a_0 d^2 \ell^4} (u - u_0)^4 + \mathcal{O}(u - u_0)^6, \quad (9.9a)$$

$$e^{2A_2(u)} = \frac{c_0}{\ell^2} (u - u_0)^2 + \frac{(a_0(2+d-d^2) - \ell^2 R_1)c_0}{6a_0 \ell^4} (u - u_0)^4 + \mathcal{O}(u - u_0)^6, \quad (9.9b)$$

where c_0 is an arbitrary positive constant. These scale factors can be read also from (3.19a) and (3.19b) by replacing $n = 1$ and $\frac{R_2}{n-1} = \frac{c_0}{\ell^2}$. Similar to the discussion (at the end of section 3.2.2) for the general S^n case we cannot have a regular end-point where AdS_d shrinks while S^1 is finite.

- **Bounces:** The analytic computations show that only the circle can have an A-bounce and the scale factor of AdS_d is always monotonic. To see this, starting from the expansions (3.32a) and (3.32b) for an AdS_d bounce, the only possible solution for coefficients is when $\hat{a}_2 = \hat{a}_3 = \dots = 0$ i.e. the scale factor of AdS_d is constant. On the other hand at the S^1 bounce, we have

$$A_1(u) = \frac{1}{2} \log(\hat{a}_0) + \hat{a}_1 \frac{(u - u_0)}{\ell} + \hat{a}_2 \frac{(u - u_0)^2}{\ell^2} + \mathcal{O}(u - u_0)^3, \quad (9.10a)$$

$$A_2(u) = \frac{1}{2} \log(\hat{s}_0) + \hat{s}_2 \frac{(u - u_0)^2}{\ell^2} + \hat{s}_3 \frac{(u - u_0)^3}{\ell^3} + \mathcal{O}(u - u_0)^4, \quad (9.10b)$$

with the following coefficients

$$\hat{a}_1 = \pm \frac{\sqrt{d(d+1) + \frac{\ell^2 R_1}{\hat{a}_0}}}{\sqrt{d(d-1)}}, \quad \hat{a}_2 = -\frac{d^2 + d + \frac{\ell^2 R_1}{\hat{a}_0}}{2d(d-1)}, \quad (9.11a)$$

$$\hat{s}_2 = \frac{d+1}{2}, \quad \hat{s}_3 = -\frac{d(d+1)\sqrt{d^2 + d + \frac{\ell^2 R_1}{\hat{a}_0}}}{6\sqrt{d(d-1)}}. \quad (9.11b)$$

Knowing all the properties above we have the following classes of solutions:

1. The regular solutions of **(R, B)** type. This describes the solution outside the horizon of the black hole i.e. stretched from the horizon to the asymptotic boundary.

2. The singular solutions of (\mathbf{R}, \mathbf{A}) type. This describes the solution behind the horizon of the black hole i.e. stretched from horizon to singularity.

3. The singular solutions of (\mathbf{A}, \mathbf{B}) type. This describes a solution that is stretched from singularity to boundary (solutions with a naked singularity).

In this case, there are also several analogs of the product space solution. One of them contains an AdS_2 wormhole. We have plotted this solution in figure 18. It will be described analytically in the next subsection.

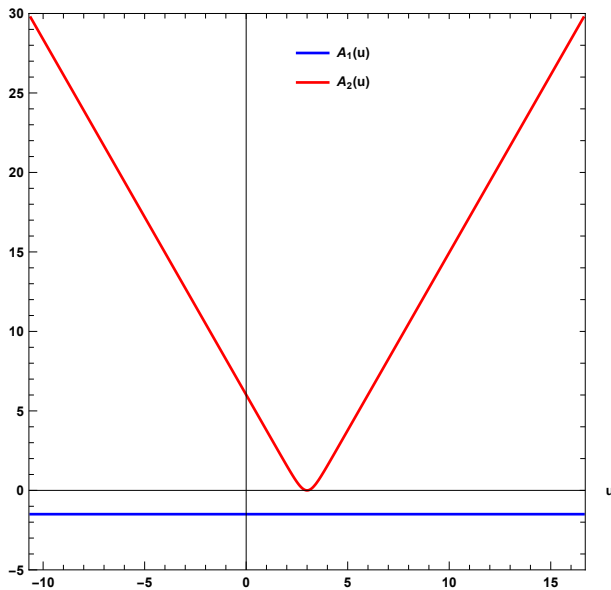


Figure 18: A wormhole solution with geometry given in equation (9.19).

9.2 Exact solutions

To proceed, from equations (9.1)–(9.3) we must distinguish two cases:

- $\dot{A}_1 = 0$

From equations of motion (9.1)–(9.3) we find

$$e^{2A_1} = -\frac{\ell^2 R_1}{d(d+1)}, \quad \ddot{A}_2 + \dot{A}_2^2 - \frac{d+1}{\ell^2} = 0. \quad (9.12)$$

We perform the following change of variable

$$A_2(u) = \log r(u), \quad (9.13)$$

so that $0 \leq r < +\infty$. The equation of motion in (9.12) becomes

$$\ddot{r} - \frac{d+1}{\ell^2} r = 0 \longrightarrow \dot{r}^2 = \frac{d+1}{\ell^2} (r^2 + k), \quad (9.14)$$

where k is the constant of integration. Therefore the relation between metrics in two coordinates u and r is given by

$$\begin{aligned} ds^2 &= du^2 + e^{2A_2(u)} d\theta^2 + e^{2A_1(u)} ds_{AdS_d}^2 \\ &= \frac{\ell^2}{d+1} \frac{dr^2}{r^2+k} + r^2 d\theta^2 - \frac{\ell^2 R_1}{d(d+1)} ds_{AdS_d}^2. \end{aligned} \quad (9.15)$$

where we have normalized the angle θ to have period 2π . Any rescaling of that period via a rescaling of r corresponds to a rescaling of the constant k . This metric describes a product space $\mathcal{M}_2 \times AdS_d$. Depending on the value of k we have different geometries for \mathcal{M}_2 :

1. For $k > 0$, the radius of S^1 shrinks to zero sizes as $r \rightarrow 0$ but the geometry is regular at this point if

$$k = \frac{\ell^2}{d+1}. \quad (9.16)$$

Otherwise, there is a conical singularity at $r = 0$.

2. For $k = 0$, the geometry is the Euclidean AdS_2 ($EAdS_2$) space in Poincaré coordinates but with one of them compact.

3. For $k < 0$, the geometry needs a better coordinate system than we now describe.

We return to the u coordinate and we have the following geometries respectively:

– For $k > 0$ we obtain

$$ds^2 = du^2 + k \sinh^2 \left[\frac{\sqrt{d+1}}{\ell} (u - u_0) \right] d\theta^2 - \frac{\ell^2 R_1}{d(d+1)} ds_{AdS_d}^2, \quad (9.17)$$

with $u \geq 0$. The parameter u_0 translates into an arbitrary radius for θ . This has a generic conical singularity.

The regular metric has k given in (9.16). and in such a case \mathcal{M}_2 is the Euclidean hyperboloid given by

$$-(x^0)^2 + (x^1)^2 + (x^2)^2 = -\frac{\ell^2}{d+1}. \quad (9.18)$$

We denote this space with $EAdS_2^+$.

– $k = 0$. The associated metric in the u coordinate is

$$ds^2 = du^2 + \exp \left[\frac{2\sqrt{d+1}}{\ell} (u + c) \right] d\theta^2 - \frac{\ell^2 R_1}{d(d+1)} ds_{AdS_d}^2, \quad u \in \mathbb{R}. \quad (9.19)$$

Again the parameter c translates into an arbitrary radius for the coordinate θ . This metric, if θ is non-compact is $EAdS_2$ in Poincaré coordinates, and it is diffeomorphic to the hyperboloid. When θ is compact, this is not true anymore. We denote this space as $EAdS_2^0$.

- $k < 0$. In this case the metric (9.15) extends from $r \in [-\sqrt{|k|}, +\infty)$. This gives the metric in the u coordinate

$$ds^2 = du^2 + |k| \cosh^2 \left[\frac{\sqrt{d+1}}{\ell} (u - u_0) \right] d\theta^2 - \frac{\ell^2 R_1}{d(d+1)} ds_{AdS_d}^2, \quad (9.20)$$

with $u > u_0$. However, this metric is not geodesically complete and one has to extend u to all real values. The manifold now is a wormhole with S^1 boundaries that is the usual $EAdS_2$. We shall denote it as $EAdS_2^-$. The constant u_0 allows an arbitrary radius for the S^1 .

All the \mathcal{M}_2 metrics above also exist when θ is taking values in the real line.

In all three cases above the Kretschmann scalar of the total $(d+2)$ -dimensional manifold is the same and is equal to

$$\mathcal{K} = \frac{2(d+1)^2(3d-2)}{(d-1)\ell^4}. \quad (9.21)$$

We can obtain Minkowski signature solutions by analytically continuing $\theta \rightarrow it$. In this case $EAdS_2^{+,0}$ becomes the AdS_2 black hole while $EAdS_2^-$ becomes AdS_2 .

- $\dot{A}_1 \neq 0$.

In this case $A_2(u)$ can be obtained from

$$A_2(u) = \int \frac{\alpha_1(d-1)\ell^2 e^{-(d+1)A_1} + 2}{2\ell^2 \dot{A}_1} du + \alpha_2. \quad (9.22)$$

Here α_2 is another constant of integration. By defining

$$A_1(u) = \log r(u), \quad (9.23)$$

equation (9.5) becomes

$$\left(\frac{dr}{du} \right)^2 \equiv f(r) = -\alpha_1 r^{1-d} + \frac{R_1}{d(d-1)} + \frac{r^2}{\ell^2}, \quad (9.24)$$

and equation (9.22) gives

$$A_2(r(u)) = \frac{1}{2} \log f(r) + \frac{1}{2} \log(\ell^2 d(d-1)) + \alpha_2. \quad (9.25)$$

Therefore the metric in these two coordinates are related as follows

$$\begin{aligned} ds^2 &= du^2 + e^{2A_1(u)} ds_{AdS_d}^2 + e^{2A_2(u)} d\theta^2 \\ &= \frac{dr^2}{f(r)} + r^2 ds_{AdS_d}^2 + \ell^2 d(d-1) e^{2\alpha_2} f(r) d\theta^2, \end{aligned} \quad (9.26)$$

where $f(r)$ is defined in equation (9.24). The last metric describes the (well-known) topological black holes with a negative cosmological constant, [61, 62], (they are reviewed in appendix F).

The function $f(r)$ in (9.24) has the following properties ($d \geq 2$).

1. $f \rightarrow +\infty$ as $r \rightarrow +\infty$.
2. $r \rightarrow 0$ is always a curvature singularity of the metrics in (9.26) and the Kretschmann scalar is given by

$$\mathcal{K} = \alpha_1^2 (d^2 - 1) d^2 r^{-2(d+1)} + \frac{2(d+1)(d+2)}{\ell^4}. \quad (9.27)$$

3. $f \rightarrow +\infty$ as $r \rightarrow 0^+$ when $\alpha_1 < 0$, and $f \rightarrow -\infty$ as $r \rightarrow 0^+$ when $\alpha_1 > 0$. As we show below when $\alpha_1 = 0$ the space is AdS_{d+2} provided α_2 is chosen appropriately.
4. At a fixed value of R_1 , there is a value $\alpha_1^{crit} < 0$ so that if $\alpha_1 < \alpha_1^{crit}$, then always $f > 0$ as $r \in [0, +\infty)$. All solutions with $\alpha_1 < \alpha_1^{crit}$ have a bad naked singularity.
5. When $\alpha_1 = \alpha_1^{crit}$ then there is a single positive double zero of f . In this case, the Minkowski signature solution has an extremal horizon. The geometry near this extremal horizon is $AdS_2 \times AdS_d$.
6. When $\alpha_1^{crit} < \alpha_1 < 0$ then f has two positive zeroes with f being negative in between the zeroes. The structure of such black holes is similar to Reissner-Nörstrom ones. In particular, the inner horizon is a Cauchy horizon. If the hyperbolic slice is a finite volume manifold, then such black holes have finite entropy.
7. When $\alpha_1 > 0$, then f has a single positive zero. Beyond this zero (at small values of r), $f < 0$.
8. $r \rightarrow \infty$ is a regular conformal boundary of the metrics in (9.26).
9. The relevant (Euclidean) solutions are all segments between a zero or a divergence of f , while $f \geq 0$.
10. Most of these solutions are singular. The only potentially regular Euclidean solutions are those between $r = +\infty$ and the first non-trivial zero

r_* for f . The regular solutions are obtained by adjusting the constant α_2 as

$$e^{2\alpha_2} = \frac{4}{d(d-1)\ell^2(f'(r_*))^2}. \quad (9.28)$$

We conclude that in this case we have two families of regular solutions in the Euclidean case:

- The solutions with $\alpha_1^{crit} < \alpha_1 < 0$ that become RN-like black holes upon analytic continuation of $\theta \rightarrow i\theta$.
- The solutions with $\alpha_1 > 0$, that become Schwarzschild-like black holes upon analytic continuation of $\theta \rightarrow i\theta$.

Minkowski signature solutions can also be obtained by giving to the AdS_d a Minkowski signature.

The “ground” state solution, is the extremal solution with $\alpha_1 = \alpha_1^{crit}$. It has zero temperature, but the asymptotic circle can have any radius. All other solutions have a fixed asymptotic circle radius that is correlated with their temperature. At a fixed asymptotic circle radius the non-extremal black holes have a lower free energy compared to the extremal one, [62].

9.3 The global AdS_{d+2} solution

The solution obtained from (9.5) and (9.22) when we choose $\alpha_1 = 0$ is

$$ds^2 = du^2 - \frac{\ell^2 R_1}{d(d-1)} \cosh^2 \frac{u-u_0}{\ell} ds_{AdS_d}^2 - e^{2\alpha_2} \ell^2 R_1 \sinh^2 \frac{u-u_0}{\ell} d\theta^2. \quad (9.29)$$

Choosing

$$e^{2\alpha_2} R_1 = -1, \quad (9.30)$$

this metric is the metric of AdS_{d+2} in global coordinates. By the following change of variables

$$-\ell^2 k \cosh^2 \frac{u-u_0}{\ell} = r^2, \quad \theta = \sqrt{\frac{k}{e^{2\alpha_2} \ell^2 R_1}} i t \quad ; \quad k \equiv \frac{R_1}{d(d-1)}, \quad (9.31)$$

the metric becomes

$$ds^2 = -f(r)dt^2 + \frac{1}{f(r)}dr^2 + r^2 ds_{AdS_d}^2 \quad ; \quad f(r) = \frac{r^2}{\ell^2} + k. \quad (9.32)$$

This is the solution that has been discussed in appendix F when $M = 0$.

9.4 Relations between parameters in two coordinates

Let us for simplicity consider $d = 3$ and $\dot{A} \neq 0$. Solving equation (9.24) gives us

$$r^2(u) = \frac{1}{24} \left(\ell^2 e^{-2\sqrt{6}c_1 - \frac{2u}{\ell}} (144\alpha_1 + \ell^2 R_1^2) + e^{2\sqrt{6}c_1 + \frac{2u}{\ell}} - 2\ell^2 R_1 \right), \quad (9.33)$$

where c_1 is the constant of integration. Moreover, there is another solution that can be found from (9.33) by replacing $u \rightarrow -u$. At large values of r or when $u \rightarrow +\infty$ we can find the expansions of scale factors in (9.7a) and (9.7b) by using equations (9.23) and (9.25) together with (9.24) if we choose

$$\bar{A}_1 = \sqrt{6}c_1 - \frac{1}{2} \log 24 \quad , \quad \bar{A}_2 = \alpha_2 + \sqrt{6}c_1 - \log 2 \quad , \quad \alpha_1 = -\frac{4C}{\ell^2} e^{4\bar{A}_1} \quad , \quad (9.34)$$

where \bar{A}_1, \bar{A}_2 and C are parameters in u coordinate while α_1, α_2 and c_1 are in r coordinate.

Now let us consider a solution which is regular at $u = u_0$ and has a boundary at $u \rightarrow +\infty$. The regularity at $u = u_0$ implies that the scale factor of A_1 is constant but $e^{A_2} \rightarrow 0$. In r coordinate this translates to a solution where at $r = r_h$

$$f(r_h) = -\alpha_1 r_h^{-2} + \frac{R_1}{6} + \frac{r_h^2}{\ell^2} = 0 \quad . \quad (9.35)$$

This describes a topological black hole with a horizon at $r = r_h$, see appendix F. Now we can compare the expansions near the regular end-points. The expansions in u coordinate are given in (9.9a) and (9.9b). The two free parameters a_0 and c_0 then are given by

$$a_0 = r_h^2 \quad , \quad c_0 = e^{2\alpha_2} \frac{(12r_h^2 + \ell^2 R_1)^2}{6r_h^2} \quad . \quad (9.36)$$

We can read the values of the sources and vevs in terms of the black hole solutions

$$\mathcal{R}_1 = \ell^2 R_1 e^{-2\bar{A}_1} = 24\ell^2 R_1 e^{-2\sqrt{6}c_1} \quad , \quad C = -\frac{1}{4} \alpha_1 \ell^2 e^{-4\bar{A}_1} = -144\omega M \ell^2 e^{-4\sqrt{6}c_1} \quad , \quad (9.37)$$

where ω and M , the mass of the black hole, are defined in (F.8) and (F.11). We can choose $\bar{A}_1 = \bar{A}_2 = 0$ for simplicity then we have $c_1 = \frac{\log 24}{2\sqrt{6}}$ and $\alpha_2 = -\frac{1}{2} \log 6$ and

$$\mathcal{R}_1 = \ell^2 R_1 \quad , \quad C = -\frac{\omega M \ell^2}{4} \quad . \quad (9.38)$$

Knowing the above parameters, we now compute the free energy of the regular solutions in both coordinates. The Euclidean action is given by

$$I_E = \frac{M_P^3}{2} V_S V_{AdS_3} \left(e^{A_1+A_2} U R_1 \Big|_{u_0}^{+\infty} - 3e^{3A_1+A_2} (3\dot{A}_1 + \dot{A}_2) \Big|_{u_0}^{u=+\infty} + e^{3A_1+A_2} (3\dot{A}_1 + \dot{A}_2) \Big|_{u_0} \right) \quad , \quad (9.39)$$

where the last term is non-zero, unlike the $n > 1$ cases. In this equation $V_{AdS_3} \sim 1/|R_1|^{\frac{3}{2}}$ is the volume of three dimensional slice and

$$V_S = \int_0^\beta d\theta \quad , \quad (9.40)$$

where β is the length of S^1 . In (9.39), U is a scalar field given by

$$(\dot{A}_1 + \dot{A}_2)U + \dot{U} + 1 = 0, \quad (9.41)$$

and by using the expansions (9.7a) and (9.7b) we find that as $u \rightarrow +\infty$

$$U(u) = -\frac{\ell}{2} + \mathcal{B}e^{-2\frac{u}{\ell}} + (C\ell - \frac{\ell^5 R_1}{576e^{4\bar{A}_1}})e^{-4\frac{u}{\ell}} + \mathcal{O}(e^{-6\frac{u}{\ell}}). \quad (9.42)$$

Moreover, near the regular end-point $u = u_0$ equations (9.9a) and (9.9b) give

$$U(u) = \frac{\mathfrak{b}}{u - u_0} - \left(\frac{1}{2} + \frac{2\mathfrak{b}}{3\ell^2}\right)(u - u_0) + \mathcal{O}(u - u_0)^3. \quad (9.43)$$

We can consider $\mathfrak{b} = 0$, so the contribution to the free energy of the first term of (9.39) at $u = u_0$ is zero. On the other hand, we can solve U in r coordinate exactly, which we find

$$\left(\frac{R_1}{3} + 4\frac{r^2}{\ell^2}\right)U + 2rfU' + 2rf^{\frac{1}{2}} = 0, \rightarrow U(r) = \frac{2c_2 - \sqrt{6}\ell r^2}{2\sqrt{6r^4 + \ell^2 r^2 R_1 - 6\alpha_1 \ell^2}}, \quad (9.44)$$

where c_2 is another constant of integration. $U(r)$ is diverging at $r = r_h$ because of (9.35). To have a regular function at this point we should have

$$c_2 = \sqrt{\frac{3}{2}}\ell r_h^2. \quad (9.45)$$

If we expand the solution (9.44) near the boundary at $r \rightarrow +\infty$ and change $r \rightarrow u$ by using (9.33) we obtain

$$\mathcal{B} = \left(4\sqrt{6}c_2 + \ell^3 R_1\right) e^{-2\sqrt{6}c_1} = \ell \left(12r_h^2 + \ell^2 R_1\right) e^{-2\sqrt{6}c_1}. \quad (9.46)$$

Returning to (9.39), if we do the proper counter-terms we can compute the renormalized action as following

$$\begin{aligned} I_E^{ren} &= \frac{1}{2}M_P^3 V_S V_{AdS_3} \left(e^{\bar{A}_1 + \bar{A}_2} R_1 \mathcal{B} - \frac{1}{\ell} a_0^{\frac{3}{2}} c_0^{\frac{1}{2}} \right) \\ &= M_P^3 V_S V_{AdS_3} \sqrt{6} e^{\alpha_2} \ell \left(-\frac{r_h^4}{\ell^2} + \frac{1}{6} R_1 r_h^2 + \frac{1}{48} R_1^2 \ell^2 \right). \end{aligned} \quad (9.47)$$

The last relation is the known result of free energy for topological black holes with negative cosmological constant and $r_h = r_+$, see appendix F for more details. By using the definition of temperature, we find that

$$\beta = \frac{2\pi}{(e^{A_2})'} \Big|_{u=u_0} \rightarrow T = \frac{c_0^{\frac{1}{2}}}{2\pi\ell}. \quad (9.48)$$

The free energy of the black hole is given by

$$\mathcal{F} = \frac{I_E^{ren}}{\beta} = (M - M_{crit}) - TS, \quad (9.49)$$

where M , M_{crit} and S are mass, critical mass, and entropy of the black hole respectively, and are given in equations (F.11), (F.14) and (F.15).

10. On general Einstein manifold solutions with constant negative curvature.

The general solutions with constant negative curvature we have found in this paper, and many previous ones provide a hierarchical construction of such solutions as conifolds of conifolds of conifolds etc.

A few examples are as follows:

In two dimensions, the solutions to Einstein's equations with a negative cosmological constant, up to diffeomorphisms consist of the family of manifolds \mathcal{M}_2 we described in the previous section.

In three dimensions, the solutions to Einstein's equations with a negative cosmological constant, up to diffeomorphisms consist of the two-parameter family of rotating AdS_3 -Schwarzschild black holes (that includes also AdS_3).

Consider now solutions in four dimensions with a negative cosmological constant. The maximally symmetric solution is AdS_4 and in global coordinates, it has $S^1 \times S^2$ slices. The Euclidean symmetry is $O(4, 1)$. In this same slicing belongs also the AdS_4 -Schwarzschild black hole with generic symmetry $O(2) \times O(3)$. The difference between these two solutions is that, in the first, it is S^2 that shrinks to zero size ending the geometry while in the second, it is the S^1 that shrinks to zero size ending the geometry.

There are however further solutions where the slices are S^3 , [10], with generic symmetry $O(4)$, as well as conifold solutions with $S^1 \times S^1 \times S^1$ solutions (tori) that correspond to AdS_4 -Schwarzschild black holes with the toroidal horizon and generic symmetry $O(2)^3$. There are also the $AdS_2 \times S^1$ solutions studied here with generic symmetry $O(2) \times O(2, 1)$. In the place of AdS_2 above we can have any of our \mathcal{M}_2 solutions. We can also replace S^1 with R .

All of these four-dimensional solutions are generically distinct and provide a large class of solutions with four-dimensional constant negative curvature. The structure of their boundaries differs. Some solutions are diffeomorphic to each other, but most are distinct manifolds. We do not know if they exhaust all solutions with the negative cosmological constant.

We now move to the next dimension which is five and describe the various conifold solutions to the constant negative curvature equations. The slices can be $(S^1)^4$, $S^1 \times S^3$, $S^2 \times S^2$, $(S^1)^2 \times S^2$, $AdS_2 \times S^2$, $AdS_2 \times (S^1)^2$, $AdS_3 \times S^1$ and $AdS_2 \times AdS_2$ and AdS_4 . For example, $(S^1)^4$ are the five-dimensional black holes with the toroidal horizon, $S^1 \times S^3$ are the five-dimensional black holes with S^3 horizon, and $(S^1)^2 \times S^2$ are the five-dimensional black holes with $S^1 \times S^2$ horizon. The $S^2 \times S^2$ solution was analyzed in [15] and exhibited Effimov phenomena. In the $AdS_2 \times S^2$ and $AdS_2 \times (S^1)^2$ solutions AdS_2 stands for the one-parameter family of AdS_2 black holes. The $AdS_3 \times S^1$ solutions contained in the slice the full two-parameter family of BTZ black holes. Finally, $AdS_2 \times AdS_2$ slices have not been systematically stud-

ied so far but we expect these solutions to have two boundaries as neither AdS_2 can shrink regularly to zero size.

This algorithm clearly generalizes to higher dimensions. The structure of the boundaries of such solutions is variable.

Acknowledgements

We would like to thank C. Behan, T. Brennan, M. Chernodub, J. Gauntlett, C. Herzog, A. Konechny, A. Lerda, V. Niarchos, M. Roberts, C. Rosen, J. Russo, A. Stergiou, E. Tonni and A. Tseytlin for helpful conversations.

This work was supported in part by CNRS grant IEA 199430. The work of A. G. is supported by Ferdowsi University of Mashhad under grant 2/60036 (1402/03/06).

APPENDIX

A. Product space ansatz for the slice

Consider the following ansatz, a block diagonal $(d + 1)$ -dimensional metric

$$ds^2 = g_{ab}dx^a dx^b = du^2 + \sum_{i=1}^n e^{2A_i(u)} \zeta_{\alpha_i, \beta_i}^i dx^{\alpha_i} dx^{\beta_i}, \quad (\text{A.1})$$

where $\zeta_{\alpha_i, \beta_i}^i$ is the d_i -dimensional metric of the i th Einstein manifold, α_i and β_i take values in the d_i coordinates of this manifold. Each Einstein manifold is associated with a different scale factor, all depending on the coordinate u only. Note that every d -dimensional slice at constant u is given by the product of n Einstein manifolds of dimension d_1, \dots, d_n .

For this ansatz, the Ricci tensor reads

$$R_{uu} = - \sum_{k=1}^n d_k (\ddot{A}_k + \dot{A}_k^2), \quad (\text{A.2a})$$

$$R_{u\alpha} = 0 \quad \text{for} \quad \alpha \neq u, \quad (\text{A.2b})$$

$$R_{\alpha_i \beta_i} = - (\ddot{A}_i + \dot{A}_i \sum_{k=1}^n d_k \dot{A}_k) g_{\alpha_i \beta_i} + R_{\alpha_i \beta_i}^{\zeta_i}, \quad (\text{A.2c})$$

$$R_{\alpha_i \beta_j} = 0 \quad \text{for} \quad i \neq j, \quad (\text{A.2d})$$

where $R_{\alpha_i \beta_i}^{\zeta_i}$ is the Ricci tensor of the d_i -dimensional Einstein metric $\zeta_{\alpha_i \beta_i}^i$. Thus, the Ricci scalar is

$$R = -2 \sum_{k=1}^n d_k \ddot{A}_k - \left(\sum_{k=1}^n d_k \dot{A}_k \right)^2 - \sum_{k=1}^n d_k \dot{A}_k^2 + \sum_{k=1}^n e^{-2A_k} R^{\zeta^k}, \quad (\text{A.3})$$

where R^{ζ^k} is the Ricci scalar of the metric ζ^k .

We consider in general an Einstein-dilaton theory in a $d + 1$ dimensional bulk space-time. The most general two-derivative action is

$$S = M_P^{d-1} \int d^{d+1}x \sqrt{-g} \left(R - \frac{1}{2} g^{ab} \partial_a \varphi \partial_b \varphi - V(\varphi) \right). \quad (\text{A.4})$$

The energy-momentum tensor $T_{\mu\nu} = \partial_\mu \varphi \partial_\nu \varphi - g_{\mu\nu} (\frac{1}{2} \partial_a \varphi \partial^a \varphi + V)$ would be as follow

$$T_{uu} = \frac{1}{2} \dot{\varphi}^2 - V, \quad (\text{A.5a})$$

$$T_{\alpha_i \beta_j} = -g_{\alpha_i \beta_j} \left(\frac{1}{2} \dot{\varphi}^2 + V \right). \quad (\text{A.5b})$$

Finally, the Einstein tensor reads

$$G_{uu} = \frac{1}{2} \left(\sum_{k=1}^n d_k \dot{A}_k \right)^2 - \frac{1}{2} \sum_{k=1}^n d_k \dot{A}_k^2 - \frac{1}{2} \sum_{k=1}^n e^{-2A_k} R^{\zeta^k}, \quad (\text{A.6a})$$

$$\begin{aligned} G_{\alpha_i \beta_i} &= \left(-(\ddot{A}_i + \dot{A}_i \sum_{k=1}^n d_k \dot{A}_k) + \sum_{k=1}^n d_k \ddot{A}_k + \frac{1}{2} \left(\sum_{k=1}^n d_k \dot{A}_k \right)^2 \right. \\ &\quad \left. + \frac{1}{2} \sum_{k=1}^n d_k \dot{A}_k^2 - \frac{1}{2} \sum_{k \neq i} e^{-2A_k} R^{\zeta^k} \right) g_{\alpha_i \beta_i} + G_{\alpha_i \beta_i}^{\zeta^i}, \end{aligned} \quad (\text{A.6b})$$

where $G_{\alpha_i \beta_i}^{\zeta^i}$ is the Einstein tensor of the metric ζ^i . Since ζ^i is an Einstein metric, we have

$$G_{\alpha_i \beta_i}^{\zeta^i} = \left(\frac{1}{d_i} - \frac{1}{2} \right) R^{\zeta^i} \zeta_{\alpha_i \beta_i} = \left(\frac{1}{d_i} - \frac{1}{2} \right) e^{-2A_i} R^{\zeta^i} g_{\alpha_i \beta_i}. \quad (\text{A.7})$$

Hence, we can rewrite the $\alpha_i \beta_i$ component of the Einstein tensor as

$$G_{\alpha_i \beta_i} = \left(-(\ddot{A}_i + \dot{A}_i \sum_{k=1}^n d_k \dot{A}_k - \frac{1}{d_i} e^{-2A_i} R^{\zeta^i}) + \sum_{k=1}^n d_k \ddot{A}_k + \sum_{k=1}^n d_k \dot{A}_k^2 + G_{uu} \right) g_{\alpha_i \beta_i}. \quad (\text{A.8})$$

Therefore, the equations of motions, given by $2G_{\mu\nu} = T_{\mu\nu}$, read

$$\left(\sum_{k=1}^n d_k \dot{A}_k \right)^2 - \sum_{k=1}^n d_k \dot{A}_k^2 - \sum_{k=1}^n e^{-2A_k} R^{\zeta^k} - \frac{1}{2} \dot{\varphi}^2 + V = 0, \quad (\text{A.9a})$$

$$-(\ddot{A}_i + \dot{A}_i \sum_{k=1}^n d_k \dot{A}_k) - \frac{1}{d_i} e^{-2A_i} R^{\zeta^i} + \sum_{k=1}^n d_k \ddot{A}_k + \sum_{k=1}^n d_k \dot{A}_k^2 + \frac{1}{2} \dot{\varphi}^2 = 0, \quad (\text{A.9b})$$

$$\ddot{\varphi} + \sum_{k=1}^n d_k \dot{A}_k \dot{\varphi} - \partial_\varphi V = 0. \quad (\text{A.9c})$$

Multiply (A.9b) by d_i , sum over i , divided by d and reorganize we obtain

$$2 \left(1 - \frac{1}{d} \right) \sum_{k=1}^n d_k \ddot{A}_k + \frac{2}{d} \sum_{i < j} d_i d_j (\dot{A}_i - \dot{A}_j)^2 + \frac{2}{d} \sum_{k=1}^n e^{-2A_k} R^{\zeta^k} + \dot{\varphi}^2 = 0, \quad (\text{A.10})$$

the symmetric version of (A.9b).

These equations are valid for any choice of n Einstein metrics $\zeta_{\alpha_i \beta_i}^i$. However, the existence of solutions is not guaranteed for an arbitrary choice. The difference between (A.9b) for different indices yields constraints on the scale factors and the curvatures

$$\ddot{A}_i + \dot{A}_i \sum_{k=1}^n d_k \dot{A}_k - \frac{1}{d_i} e^{-2A_i} R^{\zeta^i} = \ddot{A}_j + \dot{A}_j \sum_{k=1}^n d_k \dot{A}_k - \frac{1}{d_j} e^{-2A_j} R^{\zeta^j}, \quad (\text{A.11})$$

for all i and j . One can see that these constraints are satisfied by $A_i = A(u)$ and $R^{\zeta^i} = d_i \kappa$ for all i , where κ is a constant and $A(u)$ is a function of u . In this case, the equations of motion (A.9a)–(A.9c) reduce to

$$d(d-1)\dot{A}^2 - e^{-2A}R^\zeta - \frac{1}{2}\dot{\varphi}^2 + V = 0, \quad (\text{A.12a})$$

$$2(d-1)\ddot{A} + \dot{\varphi}^2 + \frac{2}{d}e^{-2A}R^\zeta = 0, \quad (\text{A.12b})$$

$$\ddot{\varphi} + d\dot{A}\dot{\varphi} - \partial_\varphi V = 0. \quad (\text{A.12c})$$

This could be foreseen since under these conditions there is only one scale factor and the product space is an Einstein manifold, since (A.12a)–(A.12c) are valid for any Einstein metric $\zeta_{\mu\nu}$.

A.1 The curvature invariants

To check the regularity of the solutions we should calculate R^2 , $R_{ab}R^{ab}$, and $R_{abcd}R^{abcd}$ for the metrics above. The first two are straightforward to compute using (A.2a)–(A.2d). The Ricci squared is

$$\begin{aligned} R_{ab}R^{ab} &= R_{uu}R^{uu} + R_{\alpha_i\beta_i}R^{\alpha_i\beta_i} \\ &= \left(\sum_{i=1}^n d_i(\ddot{A}_i + \dot{A}_i^2) \right)^2 + \sum_{i=1}^n d_i \left(e^{-2A_i} \kappa - (\ddot{A}_i + \dot{A}_i \sum_{j=1}^n d_j \dot{A}_j) \right)^2. \end{aligned} \quad (\text{A.13})$$

The Ricci scalar reads

$$R = -2 \sum_{i=1}^n d_i \ddot{A}_i - \left(\sum_{i=1}^n d_i \dot{A}_i \right)^2 - \sum_{i=1}^n d_i \dot{A}_i^2 + \sum_{i=1}^n e^{-2A_i} R^{\zeta^i}. \quad (\text{A.14})$$

The non-zero Riemann tensor components are given by

$$R_{\alpha_i u u \beta_i} = e^{2A_i} \zeta_{\alpha_i \beta_i}^i (\ddot{A}_i + \dot{A}_i^2) = -R_{u \alpha_i u \beta_i} = -R_{\alpha_i u \beta_i u}. \quad (\text{A.15a})$$

$$\begin{aligned} R_{\alpha_i \beta_j \gamma_k \delta_l} &= e^{2(A_i + A_j)} \dot{A}_i \dot{A}_j (\delta_{il} \delta_{jk} \zeta_{\alpha_i \delta_i}^i \zeta_{\beta_j \gamma_j}^j - \delta_{ik} \delta_{jl} \zeta_{\alpha_i \gamma_i}^i \zeta_{\beta_j \delta_j}^j) \\ &\quad + e^{2A_i} \delta_{ij} \delta_{kl} \delta_{ik} R_{\alpha_i \beta_i \gamma_i \delta_i}^{\zeta^i}, \end{aligned} \quad (\text{A.15b})$$

and one can see that the Riemann tensor is pairwise diagonal. So one can calculate the Kretschmann scalar as a sum of all non-zero components of the Riemann tensor

$$\mathcal{K} = 4K_1^2 + K_2^2 + 2K_3^2, \quad (\text{A.16})$$

where

$$K_1 = R_{u \alpha_i}{}^{u \beta_i} = \delta_{\alpha_i}{}^{\beta_i} (\ddot{A}_i + \dot{A}_i^2). \quad (\text{A.17})$$

Equation (A.15b) with $i = k$ and $j = l$ gives

$$K_2 = R_{\alpha_i \beta_j}{}^{\gamma_i \delta_j} = \dot{A}_i \dot{A}_j (-\delta_{\alpha_i}{}^{\gamma_i} \delta_{\beta_j}{}^{\delta_j}), \quad (\text{A.18})$$

and with $i = j = k = l$ gives

$$K_3^2 = (R_{\alpha_i \beta_j}^{\gamma_i \delta_i})^2 = e^{-4A_i} \mathcal{K}^{\zeta^i} - 4e^{-2A_i} (\dot{A}_i)^2 R^{\zeta^i} - 2d_i(d_i - 1)(\dot{A}_i)^4. \quad (\text{A.19})$$

Finally the Kretschmann scalar is

$$\begin{aligned} \mathcal{K} = & \sum_{i=1}^n \left(e^{-4A_i} \mathcal{K}^{\zeta^i} - 4e^{-2A_i} (\dot{A}_i)^2 R^{\zeta^i} - 2d_i (\dot{A}_i)^4 \right. \\ & \left. + 4d_i (\ddot{A}_i + \dot{A}_i^2)^2 \right) + \sum_{i,j=1}^n 2d_i d_j (\dot{A}_i \dot{A}_j)^2, \end{aligned} \quad (\text{A.20})$$

where \mathcal{K}^{ζ^i} is the Kretschmann scalar related to ζ^i .

B. Various global coordinates on AdS_{d+n+1} and its Euclidean version

In this appendix, we consider various coordinate systems of AdS_{d+n+1} , both standard global coordinates as well as coordinates adapted to $AdS_d \times S^n$ slices and their Euclidean versions. They will be important as benchmarks for the space of solutions we shall find.

B.1 Standard global coordinates on AdS_{d+n+1}

We consider the embedding equation that defines AdS_{d+n+1}

$$-(x^0)^2 - (x^{(-1)})^2 + \sum_{i=1}^{d+n} (x^i)^2 = -\ell^2. \quad (\text{B.1})$$

We start with the standard global coordinates. First, we parameterize

$$x^i = r_2 n^i \quad , \quad i = 1, 2, \dots, d+n \quad , \quad n^i n^i = 1 \quad , \quad r_2 \geq 0, \quad (\text{B.2a})$$

$$x^0 = r_1 \cos \theta \quad , \quad x^{(-1)} = r_1 \sin \theta \quad , \quad r_1 \geq 0. \quad (\text{B.2b})$$

The Minkowski signature metric in $(2, d+n)$ dimensions becomes

$$ds^2 = -(dx^0)^2 - (dx^{(-1)})^2 + dx^i dx^i = -dr_1^2 - r_1^2 d\theta^2 + dr_2^2 + r_2^2 d\Omega_{d+n-1}^2, \quad (\text{B.3})$$

and the constraint in (B.1) can be written as

$$-r_1^2 + r_2^2 = -\ell^2 \quad \Rightarrow \quad r_1^2 - r_2^2 = \ell^2. \quad (\text{B.4})$$

We now introduce new coordinates

$$r_1 = \ell \cosh(\rho) \quad , \quad r_2 = \ell \sinh(\rho) \quad , \quad \ell \geq 0 \quad , \quad \rho \geq 0, \quad (\text{B.5})$$

and rewrite the metric in (B.3) as

$$ds^2 = -d\ell^2 - \ell^2 \cosh^2(\rho) d\theta^2 + \ell^2 d\rho^2 + \ell^2 \sinh^2(\rho) d\Omega_{d+n-1}^2. \quad (\text{B.6})$$

AdS_{d+n+1} is obtained from the metric above by setting ℓ to be constant

$$ds_{n+d+1}^2 = \ell^2 \left(-\cosh^2(\rho) d\theta^2 + d\rho^2 + \sinh^2(\rho) d\Omega_{d+n-1}^2 \right). \quad (\text{B.7})$$

The usual AdS is obtained by extending the “time” θ from $[0, 2\pi]$ to the whole real line. We summarize the embedding map of AdS in global coordinates to the $(2, d+n)$ Minkowski space

$$x^0 = \ell \cosh(\rho) \cos \theta, \quad x^{(-1)} = \ell \cosh(\rho) \sin \theta, \quad x^i = \ell \sinh(\rho) n^i, \quad \rho \geq 0. \quad (\text{B.8})$$

The global boundary of AdS is $\rho \rightarrow \infty$ that corresponds to

$$r_1 = \left((x^0)^2 + (x^{(-1)})^2 \right)^{\frac{1}{2}} \rightarrow \infty, \quad r_2 = \left(\sum_{i=1}^{n+d} x^i x^i \right)^{\frac{1}{2}} \rightarrow \infty, \quad (\text{B.9})$$

with their ratio $\frac{r_1}{r_2}$ fixed. Indeed the topology of the boundary is $S^1 \times S^{d+n-1}$.

B.2 Coordinates fibered over $AdS_d \times S^n$

We now introduce new coordinates for the same space. We can separate the variables in x^μ with $\mu = -1, 0, 1, 2, \dots, d$ and y^i , $i = 1, 2, \dots, n$ and we parametrize the first set by AdS_d and the second by S^n

$$x^\mu = r m^\mu, \quad m \cdot m = -1, \quad y^i = \rho n^i, \quad n \cdot n = 1, \quad (\text{B.10})$$

where $r, \rho \geq 0$, and the flat $(2, d+n)$ metric is

$$ds^2 = -dr^2 + r^2 ds_{AdS_d}^2 + d\rho^2 + \rho^2 d\Omega_n^2. \quad (\text{B.11})$$

The AdS_{n+d+1} constraint is

$$-r^2 + \rho^2 = -\ell^2 \quad \Rightarrow \quad (\text{B.12a})$$

$$r = \ell \cosh(u), \quad \rho = \ell \sinh(u), \quad u > 0. \quad (\text{B.12b})$$

The induced metric becomes

$$ds_{n+d+1}^2 = \ell^2 \left(du^2 + \cosh^2(u) ds_{AdS_d}^2 + \sinh^2(u) d\Omega_n^2 \right), \quad u \geq 0, \quad (\text{B.13})$$

and has one patch $u > 0$.²⁰

²⁰In general, if we have a CFT on $AdS_d \times S^n$ the physics should depend on the ratio of the two radius scales. Here this ratio is set to one.

There is a related coordinate system where we map

$$\sinh(u) = \tan(\phi) \quad , \quad du = \frac{d\phi}{\cos(\phi)} \quad , \quad \phi \in \left[0, \frac{\pi}{2}\right] \quad , \quad (\text{B.14})$$

and the new metric becomes

$$ds^2 = \frac{\ell}{\cos^2(\phi)} \left(d\phi^2 + \sin^2(\phi) d\Omega_n^2 + ds_{AdS_d}^2 \right) \quad , \quad (\text{B.15})$$

which is conformal to $AdS_d \times S^{n+1}$. However as $\phi \in \left[0, \frac{\pi}{2}\right]$, we have only one hemisphere of S^{n+1} .

We now write explicitly (B.10)

$$x^0 = r_3 \cosh(\rho) \cos \theta \quad , \quad x^{(-1)} = r_3 \cosh(\rho) \sin \theta \quad , \quad x^i = r_3 \sinh(\rho) n^i \quad , \quad (\text{B.16a})$$

$$i = 1, 2, \dots, d-1 \quad , \quad n \cdot n = 1 \quad , \quad \rho \geq 0 \quad , \quad (\text{B.16b})$$

$$y^i = r_4 m^i \quad , \quad i = 1, 2, \dots, n+1 \quad , \quad m \cdot m = 1 \quad , \quad (\text{B.16c})$$

$$r_3 = \ell \cosh(u) \quad , \quad r_4 = \ell \sinh(u) \quad , \quad u \geq 0 \quad . \quad (\text{B.16d})$$

Consider first the limit $u \rightarrow \infty$. In this case

$$A \quad : \quad \left((x^0)^2 + (x^{(-1)})^2 \right)^{\frac{1}{2}} \rightarrow \infty \quad , \quad \left(\sum_{i=1}^d (x^i)^2 \right)^{\frac{1}{2}} \rightarrow \infty \quad , \quad \left(\sum_{i=1}^n (y^i)^2 \right)^{\frac{1}{2}} \rightarrow \infty \quad , \quad (\text{B.17})$$

in the same way but this is part of the original boundary of AdS_{d+n+1} . It does not contain the limit where $\left(\sum_{i=1}^d (x^i)^2 \right)^{\frac{1}{2}} \rightarrow \infty$ and $\left(\sum_{i=1}^n (y^i)^2 \right)^{\frac{1}{2}}$ remains finite or when $\left(\sum_{i=1}^n (y^i)^2 \right)^{\frac{1}{2}} \rightarrow \infty$ and $\left(\sum_{i=1}^d (x^i)^2 \right)^{\frac{1}{2}}$ remains finite. Therefore the part of the boundary obtained by $u \rightarrow \infty$ is $S^1 \times S^{d-1} \times S^{n-1} \subset S^1 \times S^{d+n-1}$. This piece also includes the special limit

$$B \quad : \quad \left((x^0)^2 + (x^{(-1)})^2 \right)^{\frac{1}{2}} \rightarrow \infty \quad , \quad \left(\sum_{i=1}^d (x^i)^2 \right)^{\frac{1}{2}} \rightarrow \text{finite} \quad , \quad \left(\sum_{i=1}^n (y^i)^2 \right)^{\frac{1}{2}} \rightarrow \infty \quad , \quad (\text{B.18})$$

or equivalently

$$u \rightarrow \infty \quad , \quad \rho \rightarrow 0 \quad , \quad \rho e^u \rightarrow \text{finite} \quad . \quad (\text{B.19})$$

Now the boundary of AdS_d is when $\rho \rightarrow \infty$. In terms of the embedding coordinates

$$C \quad : \quad \left((x^0)^2 + (x^{(-1)})^2 \right)^{\frac{1}{2}} \rightarrow \infty \quad , \quad \left(\sum_{i=1}^d (x^i)^2 \right)^{\frac{1}{2}} \rightarrow \infty \quad , \quad \left(\sum_{i=1}^n (y^i)^2 \right)^{\frac{1}{2}} \rightarrow \text{finite} \quad . \quad (\text{B.20})$$

This completes the missing piece of the boundary of $u \rightarrow \infty$. The topology of the three boundary pieces is

$$A + B = S^1 \times S^{d-1} \times S^{n-1} \quad , \quad C = S^1 \times S^{d-1} \quad , \quad \partial(AdS_{d+n+1}) = A \cup C \quad . \quad (\text{B.21})$$

B.3 The special case $n = 0$

Consider now the special case $n = 0$. In that case, the parametrization is

$$x^0 = r_3 \cosh(\rho) \cos \theta \quad , \quad x^{(-1)} = r_3 \cosh(\rho) \sin \theta \quad , \quad x^i = r_3 \sinh(\rho) n^i \quad , \quad (\text{B.22a})$$

$$i = 1, 2, \dots, d-1 \quad , \quad n \cdot n = 1 \quad , \quad \rho \geq 0 \quad , \quad (\text{B.22b})$$

$$y = r_4 \quad , \quad r_3 = \ell \cosh(u) \quad , \quad r_4 = \ell \sinh(u) \quad , \quad u \in R \quad , \quad y \in R. \quad (\text{B.22c})$$

The metric is now

$$ds_{d+1}^2 = \ell^2 (du^2 + \cosh^2(u) ds_{AdS_d}^2) \quad , \quad u \in R. \quad (\text{B.23})$$

Consider first the limit $u \rightarrow \pm\infty$. This is embedding coordinates correspond to

$$A \quad : \quad \left((x^0)^2 + (x^{(-1)})^2 \right)^{\frac{1}{2}} \rightarrow \infty \quad , \quad \left(\sum_{i=1}^d (x^i)^2 \right)^{\frac{1}{2}} \rightarrow \infty \quad , \quad y \rightarrow \pm\infty \quad , \quad (\text{B.24})$$

and A is topologically $S^1 \times S^{d-1} \times S^0$. This also includes

$$B \quad : \quad \left((x^0)^2 + (x^{(-1)})^2 \right)^{\frac{1}{2}} \rightarrow \infty \quad , \quad \left(\sum_{i=1}^d (x^i)^2 \right)^{\frac{1}{2}} \rightarrow \text{finite} \quad , \quad y \rightarrow \pm\infty. \quad (\text{B.25})$$

This is obtained as the two limits

$$u \rightarrow \pm\infty \quad , \quad \rho \rightarrow 0 \quad , \quad e^{\pm u} \rho \rightarrow \text{finite}. \quad (\text{B.26})$$

Here C is

$$C \quad : \quad \left((x^0)^2 + (x^{(-1)})^2 \right)^{\frac{1}{2}} \rightarrow \infty \quad , \quad \left(\sum_{i=1}^d (x^i)^2 \right)^{\frac{1}{2}} \rightarrow \infty \quad , \quad y \rightarrow \text{finite} \quad , \quad (\text{B.27})$$

and is located at the boundary $\rho \rightarrow \infty$ of the slice.

It should be stressed that all coordinate systems above, are by construction, global.

C. Analytic solutions for other signatures

In this appendix, we present two more analytic solutions that exist if the signature of the metric is changed.

C.1 The uniform solution

This solution is obtained by setting

$$e^{2A_1(u)} = \epsilon_1 e^{2A(u)} \quad , \quad e^{2A_2(u)} = \epsilon_2 e^{2A(u)} \quad , \quad (\text{C.1})$$

where $\epsilon_{1,2}$ are constants. Then, the equations (2.14), (2.15) and (2.16) without the scalar field become

$$(d+n-1)(d+n)\left(\dot{A}^2 - \frac{1}{\ell^2}\right) = (\bar{R}_1 + \bar{R}_2)e^{-2A}, \quad \bar{R}_{1,2} \equiv \frac{R_{1,2}}{\epsilon_{1,2}}, \quad (\text{C.2})$$

$$(d+n-1)(d+n)\ddot{A} + (\bar{R}_1 + \bar{R}_2)e^{-2A} = 0, \quad (\text{C.3})$$

$$\bar{R}_1 = \frac{d}{n}\bar{R}_2, \quad (\text{C.4})$$

and we have set $V = -\frac{(d+n-1)(d+n)}{\ell^2}$. Adding the two first equations we obtain

$$(e^{\ddot{A}}) - \frac{e^A}{\ell^2} = 0, \quad (\text{C.5})$$

with general solution

$$e^A = C_1 e^{-\frac{u}{\ell}} + C_2 e^{\frac{u}{\ell}}, \quad (\text{C.6})$$

Then equation (C.2) becomes

$$\dot{A}^2 e^{2A} - \frac{e^{2A}}{\ell^2} = \frac{(\bar{R}_1 + \bar{R}_2)}{(d+n-1)(d+n)} = \frac{\bar{R}_2}{n(d+n-1)}, \quad (\text{C.7})$$

which implies

$$C_1 C_2 = -\frac{\ell^2 \bar{R}_2}{4n(d+n-1)}. \quad (\text{C.8})$$

We can therefore write the general solution as

$$e^A = e^{A_0} \left[e^{-\frac{u}{\ell}} - \frac{\ell^2 \bar{R}_2}{4e^{2A_0} n(d+n-1)} e^{\frac{u}{\ell}} \right]. \quad (\text{C.9})$$

The behavior of this solution as $u \rightarrow -\infty$ does not depend on the various arbitrary constants that appear in this solution. However, such constants affect other properties of the solution.

Since $R_1 < 0$ and $R_2 > 0$, in order for (C.4) to have a non-trivial solution we must take $\epsilon_1 < 0, \epsilon_2 > 0$ or vice versa. In the first case $\bar{R}_{1,2} > 0$, while in the second case $\bar{R}_{1,2} < 0$

- If $\bar{R}_2 > 0$ then the scale factor vanishes at a finite value $u = u_0$. This is a curvature singularity of the metric. Moreover, in this case, the whole AdS_d part of the metric has a minus sign.

- If $\bar{R}_2 < 0$ then the scale factor is regular and there is a second AdS boundary at $u \rightarrow +\infty$. The solution describes a regular wormhole. In such a case the S^n part of the metric has a negative sign.

C.2 The constant A_2 solution

If we set $A_2 = \bar{A}_2$ constant the equations for A_1 become

$$d(d-1)(\dot{A}_1)^2 - e^{-2A_1} R_1 - \bar{R}_2 - \frac{(d+n-1)(d+n)}{\ell^2} = 0 \quad , \quad \bar{R}_2 \equiv e^{-2\bar{A}_2} R_2, \quad (\text{C.10})$$

$$(d+n-1)d(\ddot{A}_1 + (\dot{A}_1)^2) - d(d-1)(\dot{A}_1)^2 + e^{-2A_1} R_1 + \bar{R}_2 = 0. \quad (\text{C.11})$$

Again we can deduce that

$$e^{\ddot{A}_1} - \frac{d+n}{d\ell^2} e^{A_1} = 0, \quad (\text{C.12})$$

with general solution

$$e^{A_1} = C_1 e^{-\frac{u}{\ell}} + C_2 e^{\frac{u}{\ell}} \quad , \quad \hat{\ell} \equiv \sqrt{\frac{d}{d+n}} \ell. \quad (\text{C.13})$$

The first equation becomes

$$d(d-1) \left(\frac{d}{du} e^{A_1} \right)^2 - \left(\bar{R}_2 + \frac{(d+n-1)(d+n)}{\ell^2} \right) e^{2A_1} = R_1, \quad (\text{C.14})$$

which is satisfied if we choose A_2 and C_2 so that

$$\bar{R}_2 = -\frac{n(d+n)}{\ell^2} \quad , \quad C_2 = -\frac{\ell^2 R_1}{4(d+n)(d-1)C_1}, \quad (\text{C.15})$$

and the solution is

$$e^{A_1} = e^{\bar{A}_1} \left[e^{-\frac{u}{\ell}} - \frac{\ell^2 \bar{R}_1}{4(d+n)(d-1)} e^{\frac{u}{\ell}} \right] \quad , \quad \bar{R}_1 \equiv e^{-2\bar{A}_1} R_1, \quad (\text{C.16})$$

where we set $C_1 = e^{\bar{A}_1}$. For this solution to exist we must take the contribution of the sphere to the metric to be with a negative signature so that (C.15) be satisfied.

D. The stress-energy tensor

The vev of the stress-energy tensor is related to the constant C that appears in the Fefferman-Graham expansion of the metric near the boundary, for example, see the expansions (3.8a) and (3.8b). To show this, here for simplicity we restrict ourselves to the $d = n = 2$ case. For an asymptotically AdS space-time the metric near the boundary can be brought into the form

$$ds^2 = du^2 + \ell^2 e^{-\frac{2u}{\ell}} g_{ij}(u, x) dx^i dx^j, \quad (\text{D.1})$$

where g_{ij} has the following expansion near the boundary when $u \rightarrow +\infty$

$$g_{ij}(u, x) = g_{ij}^{(0)}(x) + e^{\frac{2u}{\ell}} g_{ij}^{(2)}(x) + e^{\frac{4u}{\ell}} \left(g_{ij}^{(4)}(x) + \frac{2u}{\ell} h_{ij}^{(4)}(x) \right) + \dots, \quad (\text{D.2})$$

where $g_{ij}^{(0)}(x)$ corresponds to the boundary condition for the metric. Since we have the second-order equations of motion, the two independent functions are $g_{ij}^{(0)}(x)$ and $g_{ij}^{(4)}(x)$ which the latter is related to the expectation value of the stress-energy tensor of the dual theory. The other functions, $g_{ij}^{(2)}(x)$ and $h_{ij}^{(4)}(x)$ are determined in terms of $g_{ij}^{(0)}(x)$

$$g_{ij}^{(2)} = \frac{1}{2}R_{ij} - \frac{1}{12}Rg_{ij}^{(0)}, \quad (\text{D.3a})$$

$$g_{ij}^{(4)} = \frac{1}{8}g_{ij}^{(0)} [(Trg^{(2)})^2 - Tr[(g^{(2)})^2]] + \frac{1}{2}(g^{(2)})_{ij}^2 - \frac{1}{4}Tr[g^{(2)}]g_{ij}^{(2)} + T_{ij}, \quad (\text{D.3b})$$

$$h_{ij}^{(4)} = \frac{1}{16\sqrt{g^{(0)}}} \frac{\delta}{\delta g^{(0)ij}} \int d^4x \sqrt{g^{(0)}} (R_{ij}R^{ij} - \frac{1}{3}R^2), \quad (\text{D.3c})$$

where the integrand in the last term, is the conformal anomaly in $d+n = 4$ dimensions [63, 64].

To read the T_{ij} we first compute $g_{ij}^{(2)}$ and the first part of $g_{ij}^{(4)}$ by using

$$g_{ij}^{(0)} dx^i dx^j = e^{2\bar{A}_1} \zeta_{\alpha\beta}^{(1)} dx^\alpha dx^\beta + e^{2\bar{A}_2} \zeta_{\mu\nu}^{(2)} dx^\mu dx^\nu, \quad (\text{D.4})$$

and we find (we set $\bar{A}_1 = \bar{A}_2 = 0$)

$$g_{\alpha\beta}^{(2)} = \frac{1}{144} (2R_1 - R_2)^2 \zeta_{\alpha\beta}^{(1)}, \quad g_{\mu\nu}^{(2)} = \frac{1}{144} (R_1 - 2R_2)^2 \zeta_{\mu\nu}^{(2)}, \quad (\text{D.5a})$$

$$g_{\alpha\beta}^{(4)} = \frac{1}{576} (R_1 + R_2)^2 \zeta_{\alpha\beta}^{(1)} + T_{\alpha\beta}, \quad g_{\mu\nu}^{(4)} = \frac{1}{576} (R_1 + R_2)^2 \zeta_{\mu\nu}^{(2)} + T_{\mu\nu}, \quad (\text{D.5b})$$

On the other hand, we can compute the scale factors from equations of motion. The results for $d = n = 2$ are given by

$$A_1 = \log a_0 - \frac{u}{\ell} + a_2 e^{\frac{2u}{\ell}} + a_4 e^{\frac{4u}{\ell}} + a_5 \frac{u}{\ell} e^{\frac{4u}{\ell}} + \dots, \quad (\text{D.6a})$$

$$A_2 = \log s_0 - \frac{u}{\ell} + s_2 e^{\frac{2u}{\ell}} + s_4 e^{\frac{4u}{\ell}} + s_5 \frac{u}{\ell} e^{\frac{4u}{\ell}} + \dots, \quad (\text{D.6b})$$

with coefficients ($a_0 = e^{\bar{A}_1}$, $s_0 = e^{\bar{A}_2}$)

$$a_2 = -\frac{\ell^2}{24} \left(\frac{2R_1}{a_0^2} - \frac{R_2}{s_0^2} \right), \quad s_2 = \frac{\ell^2}{24} \left(\frac{R_1}{a_0^2} - \frac{2R_2}{s_0^2} \right), \quad (\text{D.7a})$$

$$a_4 = -\frac{\ell^4 (5a_0^4 R_2^2 - 8a_0^2 R_1 R_2 s_0^2 + 5R_1^2 s_0^4)}{2304 a_0^4 s_0^4} - C, \quad (\text{D.7b})$$

$$s_4 = -\frac{\ell^4 (5a_0^4 R_2^2 - 8a_0^2 R_1 R_2 s_0^2 + 5R_1^2 s_0^4)}{2304 a_0^4 s_0^4} + C, \quad (\text{D.7c})$$

$$s_5 = -a_5 = -\frac{\ell^4}{192} \left(\frac{R_1^2}{a_0^4} - \frac{R_2^2}{s_0^4} \right). \quad (\text{D.7d})$$

Similar to $d + n = 8$ in (3.8a) and (3.8b) the $\frac{u}{\ell} e^{\frac{4u}{\ell}}$ terms in (D.6a) and (D.6b) are the conformal anomalous terms in $d + n = 4$.

From the above expansions we can read $g_{ij}^{(4)}$ from the near boundary expansion (D.2)

$$g_{\alpha\beta}^{(4)} = \left[\frac{\ell^4}{1152} (11R_1^2 - 8R_1R_2 - R_2^2) - 2C \right] \zeta_{\alpha\beta}^{(1)}, \quad (\text{D.8a})$$

$$g_{\mu\nu}^{(4)} = \left[\frac{\ell^4}{1152} (11R_2^2 - 8R_1R_2 - R_1^2) + 2C \right] \zeta_{\mu\nu}^{(2)}. \quad (\text{D.8b})$$

By comparing the results of (D.5b) with (D.8a) and (D.8b) we can read the stress-energy tensor components as (again we assume $\bar{A}_1 = \bar{A}_2 = 0$)

$$T_{\alpha\beta} = \frac{1}{384} (3R_1^2 - 4R_1R_2 - R_2^2 - 768C) \zeta_{\alpha\beta}^{(1)}, \quad (\text{D.9a})$$

$$T_{\mu\nu} = \frac{1}{384} (3R_2^2 - 4R_1R_2 - R_1^2 + 768C) \zeta_{\mu\nu}^{(2)}. \quad (\text{D.9b})$$

It turns out that T_{ij} and therefore C is proportional to the vev of the stress-energy tensor of the boundary CFT

$$T_{ij} = \frac{1}{4(M_P\ell)^3} \langle T_{ij} \rangle. \quad (\text{D.10})$$

Therefore we can write

$$\langle T_{ij} \rangle = 4(M_P\ell)^3 \left[\frac{T_{CFT}}{4} \begin{pmatrix} \zeta_{\alpha\beta}^{(1)} & 0 \\ 0 & \zeta_{\mu\nu}^{(2)} \end{pmatrix} + \hat{T}_{CFT} \begin{pmatrix} \zeta_{\alpha\beta}^{(1)} & 0 \\ 0 & -\zeta_{\mu\nu}^{(2)} \end{pmatrix} \right], \quad (\text{D.11})$$

where the trace part T_{CFT} and traceless part \hat{T}_{CFT} are defined

$$T_{CFT} = \frac{1}{96} (R_1^2 - 4R_1R_2 + R_2^2), \quad (\text{D.12a})$$

$$\hat{T}_{CFT} = \frac{1}{96} \left(\frac{1}{2}R_1^2 - \frac{1}{2}R_2^2 - 48C \right). \quad (\text{D.12b})$$

E. Perturbations around the product space solution

We consider a solution that is a perturbation around the product space solution. For simplicity, in notation, we choose a new variable

$$z \equiv \sqrt{\frac{d+n}{n}} \frac{(u-u_0)}{\ell}. \quad (\text{E.1})$$

The scale factors are defined as follows

$$A_1(z) = A_1^{(0)}(z) + \delta A_1(z) \quad , \quad A_2(z) = A_2^{(0)}(z) + \delta A_2(z), \quad (\text{E.2})$$

where

$$A_1^{(0)}(z) = \frac{1}{2} \log \left[-\frac{\ell^2 R_1}{d(d+n)} \right], \quad (\text{E.3a})$$

$$A_2^{(0)}(z) = \frac{1}{2} \log \left[\frac{\ell^2 R_2}{(n-1)(d+n)} \sinh^2(z) \right], \quad (\text{E.3b})$$

are the product space scale factors. We can insert (E.2) into the equation of motion (2.14) and read $\delta A'_2(z)$ and $\delta A''_2(z)$. Then by substituting these derivatives into either (2.15) or (2.16) we find the following differential equation for $\delta A_1(z)$

$$-2n\delta A_1 + n \coth(z)\delta A'_1 + \delta A''_1 = 0. \quad (\text{E.4})$$

The solution for this equation is

$$\begin{aligned} \delta A_1 = & \frac{C_1}{\cosh^{\frac{m+n}{2}}(z)} {}_2F_1\left(\frac{m+n}{4}, \frac{1}{4}(m+n+2); \frac{n+1}{2}; \tanh^2(z)\right) \\ & + \frac{C_2 \tanh^{1-n}(z)}{\cosh^{\frac{m+n}{2}}(z)} {}_2F_1\left(\frac{1}{4}(m-n+2), \frac{1}{4}(m-n+4); \frac{3-n}{2}; \tanh^2(z)\right), \end{aligned} \quad (\text{E.5})$$

where C_1 and C_2 are two constants of integration and we have defined

$$m \equiv \sqrt{n(n+8)}. \quad (\text{E.6})$$

Expanding around the end-point $u = u_0$ or equivalently $z = 0$ we read

$$\delta A_1 = C_1\left(1 + \frac{nz^2}{n+1} + \mathcal{O}(z^4)\right) + C_2 z^{-n}\left(z - \frac{n(n+5)z^3}{6(n-3)} + \mathcal{O}(z^4)\right). \quad (\text{E.7})$$

This expansion shows that in order the scale factor of *AdS* i.e. $e^{2A_1^{(0)}(u)+2\delta A_1(u)}$ be finite as $z \rightarrow 0$ we should choose

$$C_2 = 0. \quad (\text{E.8})$$

We can also expand δA_1 near the UV boundary as $z \rightarrow +\infty$

$$\delta A_1 = C_1 \frac{(m-2)2^{n-2}\Gamma\left(\frac{m}{2}-1\right)\Gamma\left(\frac{n+1}{2}\right)}{\sqrt{\pi}\Gamma\left(\frac{m+n}{2}\right)} (e^z)^{\frac{m-n}{2}} + \dots, \quad (\text{E.9})$$

which means that although the fluctuations are small near the IR end-point but grow exponentially as z moves toward the UV boundary.

The equation of motion for δA_2 in terms of the new variable z is given by

$$\coth(z) (d\delta A'_1 + (n-1)\delta A'_2) - d\delta A_1 + (n-1)\text{csch}^2(z)\delta A_2 = 0. \quad (\text{E.10})$$

The solution is obtained by

$$\delta A_2 = C_3 \coth(z) + \coth(z) \int_1^z \frac{d}{n-1} \tanh(w) (\tanh(w)\delta A_1 - \delta A'_1) dw, \quad (\text{E.11})$$

where C_3 is another constant of integration. Equation (E.11) is hard to solve but to see the series expansion of δA_2 we can solve (E.10) near $z = 0$. The series is

$$\delta A_2 = -C_1\left(\frac{d}{3(n+1)}z^2 + \frac{d(8n-3)}{45(n+1)(n+3)}z^4 + \dots\right). \quad (\text{E.12})$$

Here the constant of integration C_3 in (E.11) is related to C_1 to have a regular solution for the scale factor of the sphere A_2 . Moreover, near the UV as $z \rightarrow +\infty$ we have

$$\delta A_2 = C_1 \frac{2^{n-2} d(m-n-2) \Gamma\left(\frac{m}{2}\right) \Gamma\left(\frac{n-1}{2}\right)}{\sqrt{\pi}(n-m) \Gamma\left(\frac{m+n}{2}\right)} (e^z)^{\frac{m-n}{2}} + \dots, \quad (\text{E.13})$$

however, here unlike the δA_1 , the fluctuations remain small compared to the leading term which is growing like e^{2z} because

$$2 > \frac{m-n}{2}, \quad \text{for } n > 0. \quad (\text{E.14})$$

F. Topological Black holes with a negative cosmological constant

We consider solutions to the Einstein equation with a negative cosmological constant

$$G_{\mu\nu} = \frac{d(d+1)}{\ell^2}, \quad (\text{F.1})$$

in $d+2$ dimensions, with an ansatz

$$ds^2 = -f(r)dt^2 + \frac{dr^2}{f(r)} + r^2 h_{ij}(x) dx^i dx^j. \quad (\text{F.2})$$

$$f = k - \frac{\omega_d M}{r^{d-1}} + \frac{r^2}{\ell^2}, \quad \omega_d = \frac{16\pi G}{d \text{Vol}(h)}, \quad \text{Vol}(h) = \int d^d x \sqrt{h}, \quad (\text{F.3})$$

and h_{ij} is a constant curvature metric

$$R_{ij}(h) = (d-1)k h_{ij}. \quad (\text{F.4})$$

If the constant curvature manifold h is maximally symmetric, then

$$R_{ijkl}(h) = k(h_{ik}h_{jl} - h_{il}h_{jk}). \quad (\text{F.5})$$

The $M=0$ solution above is isomorphic to a maximally symmetric constant curvature space satisfying

$$R_{\mu\nu\rho\sigma} = -\frac{1}{\ell^2}(g_{m\rho}g_{\nu\sigma} - g_{\mu\sigma}g_{\nu\rho}). \quad (\text{F.6})$$

Therefore, the solution with $M=0$ is locally isometric to AdS_{d+2} space, but the topology depends on the sign of k . The boundary is conformally equivalent to $\text{AdS}_d \times S^1$ if we take the t coordinate to be an angle $t \in [0, 2\pi]$.

The metric above is invariant under the following rescaling

$$t \rightarrow \frac{t}{\lambda}, \quad r \rightarrow \lambda r, \quad k \rightarrow \lambda^2 k, \quad M \rightarrow \lambda^{d+1} M, \quad h_{ij} \rightarrow \frac{h_{ij}}{\lambda^2}. \quad (\text{F.7})$$

By choosing $\lambda = \frac{1}{\sqrt{|k|}}$ when $k \neq 0$ the metric can be written as

$$f = \epsilon - \frac{\omega_d M}{r^{d-1}} + \frac{r^2}{\ell^2} \quad , \quad \epsilon = 0, \pm 1 \quad , \quad \omega_d = \frac{16\pi G}{d \text{Vol}(h)} \quad , \quad \text{Vol}(h) = \int d^d x \sqrt{h} \quad , \quad (\text{F.8})$$

and h_{ij} is a constant curvature metric with

$$R_{ij}(h) = (d-1)h_{ij} \quad . \quad (\text{F.9})$$

In the maximally symmetric case, the horizon surface can be an S^d or any quotient, T^3 or any quotient, or a compact quotient of AdS_3 .

We now take $d = 3$ and set $k = -|k|$. The equation for the horizon position is

$$-|k|\ell^2 r^2 - \omega_3 M \ell^2 + r^4 = 0 \quad \rightarrow \quad r_{\pm}^2 = \ell^2 \frac{|k| \pm \sqrt{k^2 + 4\frac{\omega_3 M}{\ell^2}}}{2} \quad . \quad (\text{F.10})$$

As $r = 0$ is curvature singularity, we are interested in solutions with $r > 0$.

We can distinguish the following cases

1. $\omega_3 M < -\frac{k^2 \ell^2}{4} \equiv \omega_3 M_{crit}$.

In this case, the solutions are complex and there is no horizon.

2. $\omega_3 M = -\frac{k^2 \ell^2}{4} \equiv \omega_3 M_{crit}$.

We have a double root $r_+ = r_- = \ell \sqrt{\frac{|k|}{2}}$. This is an extremal horizon.

3. $0 > \omega_3 M > -\frac{k^2 \ell^2}{4}$. There are two distinct real roots with r_+ the largest. This is a case similar to the RN black holes and r_- is a Cauchy horizon.

4. $M = 0$. In this case $r_+ = \ell \sqrt{|k|}$ while $r_- = 0$. Now $r = 0$ is not anymore a curvature singularity and the solution is now locally AdS_5

5. $M > 0$. In this case, there is a single root $r_+ > 0$ and the black hole structure is as in Schwarzschild.

Parametrizing

$$M = \frac{r_+^{d-1}}{\omega_d} \left(\frac{r_+^2}{\ell^2} - |k| \right) \quad , \quad (\text{F.11})$$

the temperature is given in general d as

$$T = \frac{(d+1)r_+^2 - (d-1)|k|\ell^2}{4\pi\ell^2 r_+} \quad . \quad (\text{F.12})$$

When $T = 0$,

$$r_+^2 = \frac{(d-1)}{d+1} |k| \ell^2 \equiv r_{crit}^2 \quad , \quad (\text{F.13})$$

and

$$M = M_{crit} = -\frac{2}{(d+1)\omega_d} \left(\frac{d-1}{d+1}\right)^{\frac{d-1}{2}} |k|^{\frac{d+1}{2}} \ell^{d-1}. \quad (\text{F.14})$$

Using the extremal solution $M = M_{crit}$ as the reference solution, we can write the energy and entropy as

$$E = M - M_{crit} \quad , \quad S = \frac{\text{Vol}(h) r_+^d}{4G}. \quad (\text{F.15})$$

The specific heat is

$$\frac{\partial E}{\partial T} = \frac{4\pi r_+^{d-1}}{\omega_d} \frac{(d+1)r_+^2 - (d-1)|k|\ell^2}{(d+1)r_+^2 - (d-1)|k|\ell^2} = \frac{4\pi r_+^{d-1}}{\omega_d} \frac{r_+^2 - r_{crit}^2}{r_+^2 + r_{crit}^2}. \quad (\text{F.16})$$

It is clear that for $M > M_{crit}$ all solutions are thermodynamically stable.

More details, as well as the analysis of the thermodynamics and possible phase transitions, can be found in [61, 62].

References

- [1] R. C. Myers and A. Sinha, “*Seeing a c-theorem with holography,*” *Phys. Rev. D* **82** (2010), 046006 [ArXiv:1006.1263][hep-th];
“*Holographic c-theorems in arbitrary dimensions,*” *JHEP* **01** (2011), 125 [ArXiv:1011.5819][hep-th].
- [2] D. L. Jafferis, “*The Exact Superconformal R-Symmetry Extremizes Z,*” *JHEP* **05** (2012), 159 [ArXiv:1012.3210][hep-th].
- [3] J. K. Ghosh, E. Kiritsis, F. Nitti and L. T. Witkowski, “*Holographic RG flows on curved manifolds and the F-theorem,*” *JHEP* **02** (2019), 055; [hep-th].
- [4] C. Closset, T. T. Dumitrescu, G. Festuccia and Z. Komargodski, “*Supersymmetric Field Theories on Three-Manifolds,*” *JHEP* **05** (2013), 017 [ArXiv:1212.3388][hep-th].
- [5] S. L. Adler, “*Massless, Euclidean Quantum Electrodynamics on the Five-Dimensional Unit Hypersphere,*” *Phys. Rev. D* **6** (1972) 3445; Erratum: [*Phys. Rev. D* **7** (1973) 3821].
- [6] R. Jackiw and C. Rebbi, “*Conformal Properties of a Yang-Mills Pseudoparticle,*” *Phys. Rev. D* **14** (1976) 517.
- [7] C. G. Callan, Jr. and F. Wilczek, “*Infrared Behavior At Negative Curvature,*” *Nucl. Phys. B* **340** (1990) 366.

- [8] E. Kiritsis and C. Kounnas, “*Infrared regularization of superstring theory and the one loop calculation of coupling constants*,” *Nucl. Phys. B* **442** (1995) 472 [[ArXiv:hep-th/9501020](#)];
“*Curved four-dimensional space-times as infrared regulator in superstring theories*,” *Nucl. Phys. Proc. Suppl.* **41** (1995) 331 [[ArXiv:hep-th/9410212](#)].
- [9] A. Buchel, “*Quantum phase transitions in cascading gauge theory*,” *Nucl. Phys. B* **856** (2012), 278-327; [[ArXiv:1108.6070](#)] [[hep-th](#)].
- [10] J. K. Ghosh, E. Kiritsis, F. Nitti and L. T. Witkowski, “*Holographic RG flows on curved manifolds and quantum phase transitions*,” *JHEP* **05** (2018), 034; [[ArXiv:1711.08462](#)][[hep-th](#)].
- [11] C. Fefferman and C. Robin Graham, “*Conformal Invariants*”, in *Elie Cartan et les Mathématiques d’aujourd’hui* (Astérisque, 1985) 95.
- [12] J. K. Ghosh, E. Kiritsis, F. Nitti and L. T. Witkowski, “*Revisiting Coleman-de Luccia transitions in the AdS regime using holography*,” *JHEP* **09** (2021), 065; [[ArXiv:2102.11881](#)] [[hep-th](#)].
- [13] E. Witten and S. T. Yau, “*Connectedness of the boundary in the AdS / CFT correspondence*,” *Adv. Theor. Math. Phys.* **3** (1999) 1635 [[ArXiv:hep-th/9910245](#)].
- [14] M. T. Anderson, “*Geometric aspects of the AdS / CFT correspondence*,” *IRMA Lect. Math. Theor. Phys.* **8** (2005) 1 [[ArXiv:hep-th/0403087](#)].
- [15] E. Kiritsis, F. Nitti and E. Préau, “*Holographic QFTs on $S^2 \times S^2$, spontaneous symmetry breaking and Efimov saddle points*,” *JHEP* **08** (2020), 138; [[ArXiv:2005.09054](#)] [[hep-th](#)].
- [16] S. Fulling, “*Scalar quantum field theory in a closed universe of constant curvature*”, Ph.D. thesis, Princeton University (1972)
- [17] N. Birrell and P. Davies, “*Quantum Fields in Curved Space*,” doi:10.1017/CBO9780511622632
- [18] E. Mottola, “*Particle Creation in de Sitter Space*,” *Phys. Rev. D* **31** (1985) 754.
- [19] N. C. Tsamis and R. P. Woodard, “*Quantum gravity slows inflation*,” *Nucl. Phys. B* **474** (1996) 235, [[ArXiv:hep-ph/9602315](#)];
“*The Quantum gravitational back reaction on inflation*,” *Annals Phys.* **253** (1997) 1, [[ArXiv:hep-ph/9602316](#)].
- [20] A. M. Polyakov, “*Infrared instability of the de Sitter space*,” [[ArXiv:1209.4135](#)][[hep-th](#)].
- [21] L. Senatore and M. Zaldarriaga, “*On Loops in Inflation*,” *JHEP* **1012** (2010) 008, [[ArXiv:0912.2734](#)][[hep-th](#)].

- [22] J. K. Ghosh, E. Kiritsis, F. Nitti and L. T. Witkowski, “*Back-reaction in massless de Sitter QFTs: holography, gravitational DBI action and $f(R)$ gravity*,” *JCAP* **07** (2020), 040; [ArXiv:2003.09435][hep-th].
- [23] J. K. Ghosh, E. Kiritsis, F. Nitti and V. Nourry, “*Quantum (in)stability of maximally symmetric space-times*,” [ArXiv:2303.11091] [gr-qc].
- [24] J. B. Hartle, S. W. Hawking and T. Hertog, “*No-Boundary Measure of the Universe*,” *Phys. Rev. Lett.* **100** (2008), 201301; [ArXiv:0711.4630] [hep-th].
- [25] T. Hertog and J. Hartle, “*Holographic No-Boundary Measure*,” *JHEP* **05** (2012), 095 [ArXiv:1111.6090][hep-th];
J. B. Hartle, S. Hawking and T. Hertog, “*Quantum Probabilities for Inflation from Holography*,” *JCAP* **01** (2014), 015 [ArXiv:1207.6653][hep-th].
- [26] E. Kiritsis, F. Nitti and L. Silva Pimenta, “*Exotic RG Flows from Holography*,” *Fortsch. Phys.* **65** (2017) no.2, 1600120, [ArXiv:1611.05493][hep-th].
- [27] Y. Bea and D. Mateos, “*Heating up Exotic RG Flows with Holography*,” *JHEP* **08** (2018), 034 [ArXiv:1805.01806][hep-th].
- [28] U. Gursoy, E. Kiritsis, F. Nitti and L. Silva Pimenta, “*Exotic holographic RG flows at finite temperature*,” *JHEP* **1810** (2018) 173, [ArXiv:1805.01769][hep-th];
- [29] O. Aharony, E. Y. Urbach and M. Weiss, “*Generalized Hawking-Page transitions*,” *JHEP* **08** (2019), 018 [ArXiv:1904.07502][hep-th].
- [30] S. Hawking and D. N. Page, “*Thermodynamics of Black Holes in anti-De Sitter Space*,” *Commun. Math. Phys.* **87** (1983), 577
- [31] G. T. Horowitz, D. Wang and X. Ye, “*An infinity of black holes*,” *Class. Quant. Grav.* **39** (2022) no.22, 225014; [ArXiv:2206.08944][hep-th].
- [32] D. Bak, M. Gutperle and S. Hirano, “*A Dilatonic deformation of $AdS(5)$ and its field theory dual*,” *JHEP* **05** (2003), 072; [ArXiv:hep-th/0304129].
- [33] A. B. Clark, D. Z. Freedman, A. Karch and M. Schnabl, “*Dual of the Janus solution: An interface conformal field theory*,” *Phys. Rev. D* **71** (2005), 066003; [ArXiv:hep-th/0407073].
- [34] E. D’Hoker, J. Estes and M. Gutperle, “*Ten-dimensional supersymmetric Janus solutions*,” *Nucl. Phys. B* **757** (2006), 79-116; [ArXiv:0603012/hep-th].
- [35] D. Gaiotto and E. Witten, “*Janus Configurations, Chern-Simons Couplings, And The theta-Angle in $N=4$ Super Yang-Mills Theory*,” *JHEP* **06** (2010), 097; [ArXiv:0804.2907] [hep-th].
- [36] D. Gaiotto and E. Witten, “*S-Duality of Boundary Conditions In $N=4$ Super Yang-Mills Theory*,” *Adv. Theor. Math. Phys.* **13** (2009) no.3, 721-896; [ArXiv:0807.3720] [hep-th].

- [37] E. D’Hoker, J. Estes and M. Gutperle, “*Exact half-BPS Type IIB interface solutions. I. Local solution and supersymmetric Janus,*” *JHEP* **06** (2007), 021; [[ArXiv:0705.0022](#)] [[hep-th](#)].
- [38] K. Jensen and A. O’Bannon, “*Holography, Entanglement Entropy, and Conformal Field Theories with Boundaries or Defects,*” *Phys. Rev. D* **88** (2013) no.10, 106006; [[ArXiv:1309.4523](#)][[hep-th](#)].
- [39] N. Bobev, F. F. Gautason, K. Pilch, M. Suh and J. Van Muiden, “*Janus and J-fold Solutions from Sasaki-Einstein Manifolds,*” *Phys. Rev. D* **100** (2019) no.8, 081901 [[ArXiv:1907.11132](#)][[hep-th](#)].
- [40] N. Bobev, F. F. Gautason, K. Pilch, M. Suh and J. van Muiden, “*Holographic interfaces in $\mathcal{N} = 4$ SYM: Janus and J-folds,*” *JHEP* **05** (2020), 134 [[ArXiv:arXiv:2003.09154](#)][[hep-th](#)].
- [41] I. Arav, K. C. M. Cheung, J. P. Gauntlett, M. M. Roberts and C. Rosen, “*Spatially modulated and supersymmetric mass deformations of $\mathcal{N} = 4$ SYM,*” *JHEP* **11** (2020), 156; [[ArXiv:2007.15095](#)] [[hep-th](#)].
- [42] I. Arav, K. C. M. Cheung, J. P. Gauntlett, M. M. Roberts and C. Rosen, “*A new family of AdS_4 S-folds in type IIB string theory,*” *JHEP* **05** (2021), 222; [[ArXiv:2101.07264](#)] [[hep-th](#)].
- [43] N. Bobev, F. F. Gautason and J. van Muiden, “*The holographic conformal manifold of 3d $\mathcal{N} = 2$ S-fold SCFTs,*” *JHEP* **07** (2021) no.221, 221 [[ArXiv:arXiv:2104.00977](#)][[hep-th](#)].
- [44] A. Ghodsi, J. K. Ghosh, E. Kiritsis, F. Nitti and V. Nourry, “*Holographic QFTs on AdS_d , wormholes and holographic interfaces,*” *JHEP* **01** (2023), 121; [[ArXiv:2209.12094](#)] [[hep-th](#)].
- [45] A. Karch and L. Randall, “*Locally localized gravity,*” *JHEP* **05** (2001), 008; [[ArXiv:hep-th/0011156](#)].
- [46] T. Takayanagi, “*Holographic Dual of BCFT,*” *Phys. Rev. Lett.* **107** (2011), 101602; [[ArXiv:1105.5165](#)] [[hep-th](#)].
- [47] M. Fujita, T. Takayanagi and E. Tonni, “*Aspects of $AdS/BCFT$,*” *JHEP* **11** (2011), 043; [[ArXiv:1108.5152](#)][[hep-th](#)].
- [48] M. Gutperle and J. Samani, “*Holographic RG-flows and Boundary CFTs,*” *Phys. Rev. D* **86** (2012), 106007; [[ArXiv:1207.7325](#)][[hep-th](#)].
- [49] I. Arav, K. C. M. Cheung, J. P. Gauntlett, M. M. Roberts and C. Rosen, “*Superconformal RG interfaces in holography,*” *JHEP* **11** (2020), 168 [[ArXiv:2007.07891](#)][[hep-th](#)].

- [50] J. M. Maldacena and L. Maoz, “*Wormholes in AdS*,” *JHEP* **02** (2004), 053; [[ArXiv:hep-th/0401024](#)].
- [51] P. Betzios, E. Kiritsis and O. Papadoulaki, “*Euclidean Wormholes and Holography*,” *JHEP* **06** (2019), 042; [[ArXiv:1903.05658](#)][hep-th].
- [52] P. Simidzija and M. Van Raamsdonk, “*Holo-ween*,” *JHEP* **12** (2020), 028; [[ArXiv:2006.13943](#)] [hep-th].
- [53] P. Betzios, E. Kiritsis and O. Papadoulaki, “*Interacting systems and wormholes*,” *JHEP* **02** (2022), 126 [[ArXiv:2110.14655](#)][hep-th].
- [54] B. Gouteraux and E. Kiritsis, “*Generalized Holographic Quantum Criticality at Finite Density*,” *JHEP* **12**, 036 (2011) doi:10.1007/JHEP12(2011)036 [[ArXiv:1107.2116](#)][hep-th].
- [55] B. Gouteraux, J. Smolic, M. Smolic, K. Skenderis and M. Taylor, “*Holography for Einstein-Maxwell-dilaton theories from generalized dimensional reduction*,” *JHEP* **01**, 089 (2012) [[ArXiv:arXiv:1110.2320](#)][hep-th].
- [56] K. Jensen and A. O’Bannon, “*Holography, Entanglement Entropy, and Conformal Field Theories with Boundaries or Defects*,” *Phys. Rev. D* **88** (2013) no.10, 106006; [[ArXiv:1309.4523](#)] [hep-th].
- [57] R. A. Janik, J. Jankowski and P. Witkowski, “*Conformal defects in supergravity — backreacted Dirac delta sources*,” *JHEP* **07** (2015), 050; [[ArXiv:1503.08459](#)] [hep-th].
- [58] M. Billò, V. Gonçalves, E. Lauria and M. Meineri, “*Defects in conformal field theory*,” *JHEP* **04** (2016), 091; [[ArXiv:1601.02883](#)] [hep-th].
- [59] G. Cuomo, Z. Komargodski and A. Raviv-Moshe, “*Renormalization Group Flows on Line Defects*,” *Phys. Rev. Lett.* **128** (2022) no.2, 021603; [[ArXiv:2108.01117](#)] [hep-th].
- [60] D. Rodriguez-Gomez and J. G. Russo, “*Defects in scalar field theories, RG flows and dimensional disentangling*,” *JHEP* **11** (2022), 167; [[ArXiv:2209.00663](#)] [hep-th].
- [61] R. B. Mann, “*Pair production of topological anti-de Sitter black holes*,” *Class. Quant. Grav.* **14** (1997), L109-L114; [[ArXiv:gr-qc/9607071](#)].
- [62] D. Birmingham, “*Topological black holes in Anti-de Sitter space*,” *Class. Quant. Grav.* **16** (1999), 1197-1205; [[ArXiv:hep-th/9808032](#)].
- [63] M. Henningson and K. Skenderis, “*The Holographic Weyl anomaly*,” *JHEP* **07**, 023 (1998); [[ArXiv:hep-th/9806087](#)].
- [64] K. Skenderis, “*Lecture notes on holographic renormalization*,” *Class. Quant. Grav.* **19** (2002), 5849-5876; [[ArXiv:hep-th/0209067](#)].